5-2017

Developing a General Methodology for Evaluating Composite Action in Insulated Wall Panels

Jaiden Thomas Olsen
Utah State University

DEVELOPING A GENERAL METHODOLOGY FOR EVALUATING COMPOSITE ACTION IN INSULATED WALL PANELS

by

Jaiden Thomas Olsen

A thesis submitted in partial fulfillment
of the requirements for the degree

of

MASTER OF SCIENCE

in

Civil Engineering

Approved:

_____	_____
Marc Maguire, Ph.D. Major Professor	Joseph A. Caliendo, Ph.D. Committee Member
_____	_____
Paul Barr, Ph.D. Committee Member	Mark R. McLellan, Ph.D. Vice President for Research and Dean of the School of Graduate Studies

UTAH STATE UNIVERSITY
Logan, Utah

2017

ABSTRACT

Developing a General Methodology for Evaluating Composite Action in Insulated Wall Panels

by

Jaiden T. Olsen, Master of Science

Utah State University, 2017

Major Professor: Dr. Marc Maguire
Department: Civil Engineering

Thermal efficiency of Precast Concrete Sandwich Panel Walls has become a major topic when discussing the building envelope in academia. At Utah State University, research is being done to evaluate the structural and thermal efficiency of fiber reinforced polymer connectors being used today. In evaluating several different proprietary fiber reinforced polymer systems, researchers plan to develop design procedures to help engineers accurately determine minimum design requirements when using fiber reinforced polymer connectors. This largely requires a determination of the degree of composite action incurred by each system. Testing is performed by constructing small scale specimens (3 ft. by 4 ft., 0.91 m by 1.22 m). Each specimen contains one of the fiber reinforced polymer connecting systems. By constructing a five-wythe, two wall specimen, direct shear can be applied to the connectors using a push-off shear test method. By performing this test it can be determined to what degree the panel is acting compositely. Once the degree of composite action is determined, correlation can be made between design and degree of composite action. Economizing and simplifying

this procedure is key to further implementation of precast concrete sandwich panel walls in all areas of our building infrastructure.

(155 pages)

PUBLIC ABSTRACT

Developing a General Methodology for Evaluating Composite Action in Insulated Wall Panels

Jaiden T. Olsen

Precast Concrete Sandwich Panel Walls (PCSPW's) have been in use for over 60 years. They provide a very efficient building envelope for many buildings. Characteristic PCSPW's comprise an outer and inner layer (or wythe) of concrete separated by an insulating material. To use all of the material as efficiently as possible, the layers are attached by connectors which penetrate through the insulating layer and are embedded in either concrete wythe. These connectors make it possible for both layers of the wall to work together when resisting loads. The connectors are made out of plastic, or FRP, to prevent heat transfer from one side of the wall to the other.

This research is evaluates several different FRP systems by fabricating and testing 49 small scale "push-off" specimens (3 ft. by 4 ft., 0.91 m by 1.22 m). Testing of these specimens is done by applying loads perpendicular to the connectors and measuring the amount of deformation that occurs. By determining the load to deformation relationship, engineers can make more informed decisions about the full scale behavior. Using this information, the goal of this project is to validate current procedures and develop simpler, more efficient methods for predicting overall strength of this innovative building system.

DEDICATION

I would like to dedicate this thesis to my loving and supportive wife, Beckah Olsen and my son Stetson Olsen. I am so grateful for your unwavering support, love, patience, and inspiration. Without you this wouldn't be possible. My teachers and mentors have been an invaluable asset to me throughout my education and I want to thank them for their love of teaching and for taking time to make sure I am understanding. To all those that have given me support throughout my schooling, know that this couldn't have been possible without you. Thank you all!

ACKNOWLEDGMENTS

I would like to express my greatest appreciation to my graduate advisor, Dr. Marc Maguire, for his friendship, time, knowledge, direction, and encouragement during this project. I would also like to thank Dr. Joe Caliendo, Dr. Paul Barr, and Dr. Marv Halling, for their support, instruction, and friendship. I am very grateful for all of the faculty and staff at Utah State in the department of Structural Engineering.

I would like to give a special thanks to Gilbert Nichols, Ethan Pickett, Hunter Buxton, Parker Syndergaurd, and all the other research assistants at the SMASH lab. Tackling a project of this magnitude would have been impossible without so many great helping hands.

I am also incredibly grateful for the support of the Precast Concrete Institute's Daniel P. Jenny Fellowship Program. Furthermore, the donation of connectors and insulation materials by Thermomass, Dayton Superior, HK Composites, and Aslan-FRP was greatly appreciated, and was integral to the completion of this research. Special thanks to Ken Fleck and A.L. Patterson for the donated lifting devices to make our lives easier.

Jaiden T. Olsen

CONTENTS

Page

ABSTRACT iii

PUBLIC ABSTRACT v

DEDICATION vii

ACKNOWLEDGMENTS viii

LIST OF TABLES xi

LIST OF FIGURES xii

DEFINITIONS AND SYMBOLS xvii

CHAPTER

1 INTRODUCTION 1

1.1 Background 3
1.2 Research Objective 4

2 LITERATURE REVIEW 5

2.1 Concrete Sandwich Panel Wall History 5

2.1.1 1900-1990 5
2.1.2 1991-2000 12
2.1.3 2001-2010 30
2.1.4 2011-Present 37

2.2 Composite Action 51
2.3 Thermal Efficiency 51
2.4 FRP Shear Transfer Mechanism 52

2.4.1 Mold Injected GFRP 52
2.4.2 Extruded GFRP 53
2.4.3 Weaved GFRP 53

2.5 Design Methods 54

2.5.1 Principles of Mechanics 54
2.5.2 ACI Simplified Method 56
2.5.3 PCI Method 57

CONTENTS

Page

3 EXPERIMENTAL PROGRAM 59
3.1 Push-off Specimen Configurations 59
3.2 Test Matrix 60
3.2.1 Connector A 60
3.2.2 Connector B 62
3.2.3 Connector C 63
3.2.4 Connector D 65
3.2.5 Connector E 66
3.3 Construction of Wall Panels 68
3.3.1 Form Setup 69
3.3.2 Rebar Ties and Configuration 70
3.3.3 Preparing to Pour 70
3.3.4 Casting Concrete 74
3.3.5 Lifting and Storing Specimens 80
3.4 Material Properties 82
3.5 Push Test Setup 83
3.6 Instrumentation 86
3.6.1 Linear Variable Differential Transformer Locations 86

4 TEST RESULTS FOR PUSH-OFF TESTS 87
4.1 Introduction 87
4.2 Material Testing 87
4.3 Push-off Test Results 89
4.3.1 Experimental Results for Connector A 96
4.3.2 Experimental Results for Connector B 97
4.3.3 Experimental Results for Connector C 101
4.3.4 Experimental Results for Connector D 103
4.3.5 Experimental Results for Connector E 106
4.3.6 Failure Modes of Shear Connectors 106
4.3.7 Recommended Design Curves 120
4.4 Summary and Conclusions 122

5 SIMPLE MODEL TO PREDICT ELASTIC FULL SCALE BEHAVIOR . 123

CONTENTS

Page

6 SUMMARY AND CONCLUSIONS 130
6.1 Summary 130
6.2 Push-off Testing 130
6.3 Elastic Prediction Methods 131

REFERENCES 132

LIST OF TABLES

Table Page

2-1 Table to determine factors for Equation (2-22) 42

3-1 Test Matrix for Five-Wythe Push-Off Specimens 61

3-2 Material Properties of Concrete 83

3-3 Material Properties of Concrete (2) 83

4-1 Material properties of concrete for push-off specimens 88

4-2 Material Properties of Concrete for push-off specimens 89

4-3 Observed Experimental Capacity of Connector A 98

4-4 Elastic and plastic stiffness for all Connector A push-off specimens 98

4-5 Observed experimental capacity of Connector B 100

4-6 Elastic and plastic stiffness for all Connector B push-off specimens 100

4-7 Observed Experimental Capacity of Connector C 102

4-8 Elastic and plastic stiffness for all Connector C push-off specimens 103

4-9 Observed experimental capacity of Connector D 105

4-10 Elastic and plastic stiffness for all Connector D push-off specimens 105

4-11 Elastic and plastic stiffness for all Connector E push-off specimens 107

4-12 Summary of recommended design curves for all connectors 121

LIST OF FIGURES

Figure Page

1-1 Configuration of a Concrete Sandwich Panel 4

1-2 Types of Steel Connectors 4

2-1 SWP tilted while sand is sprayed from center wythe with fire hose 6

2-2 Lightweight foam concrete tilt-up SWP 8

2-3 Design charts used by designers to extract acceptable dimensional ratios 10

2-4 Stress distribution diagrams in PCSWPs due to pure bending 13

2-5 Insulation joints in SWPs 14

2-6 R-value vs % area stainless steel connectors in PCSWPs 15

2-7 R-value vs % area penetration of concrete for PCSWPs 15

2-8 Candidate FRP connectors shown in cross-sectional view of PCSWPs 17

2-9 Diagram showing the flexural test setup 18

2-10 Differential Panel Element 20

2-11 Stress distribution in a non-composite sandwich panel 25

2-12 Sample calculations for determining section properties 26

2-13 A depiction of the FEM/linear analysis model 28

2-14 Cross sectional view of the two panels tested by Lee and Pessiki 32

2-15 Maximum transverse stresses for various end conditions 34

2-16 Lateral load vs mid-span deflection with analogy model 36

2-17 Loading pattern applying point loads across unsupported span of panel 38

2-18 Photograph depicting the loading tree and end-slip measurement 38

2-19 Data collected for Naito et al.'s testing of Connector B 39

Figure Page

2-20 Shear and Moment Diagram 40

2-21 Push-off Specimen cured (left) and before concrete poured (right) 43

2-22 Observed failure modes in SWP 44

2-23 Naito et al.'s data (2011) vs Bai and Davidson's predictions 50

2-24 Evaluation of shear by principles of mechanics 55

2-25 Definition of distance, d, from Eq. (2-42) 57

3-1 Push-off Specimen diagram and photographs of each connector 59

3-2 Connector A Close-up 61

3-3 Detailed diagram of the push-off specimen design for connector A. 62

3-4 Connector B Close-up 63

3-5 Detailed diagram for push-off specimen for connector B. 64

3-6 Connector C Close-up 64

3-7 Detailed diagram for push-off specimen for connector C. 65

3-8 Connector D Close-up 66

3-9 Detailed diagram for push-off specimen for connector D. 67

3-10 Connector E Close-up 67

3-11 Detailed diagram for push-off specimen for connector E. 68

3-12 Professional Tie Wire Twister & Looped Tie Wires. 70

3-13 Tying rebar prior to inserting it in the formwork 71

3-14 Pick points attached to divider and centered within the middle wythe. 71

3-15 Seaming of the bond inhibitor using duct tape. 72

3-16 Left: Connector B, Middle: Connector C, Right: Connector D 73

Figure Page

3-17 Connector E placed in foam. 74

3-18 An example of a completed first layer. 75

3-19 Freshly removed first layer of formwork. 76

3-20 Prepared second wythe. Rebar, pick points, and form work are all in place. 77

3-21 Formwork removed after concrete for the second wythe is allowed to cure. 78

3-22 The highest set of forms is in place, ready to pour the last concrete wythe. 78

3-23 Taking special care to put a finished surface on the final wythe of the concrete 79

3-24 Finished product waiting to cure 79

3-25 Activation of the clutch around the pick point 80

3-26 Horizontal specimen ready to be lifted. 81

3-27 Specimen is vertical and ready for storage. 81

3-28 Graphical representation of the average concrete compressive strengths 83

3-29 Diagram (left) and photograph (right) of test set up. 84

3-30 Specially designed mounting bracket used to attach LVDT's to specimen. 85

3-31 Special bracket fixed to the specimen. 85

4-1 Graphical representation of average concrete compressive strengths in Table 4-2 89

4-2 Load-Deformation Curve & Visually Identifying the Yield Point 90

4-3 Ultimate Load Comparison for All Connectors Individually 92

4-4 Different types of polyisocyanurate foam and their associated face finishing .. 93

4-5 Elastic Load Limit (F_E) Comparison for All Specimen Configurations 93

4-6 Elastic Stiffness Comparison for All Connector 94

Figure Page

4-7 Inelastic Stiffness Comparison for All Connector 95

4-8 Chart of all 3-in. specimens for Connector A 96

4-9 Chart of all 4-in. specimens for Connector A 97

4-10 Chart of all three-inch specimens for connector B 99

4-11 Chart of all 4-in. specimens for Connector B push-off specimens 99

4-12 Chart of all 3-in. specimens for Connector C 101

4-13 Chart of all 4-in. specimens for Connector C 102

4-14 Chart of all 3-in. specimens for Connector D 104

4-15 Chart of all 4-in. specimens for Connector D 104

4-16 Chart of all 3-in. specimens for Connector E 106

4-17 Tensile rupture in unbonded specimen with ISO foam 108

4-18 Pullout failure in unbonded specimen with ISO foam 108

4-19 Shear fracture failure in unbonded specimen with EPS foam 109

4-20 Dowel action causing delamination occurring along the width of ..... Connector B 110

4-21 Dowel action failure of Connector B 110

4-22 Dowel action occurring along the length of Connector B 111

4-23 Shear fracture observed in Connector B 111

4-24 Pullout occurring with Connector B in combination with bending fracture 112

4-25 Shear fracture of Connector B 112

4-26 Delamination observed in a 4-in. unbonded XPS specimen 113

4-27 Dowel action in a 4-in. bonded XPS specimen 114

Figure Page

4-28 Delamination / shear rupture in a 4-in. bonded XPS specimen 114

4-29 Shear fracture and dowel action of Connector C 115

4-30 Punch through observed in all 3-in. specimens with Connector C 115

4-31 Punch through close-up..... 116

4-32 Shear fracture of Connector D (full specimen)..... 117

4-33 Shear fracture of Connector D, both ends fractured 117

4-34 Close-up of shear fracture of connector D..... 118

4-35 Three inch bonded EPS connector E tensile rupture of all connectors..... 119

4-36 Tensile rupture of connector E, note compression leg still intact..... 119

4-37 Tensile rupture of tension strut in truss..... 120

5-1 Simple FEM model used to predict full-scale behavior..... 124

5-2 Comparison of the Beam Spring Model in elastic range 125

5-3 Deflection comparison with different connector distributions. 126

5-4 Force per connector for different connector distributions. 127

5-5 Example elastic load versus deformation relationship for various levels .....

of shear connector intensities..... 128

DEFINITIONS AND SYMBOLS

- *Cast-in-place Concrete*- Concrete that is cast where it will be used. Cast-in-place concrete makes up the majority of concrete used today.
- *CFRP*-An acronym for Carbon Fiber Reinforced Polymer. Though there are no CFRP shear connectors used in this study, they are a very common alternative to GFRP or traditional steel shear connectors in the industry.
- *Composite Action*- A principle that describes the degree to which two or more independent bodies cooperate to accommodate a specified loading scenario. Composite action occurs when there is a shear transfer mechanism which transfers load from one element to another. Essentially, a shear transfer mechanism creates a point of fixity between one interface and another. This fixity prevents independent association of structural elements. The forced interaction that takes places requires equivalent load distribution and strain compatibility.
- *Composite Material*-Refers to any material made from two or more component materials with independent characteristics and affixed in such a way that they behave as one. Examples of composite materials include CFRP, GFRP, and concrete. For the purposes of this report, composite material will refer to fiber reinforced polymer materials.
- *Concrete Wythe*- Refers to either layer of the PCSPW that is made up of concrete. For full scale specimens, these are the outside wythes. For the push-off specimen, this can be the outside or the very center wythe.

- *Connectors*- Specifically for this thesis, connectors will be referred to as any one of the proprietary shear connectors used to connect concrete wythes. Connectors are used to transfer shear force within a PCSPW.
- *EPS*-An acronym for expanded polystyrene. Expanded polystyrene is used as a rigid thermal insulation. As a possible component of PCSPW's, it may constitute the center wythe of a panel.
- *FRP*-An acronym for Fiber Reinforced Polymer. Used as an ambiguity in referring to FRP shear connectors.
- *Fully Composite Panels*- Specifically in reference to PCSPW's, fully composite panels distribute the load through the shear connectors such that the components of the PCSPW move and distribute stresses together.
- *GFRP*-An acronym for Glass Fiber Reinforced Polymer. All of the shear connectors tested in this thesis are made of GFRP. GFRP has many different manufacturing processes which include: extrusion, mold injection, and weaving.
- *Insulation*-For this thesis, insulation will refer to the material used as a thermal barrier and will be placed in the center Wythe of a 3-wythe panel.
- *ISO*-An acronym for polyisocyanurate. Polyisocyanurate is a thermo-plastic used as a rigid insulation.
- *Non-Composite Panels*-Specifically in reference to PCSPW's, non-composite panels exist when wythes act independent of one another.
- *Non-Structural Wythe*- Any layer of a PCSPW that is not designed to take load (can be either concrete or insulation). A non-structural wythe could be used as an

architectural cladding or simply as an outer layer to protect the insulation in the center wythe.

- *Partially Composite Action*- Any number of elements that work together to sustain loading conditions, where the bodies are somewhat independent of one another yet share the load.
- *Partially Composite Panels*- A sandwich panel which distributes some load through shear connectors, but an unbalanced load case does exist. Wythes do not cooperate independently, nor are they completely dependent.
- *PCSPW*-Short for Precast Concrete Sandwich Panel Walls. Precast Concrete Sandwich Panel Walls are structural elements used as a building envelope and can also be used as the lateral resisting system and the gravity resisting system. They are made up of 3 layers of varying thicknesses, materials, and levels of composite action. The panels are commonly described by a three-digit sequence of numbers where each digit in the sequence denotes the thickness of one of the layers in the panel. For example, a 5-3-4 panel is comprised of a 5 inch thick interior wythe, a 3 inch thick insulation wythe, and a 4 inch thick exterior wythe.
- *Pick-Point*- Often referred to as a lifting anchor, or is the location designed to lift and maneuver precast members. For this project, pick-points were provided by A.L. Patterson, and are recessed into the concrete. A special clutch is used to attach the hook of the crane for lifting.
- *Precast Concrete*- Precast concrete is a building product that is manufactured in a controlled environment in reusable forms. It is then transported to the job site and erected into place.

- *Push-off Specimen*- The specimens used in this research. A push-off specimen is a test specimen designed to apply direct shear force on the connectors.
- *R-Value*- The capacity of an insulating material to resist heat transfer. Often measured in hr•ft^2 •°F/Btu (SI-Units = m^2•K/W).
- *Shear Connector*- A connector used to transfer shear forces between concrete wythes in a PCSPW.
- *Structural Wythe*-A structural wythe is any layer of a PCSPW that is designed to take load (typically made of concrete).
- *Tilt-up Concrete*- Unlike Precast Concrete, Tilt-up concrete is cast on site and then lifted into place.
- *Wythe*-A vertical section or layer of a PCSPW. A wythe can be structural or nonstructural and can be made up of any number of materials.
- *XPS*-An acronym for extruded polystyrene. Extruded polystyrene is used as a rigid thermal insulation. As a possible component of PCSPW's, it may constitute the center, insulating wythe of a panel.

CHAPTER 1

INTRODUCTION

Precast Concrete Sandwich Panel Walls (PCSPWs) have been in use for over 60 years. They provide a very efficient building envelope for many buildings. Sandwich panel walls combine structural and thermal efficiencies into one simplistic design. This system is advantageous over conventional methods because of its rapid construction and erection methods. Characteristic PCSPW's comprise an outer and inner layer (or wythe) of concrete separated by an insulating material. To achieve maximum structural efficiency, the wythes are connected by shear transfer mechanisms, which penetrate through the insulating layer and can provide various levels of composite action. More stringent energy building codes demand greater thermal efficiency which therefore increases the implementation of PCSPW's. As these connectors become more widely used, the demand for a reduction in thermal bridging fostered the development of connectors made of many different materials.

Sandwich panel walls have been in production in the United States for more than 100 years. One of the earliest examples of sandwich panel walls was built in 1906. This *tilt-up* wall was produced by casting a 2-inch layer of concrete, covered by a 2-inch layer of sand. An additional layer of concrete was then cast superior to the sand. The concrete panels were connected using steel ties with an unknown design. After curing, the panel was tilted and the sand was washed out with a fire hose as it was put into place. Other early PCSPW's were built in 1951 in New York City, New York. The production lines

used to build these precast insulated wall panels were 200 feet long. The panels were six feet high and ten feet wide. The panels were cast and then transported to British Columbia, Canada. “[The panels] consist of a 2-inch thick layer of cellular glass insulation and two wire-mesh reinforced slabs of 3000-psi concrete, tied together with channel-shaped strips of expanded metal. These ties also serve as shear reinforcing (Collins, 1954).” These panels had an overall thickness of 5.5 inches.

Precast sandwich panel walls constructed between 1951 and the mid 1990’s largely had identical components with varying insulation types, dimensions, and wythe connection design. Reinforced concrete wythes, foam insulation, and shear transfer mechanisms were components of every panel. With the huge push for Leadership in Energy and Environmental Design Certified buildings (or LEED certified buildings), there is a rapidly increasing demand for these thermally and cost efficient structural elements. The research performed on PCSPW’s in the last two and a half decades, has focused on designing with thermally efficient connectors. Thermal bridging is still a significant challenge for PCSPWs, particularly in structurally composite panels. There have been many proposed solutions to enable composite action without thermal bridging, and many have been implemented and are currently in use across the United States. Fiber Reinforced Polymer (FRP) connectors make up the largest part of today’s cutting edge shear connectors.

The research presented in this paper is aimed at developing general tools for PCSPW designers to use in everyday practice, specifically through component level testing and simplified modeling. Using this component level testing, the goal of this

project is to validate a simple model to predict elastic stresses and deflections in PCSPWs, which are currently a major concern for design engineers.

1.1 Background

Precast Concrete Sandwich Panel Walls (PCSPW's) have been in use for over 60 years. They provide a very efficient building envelope for many buildings. They combine structural and thermal efficiencies into one simplistic design. They are also advantageous over conventional methods because they eliminate many delays due to field work as well as the need for several sub-contractors. Characteristic PCSPW's comprise an outer and inner layer (or wythe) of concrete separated by an insulating material (See Figure 1-1). To achieve maximum structural efficiency, the wythes are connected by shear connectors that penetrate through the insulating layer which can provide various levels of composite action. More stringent energy building codes have demanded greater thermal efficiency. Therefore, these shear connections are often made of various composites to eliminate thermal bridging.

The majority of sandwich panel walls between 1906 and the mid 1990's have had nearly identical components with varying insulation types, dimensions, and wythe connection design. Figure 1-2 shows many of the connector configurations used in these early panels. All connectors were made of steel, or monolithically cast concrete ribs.

Reinforced concrete wythes, insulation, and steel connectors were components of nearly every panel. Thermal bridging is still a massive problem with precast sandwich panel walls. There have been many proposed solutions and many have been implemented across the United States. The goal of increasing thermal efficiency has led to simple eradication of many steel components within the sandwich panel wall. Though the focus

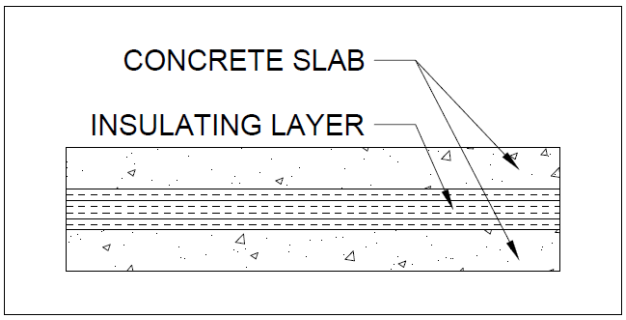

Figure 1-1 Configuration of a Concrete Sandwich Panel

has generally been to prevent any steel from penetrating the thermal barrier, research has proven that elimination of steel components embedded in the concrete can improve thermal efficiency. The most effective solutions are FRP based materials which are currently available to replace longitudinal reinforcement and shear transfer mechanisms.

1.2 Research Objective

This research involves the evaluation of several different proprietary FRP systems by fabricating and testing 49 small scale “push-off” specimens. Testing involves the application of direct shear to each connecting system. By determining the shear load versus shear deformation behavior of each system at the specimen and component levels, engineers can make more informed decisions about the full scale behavior of panels. Using the component level testing, the goal of this project is to validate mechanics-based procedures for predicting stresses, deflections, and nominal strength.

Figure 1-2 Types of Steel Connectors

CHAPTER 2

LITERATURE REVIEW

2.1 Concrete Sandwich Panel Wall History

This section contains a history of today's precast concrete sandwich panel walls, starting with its earliest predecessor, tilt-up sandwich panel walls. Records of concrete sandwich panel walls go back as far as 1906. Since their inception, PCSWPs have become a fundamental building envelope alternative in the United States.

2.1.1 1900-1990

Collins (1954) presented a project from the early 1900s. This is the earliest documented project completed using sandwich panel construction. At the time, the new tilt-up sandwich panel system was a novelty to designers and contractors. The panels were constructed by pouring a 2-in. layer of concrete while embedding steel ties into the concrete wythes. Steel tie configuration is unknown. After the concrete cured, a 2-in. layer of sand was poured across the panel on top of which a second 2-in. layer of concrete was poured. After an unspecified amount of time, the panels were tilted on an angle at which the sand was washed out of the panel with a fire hose (See Figure 2-1), leaving an air gap between the inside and outside wythes. This air gap created a simple thermal barrier. After the sand was washed out of the panel, it was tilted upright and fixed into place.

Modern machinery enabled the invention of *precast* sandwich wall panels in 1951. Some of the earliest PCSWPs were built in 1951 in New York City, New York.

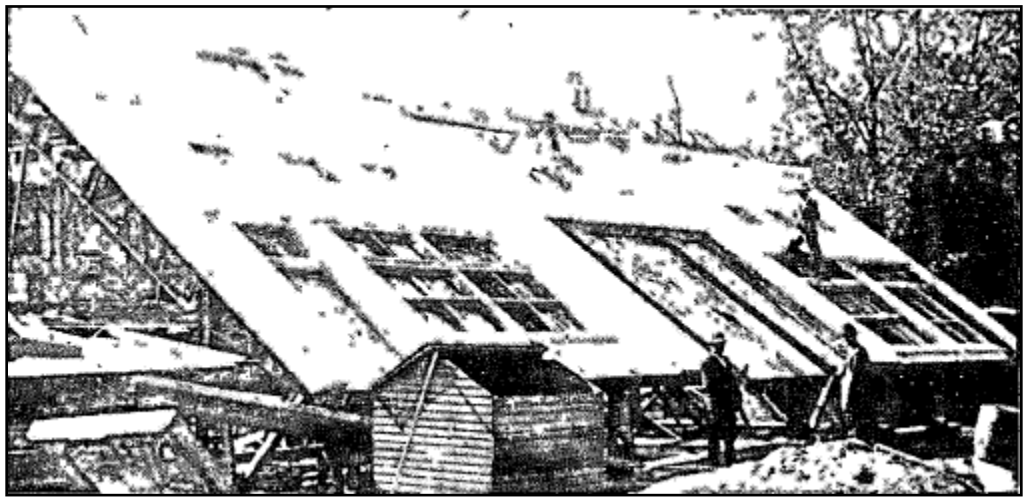

Figure 2-1 SWP tilted while sand is sprayed from center wythe with fire hose (Collins 1954).

The production lines used to build these precast insulated wall panels were 200 feet long. The panels were six feet high and ten feet wide. The panels were cast and then transported to British Columbia, Canada. “[The panels consisted] of a 2-in. thick layer of cellular glass insulation and two wire-mesh reinforced slabs of 3000-psi concrete, tied together with channel-shaped strips of expanded metal. These ties also serve as shear reinforcing.” These panels had an overall thickness of 5.5 inches. Over time, sandwich panel wall designs became much more structurally and thermally efficient.

One project in particular helped Collins develop a design procedure in which he explored different materials to be used as an insulating barrier, different types of shear connectors, and different connector configurations. Figure 2-2 shows one of his twelve-inch (2-8-2) tilt-up sandwich panels. The outer wythes were constructed of reinforced concrete (150 pounds per cubic foot) and the inside wythe was a lightweight foam

concrete (28 pounds per cubic foot). The shear connectors used were a thin-gage expanded steel mesh. The available insulating materials (or materials with a high R-value suitable for the constitution of the center wythe) were divided into the following categories:

1. Cellular glass materials and plastic foam
2. Compressed and treated wood fibers in cement
3. Foam concrete
4. Lightweight concrete

These materials were advantageous for their compressive strength, thermal properties, and unit weight. Insulating concretes are not very common today. The shear connectors that were used were all made of steel: thin-gage expanded mesh, electrically welded wire mesh, bent-wire with welded anchors, and “J” bar (a pin with one hooked end). Collins points out advantages of early sandwich panel walls including thermal efficiency, extended fire rating, and reduced dead weight. These benefits are all similar to contemporary PCSWP.

Collins (1954) suggested that there be a minimum concrete design strength of 3,000 psi for the outside wythes and 2,500 psi for the center insulation (lightweight insulating concrete). He also outlined minimum wythe thicknesses for both the inner and outer wythes. He concluded that the minimum required thicknesses for a panel should be 1.25-2-1.25, or an overall panel thickness of 4.5 inches. The design recommendation took an allowable stress design approach to determine panel dimensions. This iterative design procedure is outlined as follows:

Figure 2-2 Lightweight foam concrete tilt-up SWPwith 2” outer wythes and 8” center wythe (Collins 1954).

1. Begin with the minimum required wythe thickness to obtain an R-value of 4.5 (°F) ft^2 hr/BTU. This is dependent upon the material used (one of the four categories listed previously) for the center wythe.
2. Calculate biaxial maximum design bending moment by checking wind and seismic forces.
3. Calculate the section modulus and determine the associated required area of steel.
4. Increase the wythe thickness until allowable stresses are met.

Adams et al. (1971) outlined design procedures for precast concrete wall panels that standardized this procedure for designers. The design procedure covered the design of solid, ribbed, hollow core, and sandwich panel walls. The design approach to sandwich

panel walls, as indicated by the committee, is to use an “effective section” approach. The recommendation was made that “shearing stress should not be transferred through the nonstructural insulation core. Compressive stress and bending stress should be carried by the concrete sections only (Adams et al. 1971).” The outside wythes of concrete were connected using mechanical steel shear ties or by monolithically cast concrete ribs. It was recommended by the committee that insulation used be either a cellular or mineral based aggregate in lightweight concrete.

The design procedure outlined by Adams et al. (1971) was an allowable stress design approach. By determining the allowable stresses in the panel, an engineer could read a required dimensional ratio of height times width divided by thickness ($h*b/t_e$) from a plot (see Figure 2-3) based on concrete unit weight and compressive strength. In order to determine the correct design stress, two scenarios were considered: vertical compressive stress for concentric loads based on panel buckling stability, and out-of-plane compressive stress for panels between columns, supports, or isolated footings.

Adams et al. (1971) derived equations for determining the allowable stresses in a panel.

For vertical compressive stress with $F_a < 0.11f_c'$

$$F_a = 0.225f_c' \left[1 - \frac{\sqrt{f_c'}}{w^{1.5}} \left(\frac{h}{9t_e} \right)^2 \right] \qquad (2\text{-}1)$$

And for vertical compressive stress with $F_a \geq 0.11f_c'$

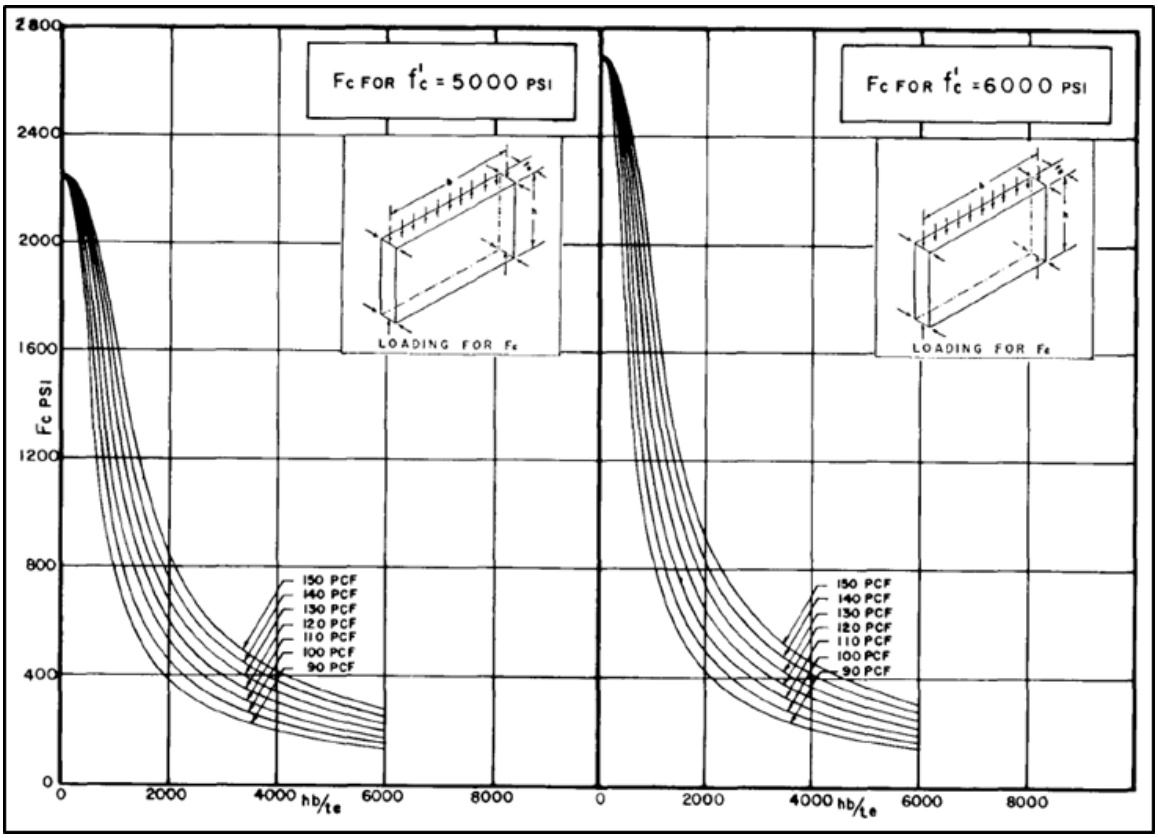

Figure 2-3 Design charts used by designers to extract acceptable dimensional ratioswith a calculated stress and predetermined concrete compressive strength (Adams et al. 1971).

$$F_a = 5w^{1.5}\sqrt{f_c'}\left(\frac{t_e}{h}\right)^2 \tag{2-2}$$

For horizontal compressive stress with $F_c > 0.3f_c'$

$$F_c = 0.45f_c'\left[1 - \frac{f_c'}{w^3}\left(\frac{bh}{75t_e}\right)^2\right] \tag{2-3}$$

And for horizontal compressive stress with $F_c \leq 0.3f_c'$

$$F_c = 13w^{1.5}\sqrt{f_c'}\left(\frac{t_e}{bh}\right) \tag{2-4}$$

Where:

F_a = allowable direct compressive stress, psi

F_c = allowable horizontal compressive stress, psi

f_c' = specified compressive strength of the concrete at 28 days, psi

w = unit weight of concrete, pcf

h = unsupported height of panel, in

t_e = effective thickness of precast wall, in

The stress which returned the lowest value would govern design. Recommendations were also provided for panel dimension ratio requirements for panels subjected to both vertical and horizontal direct uniaxial or biaxial bending stresses, as follows:

For vertical loads:

$$\frac{f_a}{F_a} + \frac{f_{b1}}{F_b} + \frac{f_{b2}}{F_b} \leq 1 \quad (2\text{-}5)$$

For horizontal loads:

$$\frac{f_c}{F_c} + \frac{f_b}{F_b} \leq 1 \quad (2\text{-}6)$$

Adams et al. also provide details on the maximum bearing pressure under a panel (applied on the footprint of the erected panel), to be:

$$F_{br} = 0.4 f_c^{'} \sqrt[3]{\frac{A_c}{A_b}} \leq f_c^{'} \quad (2\text{-}7)$$

Where:

A_c = maximum area of the of supporting member that is geometrically similar to and concentric with the bearing area of the precast panel, in^2

A_b = bearing area of precast panel in contact with supporting frame, in^2

f_a = computed direct compressive stress, psi

$f_b = f_{b1} = f_{b2}$ = computed bending stress, psi, for panels loaded perpendicular to the plane of panel

F_b = allowable maximum bending stress, psi, for panels loaded perpendicular to panel plane

Adams et al. required specific shear connector spacing requirements as well, stating that the connectors should not be placed near the edge of the panel and that the connector composition should be out of a fireproof ductile material. These requirements were to ensure that connectors would be designed to accommodate all shear, bending, tension, and compression forces even in the case of a fire. The conservative assumption was made that the wythes of sandwich wall panels do not work compositely. Though it was a very conservative approach, it made designing PCSWPs very simple.

2.1.2 1991-2000

Einea et al. (1991) presented detailed information on the design and construction of fully-composite, partially-composite, and non-composite PCSWPs in addition to discussing then common building materials. They discussed the principles of fully-, partially, and non-composite panels (Figure 2-4) and introduced the plausibility of many different types of insulations, outlining details on how to conjoin wall panels. They explored many different configurations of steel shear connectors designed to accommodate some degree of composite action as well as the option of non-composite

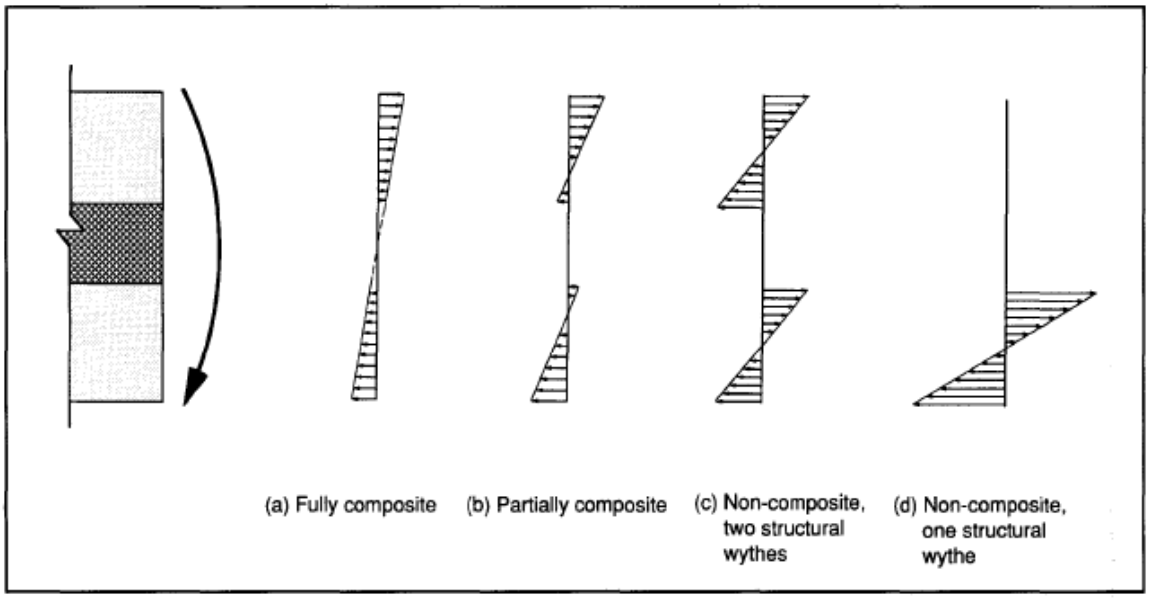

Figure 2-4 Stress distribution diagrams in PCSWPs due to pure bending (Einea et al. 1991)

ties used for attaching architectural cladding and other non-structural elements. Their discussion extensively covered the design and analysis of sandwich panel walls, addressing many failure modes common to PCSWPs.

Einea et al. (1991) introduced the subject of rigid insulation joints. Rigid insulation joints occur when staging the center wythe and preparing to pour the second outside wythe. Rigid insulation comes pre-fabricated in sheets as long as twelve feet. Joints can cause pockets of stagnant air and also concrete ribs that penetrate the thermal barrier, both of which cause a decreased R-value, thus hurting the thermal efficiency of the panel. The easy joint option is called a “butt joint” and is simply two square edges butted up to one another. Recommendations provided by Einea et al. include four much

better alternatives, pictured in Figure 2-5; staggered sheets, perpendicular lapping, inclined lapping, and curved lapping.

Studies were performed to plot the reduction in R-value to the percentage of both steel and concrete penetrating through the center wythe. For example, if 0.1% of the area occupied by one wythe is bridged through the panel via stainless steel, there is a 41% reduction in R-value. For concrete penetrations, 1% of the area occupied by one wythe is equivalent to a 37% reduction in R-value.

Figure 2-6 and Figure 2-7 plot this relationship of R-value versus percentage of area penetrating the center wythe.

This study presented the need for further research aimed at maximizing thermal efficiency. Other areas of research they suggested include thermal efficiency, fire protection, volume changes, and transient versus steady-state temperature effects.

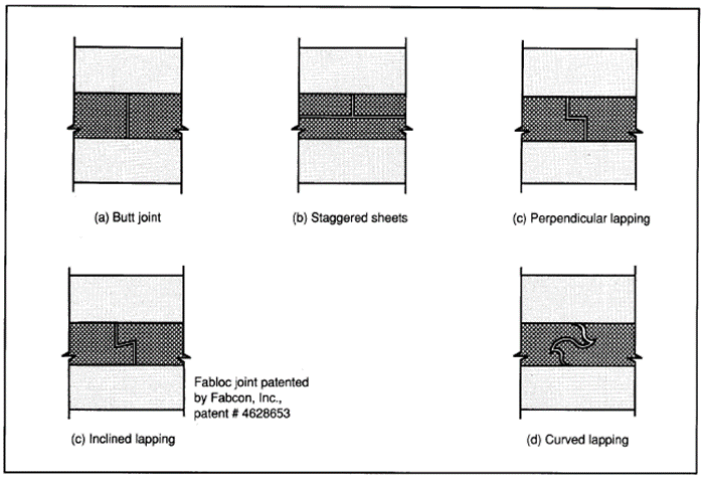

Figure 2-5 Insulation joints in SWPs: a) butt joints, b) staggered sheets, c) perpendicular/inclined lapping, d) curved lapping (Einea et al. 1991)

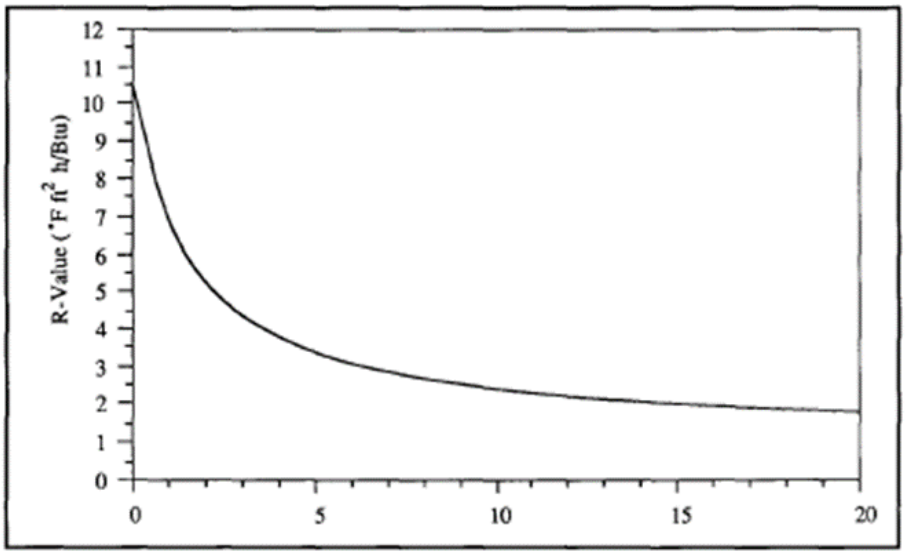

Figure 2-6 R-value vs % area stainless steel connectors in PCSWPsdue to thermal bridging (Einea et al. 1991).

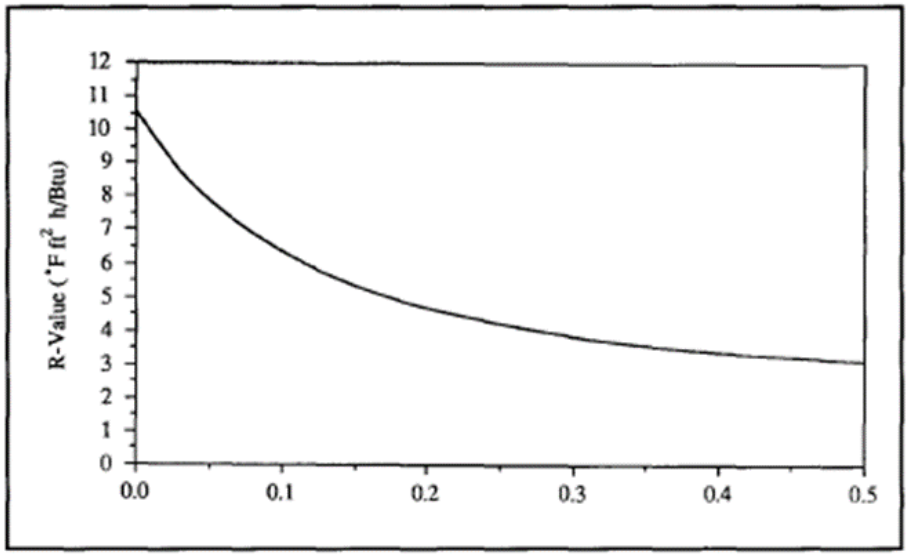

Figure 2-7 R-value vs % area penetration of concrete for PCSWPs due to thermal bridging (Einea et al. 1991).Einea et al. (1994), introduced a new sandwich panel system incorporating “fiber-reinforced plastic [polymer],” (FRP) material. Rather than using traditional steel connectors to create a load path between cooperating wythes, Einea et al.

implemented the use of FRP shear connectors. The motivation behind implementing plastic shear connectors as part of a sandwich panel wall was to reduce heat transfer between concrete wythes. Einea et al. identified the thermal insufficiency of using steel connectors, pointing out that it greatly reduces the thermal potential of PCSWPs (Einea et al. 1991). The authors noted that although implementing FRP connectors increases the initial cost, it proves to have positive economic impact through the life of the structure in heating and cooling costs. Another crucial aspect mentioned by Einea et al. involves the circulation of three components that thermally and structurally efficient precast concrete sandwich panels must incorporate:

1. The connectors must be strong and stiff enough to develop composite behavior of the panels.
2. The connectors must have a high thermal resistance.
3. No concrete penetrations through the insulation layer should exist.

Four different configurations of FRP shear transfer mechanisms were submitted for consideration: wide flange FRP connector, specially fabricated “dog-bone” connector, FRP diagonal strap connectors, and bent bar connector. (See Figure 2-8). The only connector that made it through the first stages of consideration was the bent bar connector. The bent bar connector is a deformed helix that is then threaded with two

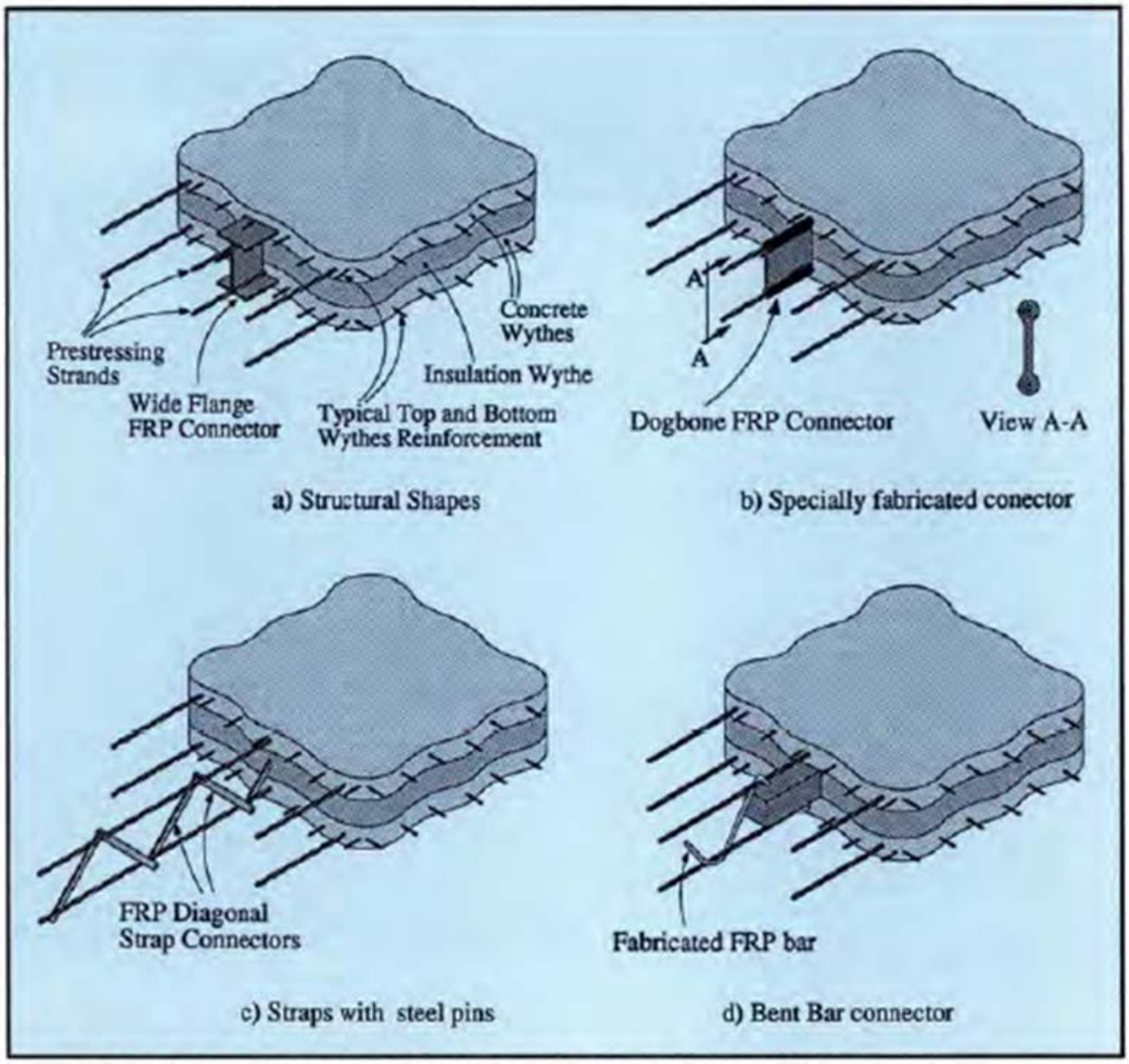

Figure 2-8 Candidate FRP connectors shown in cross-sectional view of PCSWPs (Einea et al. 1994)

prestressing strands. Further, the prestressing strands are embedded in either outside wythe to ensure positive connection between the FRP bar and the concrete.

Shear testing was performed via push-off specimen to determine the shear capacity and shear stiffness of the connector. It was determined that the shear capacity of

the connector is governed by the axial strength of the FRP bar. In other words, the majority of the connectors failed between either of the concrete-foam interfaces. It was also noted that the uninhibited surface of the insulation board bonded with the inner faces of the concrete and contributed up to ten percent of the shear capacity of the specimen.

Flexural testing was also performed to evaluate flexural performance. A single FRP bent bar connector was placed within a three-wythe panel and loaded in two phases. For the first phase, load was applied perpendicular to the panel (Figure 2-9) until the bottom edge of the opposite wythe began to crack. This was done to ensure linearity during a second loading phase. Once cracking occurred the panel was unloaded. The setup for the second phase of loading mimicked the first, only load was applied until specimen failure. This test was performed on two specimens.

During this initial phase of testing on FRP shear transfer mechanisms, it was determined that in addition to being thermally superior to their predecessors, FRP bars satisfy all structural performance guidelines outlined by the researchers. It was observed

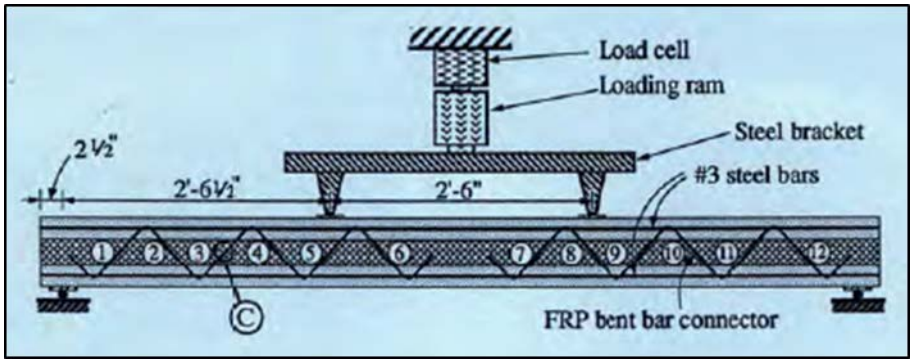

Figure 2-9 Diagram showing the flexural test setup (Einea et al. 1994).

that, though FRP is inherently brittle in nature and fractures at ultimate capacity without any warning, ductile behavior was observed. “[This] ductile behavior is likely caused by cracking in the connections between the bent bar connector and the concrete that leads to a gradual loss of composite action and hence, larger deflections (Einea et al. 1994).” Einea et al. suggested that further research be performed in the following categories:

1. “The effect of long term loading on the proposed system.
2. Cyclic load testing to investigate the ductility and energy dissipation characteristics of the panels for use in high seismic risk areas.
3. Development of lifting and connection inserts to maintain the thermal and structural efficiency of panels. Research is required to develop, test, and obtain design parameters for such accessories.
4. Determination of the fire rating of the proposed panel system. FRP material loses a large portion of its strength when exposed to fire or a high temperature environment. Investigation of concrete cover or other means to prolong the fire rating of the system is needed.
5. Determination if lateral support provided by insulation and concrete wythes is sufficient to prevent instability of the connectors when small bars are used.
6. Experiments to determine the nature of load-slip behavior of the connectors inside the wythes to more accurately predict the stiffness of the panels” (Einea et al. 1994).

These suggestions were published more than twenty years ago. Researchers are still searching for many of these solutions today.

Salmon and Einea (1995) sought to determine a method to predict panel deflections. This is one of the first studies to use finite element methods (FEM) in predicting concrete sandwich panel deflections. The first of two determinations made as a result of this research was that predicting deflections caused by thermal bowing using FEM was found to be acceptable. The second was that "long insulated sandwich panels with low connecting-layer stiffness will experience nearly the same amount of thermal bowing as fully-composite panels." In searching for an accurate design procedure, Salmon and Einea looked at an element of a PCSWP being loaded and closely analyzed the deformation (See Figure 2-10). They found that the panel deformation consists of two components. The first is due to the curvature of the panel. The second is as a result of the

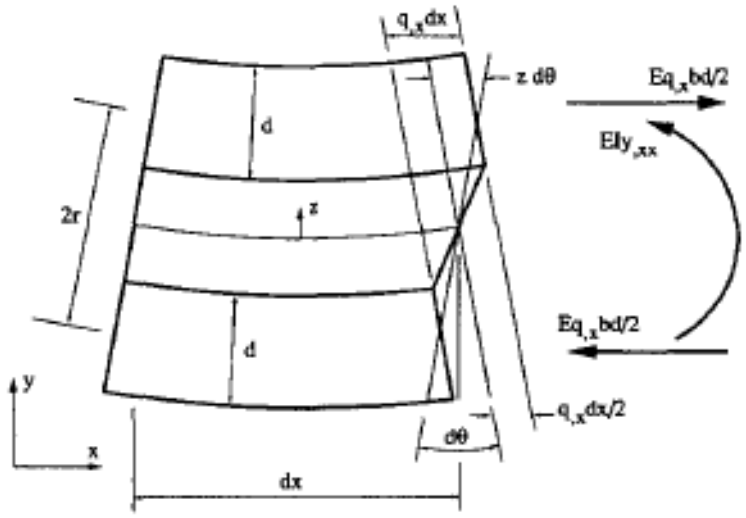

Figure 2-10 Differential Panel Element (Salmon and Einea 1995)

offset that occurs between wythes as a result of the shear stresses involved.

Mathematically, these phenomena can be expressed as:

$$y_{xx} = \frac{M}{EI} + \frac{\alpha^2}{2r} q_x$$

$$\alpha = \frac{(I - 2I_w)}{I} \tag{2-8}$$

Where

x = distance along the length of the panel

y = upward displacement of the panel

q = relative shear displacement of the centroid of the top and bottom wythes

b = width of the panel

M = applied moment

E = wythe modulus of elasticity

I_w = moment of inertia of each wythe

I = moment of inertia of the entire panel cross section

In continuing with the differential equations and performing several derivations similar to the one pictured in

Figure 2-10, Salmon and Einea develop an equation to predict displacement they called the continuum model:

$$\delta = \delta_0 \left[1 - \frac{2}{\psi^2}(1 - \operatorname{sech}\psi)\right] \tag{2-9}$$

Where

$$\delta_0 = -\frac{M_T L^2}{8EI} \tag{2-10}$$

$$\psi = \frac{\chi L}{2\beta} \tag{2-11}$$

$$\beta^2 = \frac{1}{1 + 12\left(\frac{r}{d}\right)^2} \tag{2-12}$$

$$\chi^2 = \frac{2K}{Ed} = \frac{A_c m}{4\sqrt{2}r^2 b}\frac{E_c}{E}\frac{1}{d} = \frac{1}{4\sqrt{2}}\frac{A_c mn}{rb}\frac{1}{rd} \tag{2-13}$$

Where

δ = center panel deflection

δ_0 = fully-composite center panel deflection

ψ = $\frac{\chi L}{2\beta}$

M_T = equivalent end moment caused by change in temperature ΔT

L = panel length

E = modulus of elasticity of connectors

I = panel moment of inertia

β = constant: $\beta^2 = 1 - \alpha^2$

χ = constant: $\chi^2 = \frac{2K}{Ed}$

r = distance between structural wythe centroids

d = structural wythe thickness

K = shear stiffness of connecting layer

A_c = cross-sectional area of connectors

m = number of connectors across panel width

E_c = modulus of elasticity of the concrete

n = modular ratio, $\frac{E_c}{E}$

Though no full-scale testing was done at the time of publication, a comparison between the continuum model and finite element model proved quite successful. For the panels analyzed, results were within 1% of each other.

In March of 1997, the Precast Concrete Institute (PCI) published a PCI Committee Report titled, “State-of-the-Art of Precast/Prestressed Sandwich Wall Panels.” Kim E. Seeber acted as the chairman for 24-member committee. Unlike the 1991 state-of-the-art paper by Einea et al., wythe and panel dimensions were no longer governed by allowable stress in the panel. A minimum wythe thickness was suggested to be two inches, however, overall panel width could be as low as five inches. Although no maximum wythe thickness was imposed, most designs were to make the panels as thin as possible, with required fire resistivity often designating the thickness of the wall panels. Wythe thickness ratios were dependent upon the type of panel; composite, non-composite, or partially composite. The wythes of composite panels were often symmetrical whereas non-composite panels often had a thicker structural wythe. Panel dimensions were “…limited only by the handling capability of the plant, erection equipment, transportation restrictions, and the ability of the panel to resist the applied

stresses" (Seeber et al. 1997). Panels had been as tall as 75 feet and as wide as 14 feet. Most panels ranged between 6 and 12 inches thick, 8 to 12 feet wide, and 10 to 50 feet tall.

Bowing considerations were addressed by the article as well. There are many variables that make it difficult to predict bowing at any given time. These variables include shrinkage, creep, cracking of the concrete (and, consequently, inconsistent modulus of elasticity), thermal gradients between panels, boundary conditions (including indeterminate fixity), and uncertainty in the degree to which the wythes of the panel are acting compositely. In this report, the researchers noted that bowing most often occurred toward the outside of the building. Panels exposed to the sun in the warmer part of the day experienced more bowing than other panels (i.e. south and west panels see more sunlight throughout the day than the north and east panels). Bowing was also constantly changing throughout the day. Due to differing climate on either side of the wall (post erection), it was also noted that differential shrinkage could occur and cause exaggerated effects. It was also observed that asymmetrical panels (due to differing dimension, concrete strength, or prestressing force) experienced more exaggerated bowing effects as well.

Panel design was also approached differently than the previous state-of-the-art article (Einea et al. 1991). The recommendation for non-composite panels was to simply design them like solid section concrete panels, with the assumption that only one wythe would resist all the vertical loads. In the case of lateral loading, it was considered

acceptable to account for the independent flexural stiffness of each wythe. An example is provided for calculating the stresses associated in a 2-1-3 panel in Figure 2-11.

The approach recommended for composite panels was to design the panel similar to that of a solid panel with the same cross-sectional thickness. It was assumed that the panel would remain fully-composite for the entire life of the structure. The authors noted that consideration must be taken for the horizontal shear load that needs to be transferred between the wythes. They also mention that when determining the section properties for design, an account must be made for the lack of stiffness in the center wythe as pictured in Figure 2-12. Recommendations were provided for calculating the force required to be transferred through the shear transfer mechanisms as found in the PCI Design Handbook (Section 4.3.5) (Seeber et al. 2004).

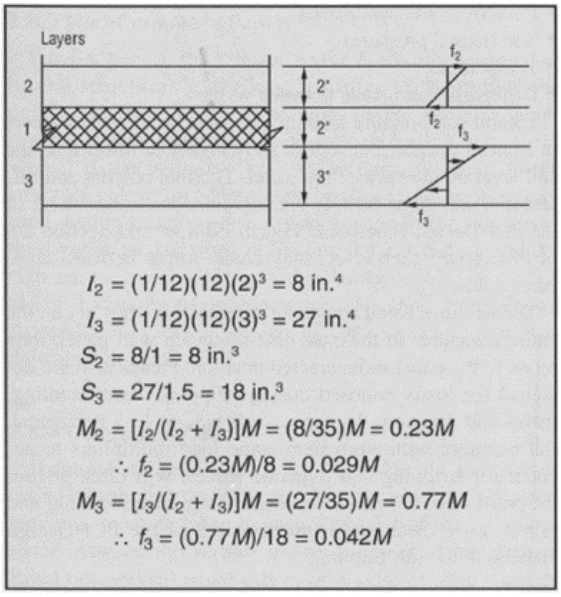

Figure 2-11 Stress distribution in a non-composite sandwich panel (Seeber et al. 1997)

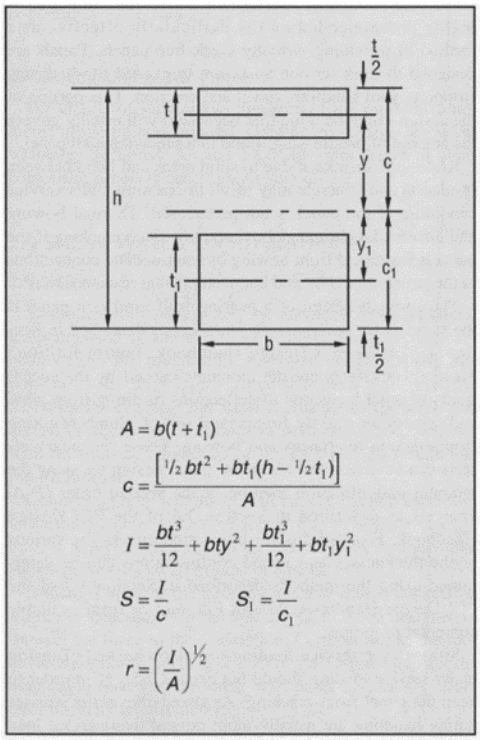

Figure 2-12 Sample calculations for determining section propertiesof fully-composite SWP (Seeber et al. 1997)

Semi-composite panels were designed for two different stages. The assumption was made that the panel works compositely through stripping, release, handling, transportation, and erection processes. The panel was then assumed to be non-composite following erection. This assumption was made because of the concrete-foam interface bond that was initially present in PCSWPs. This bond was known to deteriorate with time. It was unsafe to rely on this bond for the life of the structure. In reality, composite action can be assumed for the panel at the time of release because of the shear capacity of the concrete-foam interface bond in conjunction with shear connectors. After the concrete-foam interface bond is broken, there is still a degree of composite action that takes place as a result of the shear connectors. This was not understood at the time.

Another suggested design procedure for partially composite panel was to perform lateral load tests on an experimental panel that is an exact replication of the design panel. By loading the experimental panel and comparing measured deflections to the calculated fully-composite and non-composite dimensional equivalent, a degree of composite action could be derived by linear interpolation.

For bearing wall design of non-composite panels, the structural wythe was designed to accommodate all bearing loads, including the dead weight of the non-structural wythe if the non-structural wythe did not bear on the structure below. The design was required to comply with the design prescriptions outlined in the PCI Handbook for bearing walls (Seeber et al. 2004).

For composite panels, the bearing loads were required to be positively transferred to both structural wythes. Measures were to be taken to ensure transfer between wythes via positive shear transfer mechanisms. Again, the design was required to comply with the design prescriptions outlined in the PCI hand book for bearing walls.

Semi-composite panels had to be considered as non-composite for bearing loads. In checking for buckling, the independent moments of inertia were to be used. Note this is not the composite section, but the independent wythe section properties.

For shear wall design, lateral load resistance was to be attributed to the structural wythe for non-composite panels. For composite panels, the composite section was allowed to be used to accommodate lateral loads. Semi-composite panels were designed just like non-composite panels.

Included in the article, Seeber et al. outlined design procedures for external connections, panel roof connections, corner connections, floor connections, and panel to panel connections. Also discussed were detailing considerations, reinforcement requirements, fire resistance, insulation types, energy performance, and sandwich panel wall fabrication, transportation, erection, and inspection. This article was ascribed as the most comprehensive design provision published at the time.

Salmon et al. (1997) tested four full-scale specimens to compare results from a control group (two panels with a standard steel truss shear connector) to the results of panels containing the FRP truss introduced by the same group of researchers in 1994 (Einea et al. 1994). This research was geared towards the observation of partially-composite action and ultimate strength comparison. It was determined by the researchers that results between each type of shear connector were very similar.

The beam elements in the FEM model, shown in Figure 2-13, were assigned a moment of inertia corresponding to each wythe. The truss elements represented the FRP

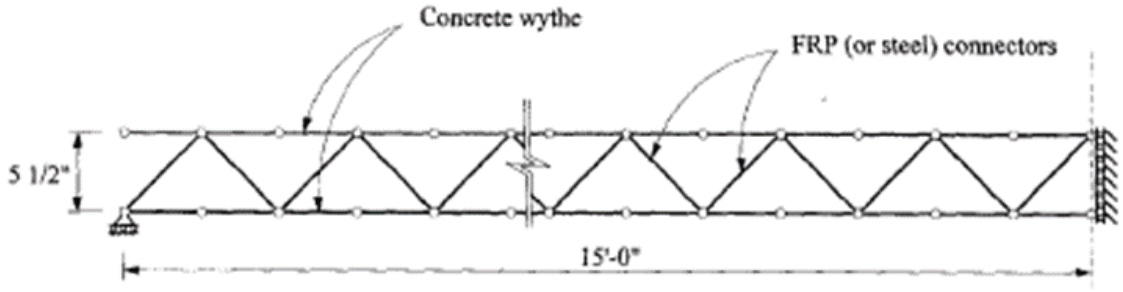

Figure 2-13 A depiction of the FEM/linear analysis model (Einea et al. 1997)

truss or steel truss, depending on the model. Load was applied to the model to generate elastic performance. The results were compared to determine accuracy. Salmon et al. derived an equation from the linear analysis to predict the effective moment of inertia for partially composite panels.

Note, Eq. (2-14) does predict the effective moment of inertia. However, the FEM model is optimized to mimic the data determined from experimental methods. After the researchers calculated the effective moment of inertia, the cracking moment was calculated as follows:

$$I_e = \frac{Mh}{f_b - f_t} \tag{2-14}$$

Where

I_e = the effective moment of inertia

f_b = the stress at the bottom face of the panel

f_t = the stress at the top face of the panel

M = applied moment

h = unsupported length of the panel

$$M_{cr} = \left(6\sqrt{f_c'} + \frac{f_{ps}A_{ps}}{A_w}\right)\frac{I_e}{c} \tag{2-15}$$

Where:

M_{cr} = bending moment that causes cracking

f_c' = concrete compressive strength

f_{ps} = effective prestress in the strand

A_{ps} = prestressed steel area in tension wythe

A_w = cross sectional area of the concrete wythe

c = distance from panel centroid to compression face

The design recommendations given included specifications on adequate FRP to achieve composite action, and not over-reinforcing the concrete wythes.

2.1.3 2001-2010

Pessiki and Mlynarczyk (2003) performed a series of research projects on PCSWPs containing steel truss shear connectors. This project involved the evaluated composite behavior of PCSWP. By designing four full-scale 3-wythe panels of identical dimensions, Pessiki and Mlynarczyk derived an equation to determine the experimental moment of inertia shown in Eq. (2-16). Because this value is an experimental value, it was the actual moment of inertia of the partially composite panel. Pessiki and Mlynarczyk were able to evaluate the degree of composite action using Eq. (2-17), which calculated the percent composite action using the assumption that the relationship between non-composite and fully-composite panels is linear.

$$I_{exp} = \frac{5wL^4}{384\Delta E_c} \tag{2-16}$$

$$\kappa = \frac{(I_{exp} - I_{nc})}{(I_c - I_{nc})} \tag{2-17}$$

Where:

I_{exp} = experimentally determined moment of inertia

w = uniformly distributed load per length

L = span length of test panel

Δ = midspan lateral deflection

E_c = modulus of elasticity of concrete

κ = factor to describe percent composite action of panel

I_c = moment of inertia of the fully-composite section

I_{nc} = moment of inertia of the non-composite section

The first full-scale specimen was a typical PCSWP. Shear forces were transferred between wythes via regions of solid concrete, steel shear connectors, and concrete-insulation interface bond. The other three specimens were constructed such that only one shear transfer mechanism was incorporated into each panel. By testing all four panels with a uniform lateral pressure and determining relative stiffnesses, it was found that the solid concrete regions provided the majority of the composite action in the wall panel. The recommendation of the researchers was that "solid concrete regions be proportioned to provide all of the required composite action in a precast sandwich wall panel." Though significant, this research fueled a need to create a more efficient shear connector and spurred research on full-scale panels that did not contain any solid concrete regions in the panel.

Lee and Pessiki (2008) performed testing involving the lateral load testing of three-wythe (three concrete wythes, two foam wythes) panels with steel truss shear connectors. They tested two panels, each with a different cross-section (See Figure 2-14).

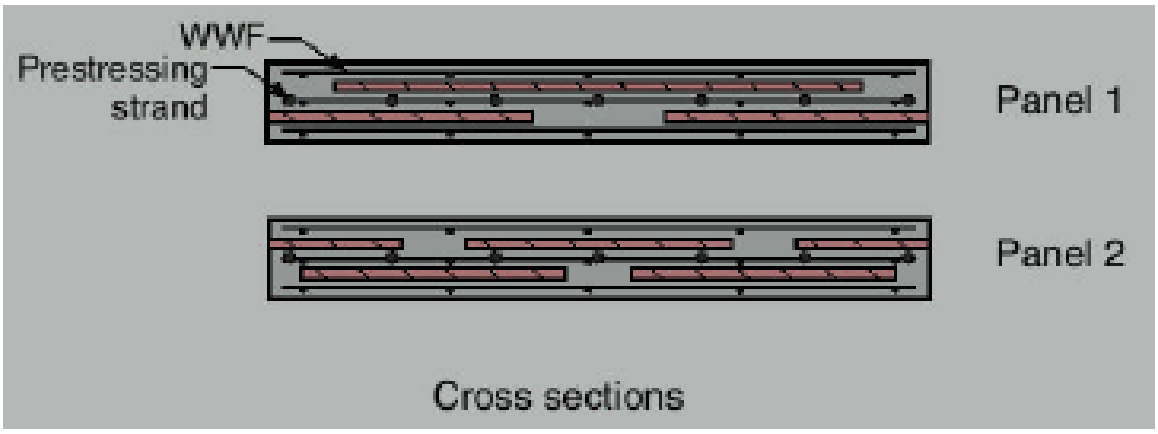

Figure 2-14 Cross sectional view of the two panels tested by Lee and Pessiki (2008)

This research was performed to enhance the knowledge acquired because of Lee and Pessiki (2007), proving that five-wythe panels were more thermally efficient than their three-wythe counter parts. This motivated research to determine structural performance of different five-wythe configurations. The PCSWPs were tested by placing each specimen horizontally on top of an air bladder and placing reaction beam structures on each end to mimic pin-and-roller end conditions. Upon inflation of the bladder, the panel would experience a uniformly distributed loading condition. This uniformly distributed load was incrementally increased until failure. Load and deflection were measured for both panels and then compared. It was determined that Panel 2 was stiffer than Panel 1. Because of the abrupt failure noted, Lee and Pessiki made the recommendation that the design tensile strength should be reduced for five-wythe panels. They also noted that current codified design methods were acceptable for five-wythe sandwich panel design. The recommendation made to reduce the tensile strength is a result of Eq. 2-18.

$$\alpha\sqrt{f_c'} = \frac{Mc}{I} + f_{pe} \quad (2\text{-}18)$$

Where:

α = is a multiplier (typically = 7.5)

f_c' = compressive strength of concrete

M = the moment when cracking occurs

c = distance from the centroid to extreme tension fiber

f_{pe} = effective prestress of the panel

Lee and Pessiki observed a considerably reduced cracking moment. As a result of Eq. (2-18), they recommended that the value of α be equal to 3.7 rather than 7.5 for PCSWP design. Another aspect of this research incorporated the generation of design graphs to help designers determine the maximum transverse stresses for various end conditions. These graphs are shown in

Figure 2-15, where each line is representative of a different type of panel. The graphs were interpreted by the number of strands or the initial prestress in the panel (psi). The upper graph is for center wythe stresses, while the lower schematic shows the outer wythe stresses.

The most relevant observations and recommendations of Lee and Pessiki's project included the following

1. Early flexural cracking was observed for both panels (leading to the recommendation that design tensile strength be $3.7\sqrt{f_c'}$).

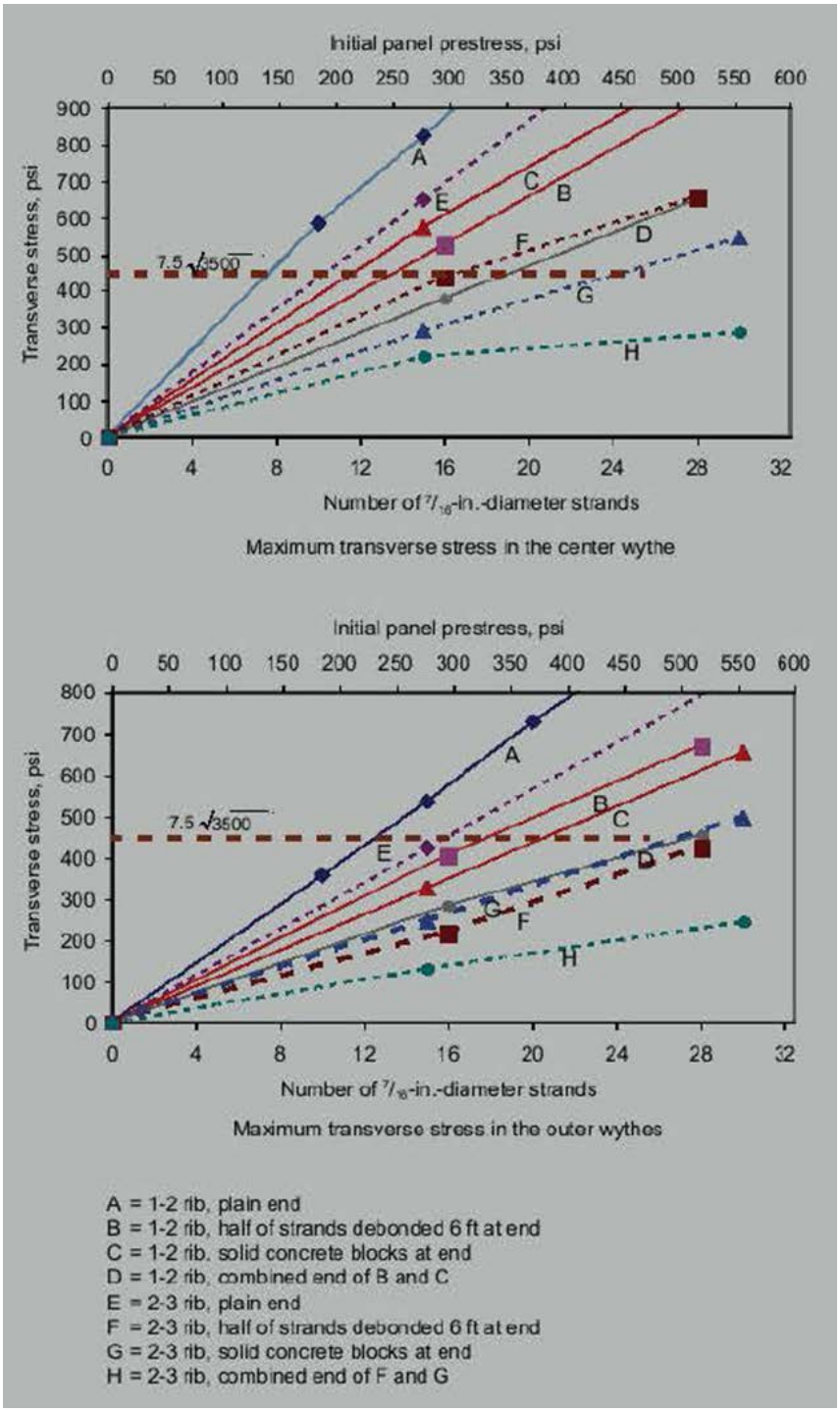

Figure 2-15 Maximum transverse stresses for various end conditions (Lee and Pessiki 2008)

2. The design for transverse bending stresses could be addressed by incorporating additional stiffness at either terminal of the panel (i.e. shear connector, debonded strands, or discontinuous concrete ribs).
3. A correlation existed between the experimental results and FEM analysis, indicating that the FEM analysis could be used to predict cracking.
4. Design codes of the day proved sufficient for three-wythe panel design,
5. A T-beam approach was recommended to predict flexural capacity.
6. Transverse stresses could be checked using
7. Figure 2-15.

Pantelides et al. (2008) sought to determine the adequacy of a new hybrid glass fiber-reinforced polymer (GFRP) composite shell steel connector in PCSWPs. This connector mimicked the design of a steel truss in geometry, but utilized FRP in the web in place of steel. This greatly reduced thermal bridging through the panel. Other FRP connectors were also used in the research. Specimens were created using the FRP shear connectors and were laterally loaded to determine the stiffness of the panels. It was determined that for the panels tested, composite action was achieved with the FRP shear connectors. Pantelides et al. developed a bilinear approximation to predict the deflection at yield:

$$\Delta_{my} = \frac{\left(0.5P_y\right)a}{24E_cI_{cr}}\left(3L^2 - 4a^2\right) \qquad (2\text{-}19)$$

Where:

Δ_{my} = midspan deflection at yield

P_y = total applied load at yield

A = shear span

E_c = modulus of elasticity of the concrete

I_{cr} = moment of inertia of the fully-cracked section

L = clear span length

The elastic and plastic regions can be visually estimated from the results of their testing (Figure 2-16).

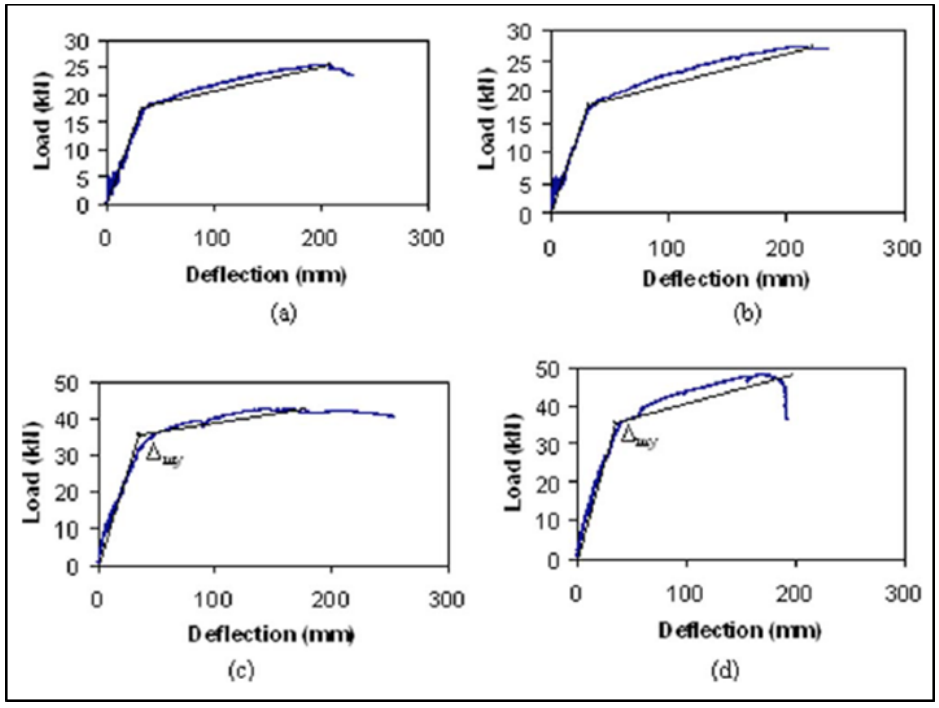

Figure 2-16 Lateral load vs mid-span deflection with analogy model: a) epoxy-cured GFRP single cage; b) urethane-cured GFRP single cage; c) epoxy-cured double cage; and d) urethane-cured double cage (Pantelides et al. 2008)

2.1.4 2011-Present

Naito et al. (2011) performed research on non-load bearing sandwich panel walls that is considered one of the most comprehensive studies done on PCSWPs. Naito et al. tested fifty-six full-scale specimens to failure using a variety of connectors including metallic, carbon fiber-reinforced polymer (CFRP), and GFRP shear connectors. The research covered both prestressed and regular reinforced concrete wythes, and both structural and non-structural scenarios were also considered. Wythe configurations had various symmetries and also asymmetries. Fully-composite, partially composite, and non-composite shear ties were tested. Three different insulation types were tested as well. For every configuration, the test was duplicated either two or three times depending on material availability, with 21 different configurations in total. The specimens were constructed off sight and transported to the testing facility. For this reason, concrete types varied significantly. Various pre-casting companies helped to fabricate the specimens. Every specimen configuration was accompanied by an idiosyncratic schematic. Every specimen was tested by applying an iterative loading sequence across the unsupported length of the panel (see Figure 2-17). End conditions were considered pin-and-roller during the experimental procedure. In reality, the specimen was not fixed in the longitudinal direction, but was fixed laterally. This was the case to ensure any panel deformation inconsistencies, or slip, could be measured (See Figure 2-18). Equation (2-20) shows the calculation for rotation at the support.

$$\theta = tan^{-1}\left[\frac{2\Delta_{mid}}{L}\right] \quad (2\text{-}20)$$

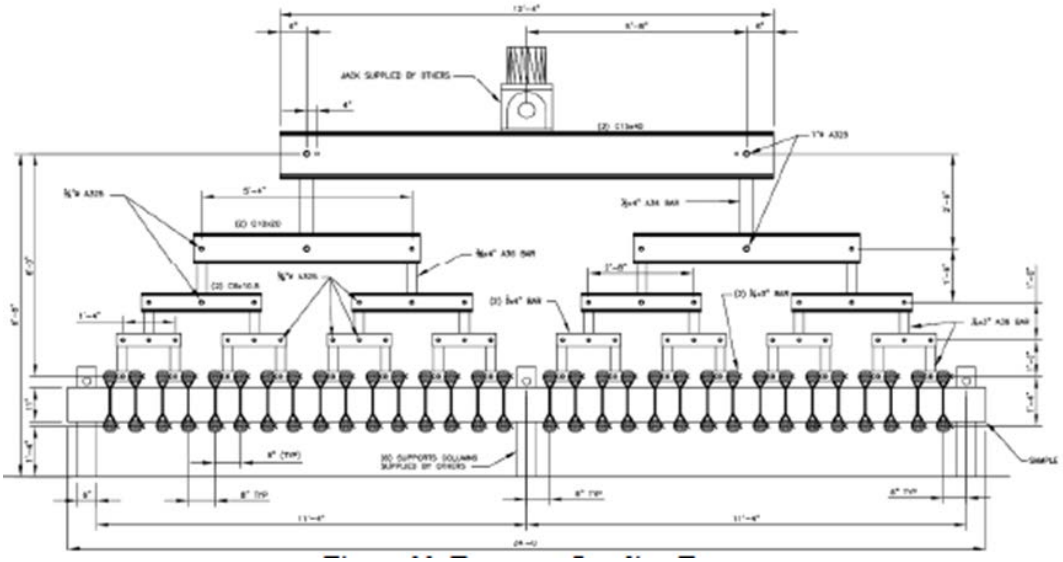

Figure 2-17 Loading pattern applying point loads across unsupported span of panel (Naito et al. 2011)

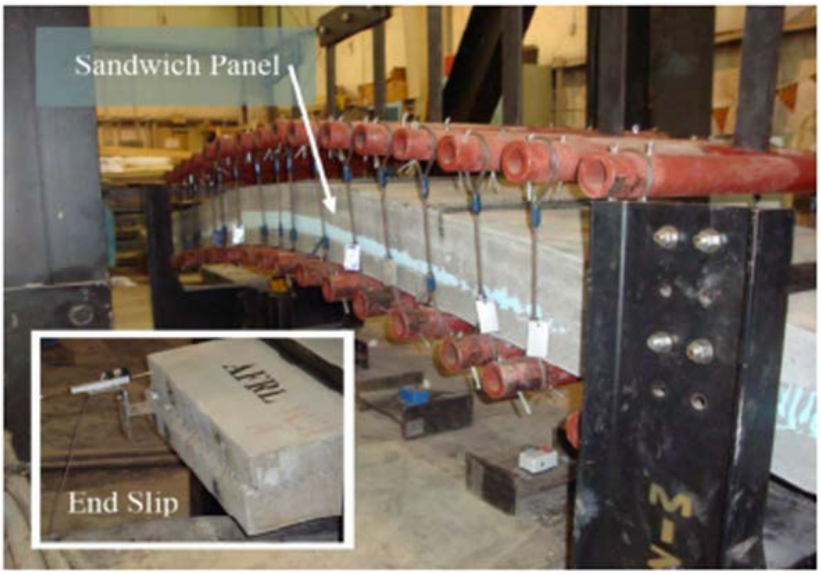

Figure 2-18 Photograph depicting the loading tree and end-slip measurement (Naito et al. 2011)

The load pattern was applied in order to simulate a uniformly distributed load. After loading each specimen to failure, plots were created displaying pressure vs. midspan displacement. Tabulated values of specimen name, age of concrete, max load, max pressure, corresponding displacement, east and west slip, boundary rotation, and measured moment capacity were also created for each specimen configuration. An example of specimen “PCS5” is included. Data from Figure 2-19 was also referenced by Bai and Davidson (Bai and Davidson 2015).

Specimen	Age at Test [days]	Max Load [lbs]	Max Pressure [psi]	Corresponding Displacement [in]	East Slip [in]	West Slip [in]	Rot. [deg]	Measured Moment Capacity [k-in]
PCS5-A	101	17770	4.628	4.765	0.527	0.604	4.541	266.55
PCS5-B	112	19910	5.185	5.118	0.500	0.562	4.875	298.65
PCS5-C	113	18252	4.753	5.536	0.633	0.637	5.272	273.78
	Average	18644	4.86	5.14	0.55	0.60	4.90	279.7

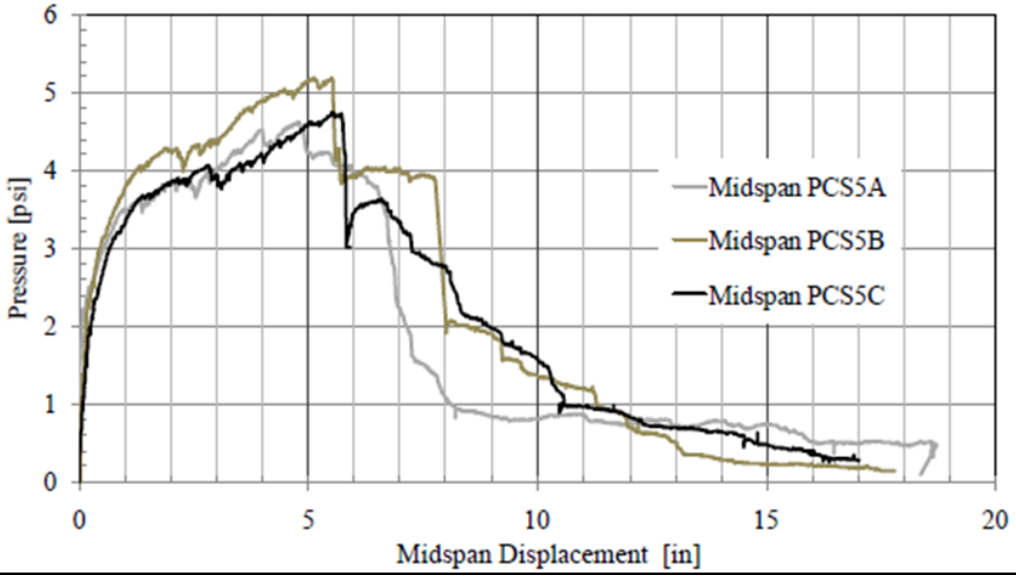

Figure 2-19 Data collected for Naito et al.'s testing of Connector B (Naito et al. 2011)

Frankl et al. (2011) researched behavior of PCSWP reinforced with CFRP shear grid connectors. This research was modeled after research performed by Naito et al. in the previous section, except that loading was performed vertically. Full-scale panels were tested by applying two equidistant point loads to generate a constant moment region across the midspan of the panel (See Figure 2-20). Similar plots were derived and strain profiles were generated. Frankl et al. included in their report several of the observed failure modes of the CFRP shear grid. The researchers implemented the following equation, Eq. (2-21), from Bischoff and Scanlon to determine the effective moment of inertia.

$$I_{eff} = \frac{I_{cr}}{1 - \left(\frac{M_{cr}}{M_a}\right)^2 \left[1 - \frac{I_{cr}}{I_g}\right]} \leq I_g \qquad (2\text{-}21)$$

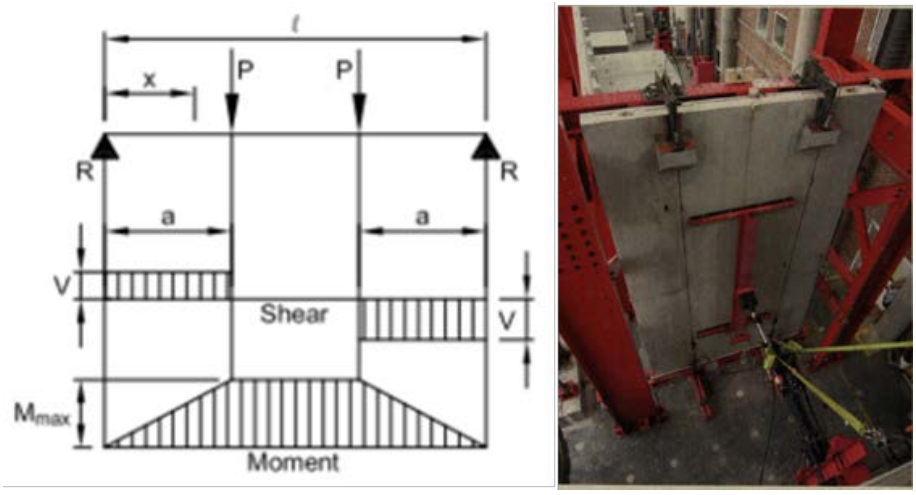

Figure 2-20 Shear and Moment Diagram from PCI Handbook (left) and testing of vertical panel (right) (Seeber et al. 2004; Frankl et al. 2011)

Another state-of-the-art paper was published by Losch et al. in the March 2011 PCI Journal regarding PCSWPs. Like many of the previous “State-of-the-Art” papers published by the PCI, this article highlighted many of the iconic PCSWP buildings constructed in the past decade. This article served the purpose of updating much of the current design procedures to include recommendations for FRP shear connectors and other pertinent information and findings of recent research. It goes into extensive detail about wythe thickness and prestressing strand sizing, wythe connectors, panel width thickness and span, bowing, flexural design, load bearing design, shear wall considerations, external connections, detailing considerations, thermal performance, manufacturing processes, product tolerances, transportation, erection and inspection of PCSWPs. This is the most recent document published by PCI regarding PCSWP design for engineers, though it is nearly identical to the standards presented in the PCI Handbook published in 2004 (Seeber et al. 2004). A few changes included consideration of fully-composite as well as non-composite shear connectors and there is also a lot more detail on panel connections.

Bunn (2011) published data on push-off specimens rather than full-scale specimens. The data collected considered vertical and transverse alignment of the connectors; foam to concrete interface bond variations; panels without shear connectors; panels with missing shear connectors; variations in panel dimensions, grid spacing, wythe thickness, and foam type. For every specimen tested, plots were generated displaying shear flow versus deflection. This was done to compare specimen and connectors stiffness. The design approach taken by Bunn, is to predict a Nominal shear flow capacity based on four variables and one constant. The equation is shown in Eq. 2-22.

$$q_n = \gamma_{type} * \gamma_{thickness} * \gamma_{spacing} * \gamma_{orientation} * q_{baseline} \quad (2\text{-}22)$$

Where:

q_n = Nominal shear flow capacity of grid, lb/in

γ_{type} = factor for insulation type (See Table 2-1)

$\gamma_{thickness}$ = factor for insulation thickness

$\gamma_{spacing}$ = factor for grid spacing

$\gamma_{orientation}$ = factor for grid orientation (either vertical or transverse)

$q_{baseline}$ = constant of 100 lb/in (based on the grids shear flow capacity)

Table 2-1 Table to determine factors for Equation (2-22) (Bunn 2011)

	γ_{Type}	Insulation Thickness (in.)	$\gamma_{thickness}$	Spacing (in.)	$\gamma_{spacing}$	Orientation	$\gamma_{orientaion}$	$q_{baseline}$
EPS	1.77	2	1.53	12	0.95	Vertical	1	100
		4	1.34	18	1.12			
		6	1.11	24	1.18	Transverse	0.8	
		8	1.11	36	1.56			
XPS	γ_{Type}	Insulation Thickness (in.)	$\gamma_{thickness}$	Spacing (in.)	$\gamma_{spacing}$	Orientation	$\gamma_{orientaion}$	$q_{baseline}$
	1.28	2	1.27	12	1.34	Vertical	1	100
				18	1.19			
		4	1.18	24	1.05	Transverse	0.8	
				36	0.99			

Equation (2-22) takes a relatively straight forward approach but was proven accurate when predicting the experimentally tested specimens. The equation was optimized using a spreadsheet and derived from the test results collected from the experimental program.

Woltman, Tomlinson, and Fam (2013) investigated the performance of non-composite GFRP shear connectors. The connector tested was simply a GFRP dowel, which is deformed on either end to achieve sufficient embedment in the outer concrete wythes in a push-off specimen (Figure 2-21). The setup allowed the concrete to be poured monolithically.

Figure 2-21 Push-off Specimen cured (left) and before concrete poured (right) (Woltman et al. 2013)

Push-off specimens were tested to failure, load and deflection were measured and plotted to compare stiffness. Woltman et al. makes significant observations regarding the modes of failure. The specimens experienced both strong and weak axis failures of the connector, cracking of the concrete embedment, as well as dowel action of the GFRP dowel (See Figure 2-22).

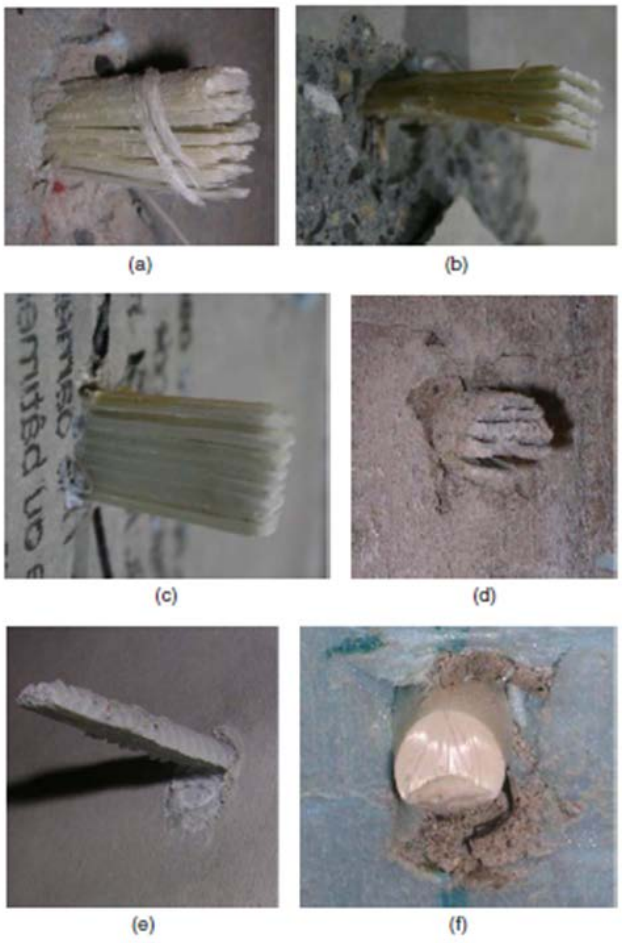

Figure 2-22 Observed failure modes in SWP: a) weak axis and b) strong axis fracture, c) dowel action, d) concrete cracking, e) polymer brittle fracture (Woltman et al. 2013)

Woltman et al. (2013) were able to create an analytical model that explained the behavior of the FRP shear connectors and also correlated the dowel shear strength based on the thickness of the insulation, observing that shear strength is reduced as thickness increases. It was determined that if flexural failure governs, then Eq. (2-23) ought to be used. If shear failure governs, however, then Eq. (2-24) would be appropriate.

$$M = \frac{2If_u}{D} \tag{2-23}$$

$$\tau_{mas} = k\frac{V}{A} \tag{2-24}$$

Where:

M = governing moment of the connector

I = cross-sectional

f_u = flexural capacity of the GFRP connector

D = the diameter of the GFRP connector

τ_{max} = governing shear stress of the connector

k = shape factor (1.33 for round connectors)

A = cross-sectional area of the connector

V = $2M/X$

M = governing moment of the connector

X = thickness of the foam wythe

It was determined that for the non-composite shear connectors the load displacement curves have an initial elastic peak response due to the added shear strength of the foam-concrete interface bond. After this bond deteriorates, the connectors begin to plasticize and form longitudinal cracks. A rapid and significant deformation takes place at this instant. Because of this plasticization, the response continues, but at a reduced stiffness. Once ultimate capacity is reached, the load gradually decreases as connectors fail one by one. As previously stated, the connectors fail mostly by delamination or dowel action.

Bai and Davidson (2015) analyzed partially composite, foam-insulated, concrete sandwich structures to derive mathematically the correlation between the degree of composite action (for partially composite panels) and the combined stiffness of the shear connectors within the panel. They did this to predict bearing and flexural behavior of PCSWPs. Bai and Davidson derived the non-trivial mathematical solution to predict deflection, bending moment, axial force, slip between wythes, and middle layer shear stress. These equations are as follows:

Panel Deflection:

$$y_1 = \frac{5}{384}\frac{qbl^4}{E_w I_{total}}\left[1 - \frac{24}{5}\left(\frac{x}{l}\right)^2 + \frac{16}{5}\left(\frac{x}{l}\right)^4\right] \ldots$$
$$+\frac{1}{16}\frac{qbl^4}{E_w I_{total}}\left(\frac{\alpha}{\beta}\right)^2\left(\frac{2\beta}{\chi l}\right)^2\left[\left(\frac{2\beta}{\chi l}\right)^2\left(\frac{cos\,h\left(\frac{\chi}{\beta}\right)\chi}{cos\,h\left(\frac{\chi l}{2\beta}\right)} - 1\right) + \frac{1}{2}\left(1 - \left(\frac{2\chi}{l}\right)^2\right)\right] \quad (2\text{-}25)$$

$$y_2 = \pm\frac{q}{4k} \quad (2\text{-}26)$$

$$y_3 = \pm\frac{\sqrt{2}}{2}\frac{qbl}{E_w I_{toatl}}\frac{l_0}{\beta^2}\frac{1}{\Psi}\left(\phi_1^0\phi_1 + \phi_3^0\phi_3\right) \quad (2\text{-}27)$$

$$\begin{cases} y^{ex} = |y_1| + |y_2| + |y_3| \\ y^{in} = |y_1| - |y_2| - |y_3| \end{cases} \tag{2-28}$$

Bending Moment:

$$M1=18qbl2\alpha22\beta\chi l21-cosh\chi\beta\chi cosh\chi l2\beta+12\beta21-2\chi l2 \tag{2-29}$$

$$M2=0 \tag{2-30}$$

$$M3=-24abl2l0l1\psi\ \phi30\phi1+\phi10\phi3 \tag{2-31}$$

$$Mex=M1-M3Mex=M1+M3 \tag{2-32}$$

Axial Force:

$$N_1 = \frac{1}{8}\frac{qbl^2}{r}\ \alpha^2 \left[-\left(\frac{2\beta}{\chi l}\right)^2 \left(1 - \frac{\cosh\left(\frac{\chi}{\beta}\right)\chi}{\cosh\left(\frac{\chi l}{2\beta}\right)} \right) + \frac{1}{2}\left(1 - \left(\frac{2\chi}{l}\right)^2 \right) \right] \tag{2-33}$$

$$N_2 = 0 \tag{2-34}$$

$$N_3 = 0 \tag{2-35}$$

$$\begin{cases} N^{ex} = -|N_1| \\ N^{ex} = |N_1| \end{cases} \tag{2-36}$$

Slip Between Wythes:

$$\phi = \frac{1}{4}\frac{qrbl^3}{E_w I_{total}} \left(\frac{2\beta}{\chi l}\right)^2 \frac{1}{\beta^2} \left[\frac{2\beta}{\chi l}\left(\frac{\sinh\left(\frac{\chi}{\beta}\right)\chi}{\cosh\left(\frac{\chi l}{2\beta}\right)} \right) - \frac{2\chi}{l} \right] \tag{2-37}$$

Middle Layer Shear Stress:

$$\tau = \frac{1}{4}\frac{ql}{r}\alpha^2\left[\frac{2\beta}{\chi l}\left(\frac{\sinh\left(\frac{\chi}{\beta}\right)\chi}{\cosh\left(\frac{\chi l}{2\beta}\right)}\right) - \frac{2\chi}{l}\right] \quad (2\text{-}38)$$

Where: y_1, y_2, *and* y_3 = deflection cases used for super-position

M_1, M_2, *and* M_3 = moment cases used for super-position

N_1, N_2, *and* N_3 = axial force cases used for super-position

y^{ex} = external deflection

y^{in} = internal deflection

M^{ex} = external bending moment

M^{in} = internal bending moment

N^{ex} = external axial force

N^{in} = internal axial force

Φ = slip between wythes

τ = shear stress in the middle layer

q = lateral pressure applied to the face of the wythe

k = vertical compressive stiffness of middle wythe

b = wythe width

d = thickness of wythe

l = span length

l_0 $= \sqrt[4]{E_w \cdot \frac{i}{2k} \cdot b}$

$i = 2 \cdot I_{sgl}$

$I_{sgl} = \frac{bd^3}{12}$ = moment of inertia of each wythe

E_w = moduli of elasticity of wythes

I_{Total} = $2I_{sgl} + 2r^2A$ = moment of inertia of the whole cross-section

A = cross-sectional area of wythe

χ $= \sqrt{\frac{2Kb}{E_w A}}$

K = shear stiffness of the middle layer

α $= \sqrt{\frac{2r^2 A}{I_{total}}}$

β $= \sqrt{1 - \alpha^2}$

k = vertical compressive stiffness of middle layer

Ψ $= \phi_1^0(\phi_2^0 + \phi_4^0) - \phi_3^0(\phi_2^0 + \phi_4^0)$

$\phi_1{}^0 = \cos\lambda \cdot \cosh\lambda$

$\phi_2{}^0 = \cos\lambda \cdot \sinh\lambda$

$\phi_3{}^0 = \sin\lambda \cdot \sinh\lambda$

$\phi_4{}^0 = \sin\lambda \cdot \cosh\lambda$

$\lambda = \frac{\sqrt{2}}{4}\left(\frac{l}{l_0}\right)$

ϕ_1 $= \cos\varepsilon \cdot \cosh\varepsilon$

ϕ_3 = $\sin \varepsilon \cdot \sinh \varepsilon$

r = distance from neutral axis of wythe to the overall neutral axis

Predicted panel behavior was then compared to observed behavior from Naito's 2011 research (Naito et al. 2011), where most predictions were relatively close, though some were significantly inaccurate (See Figure 2-23).

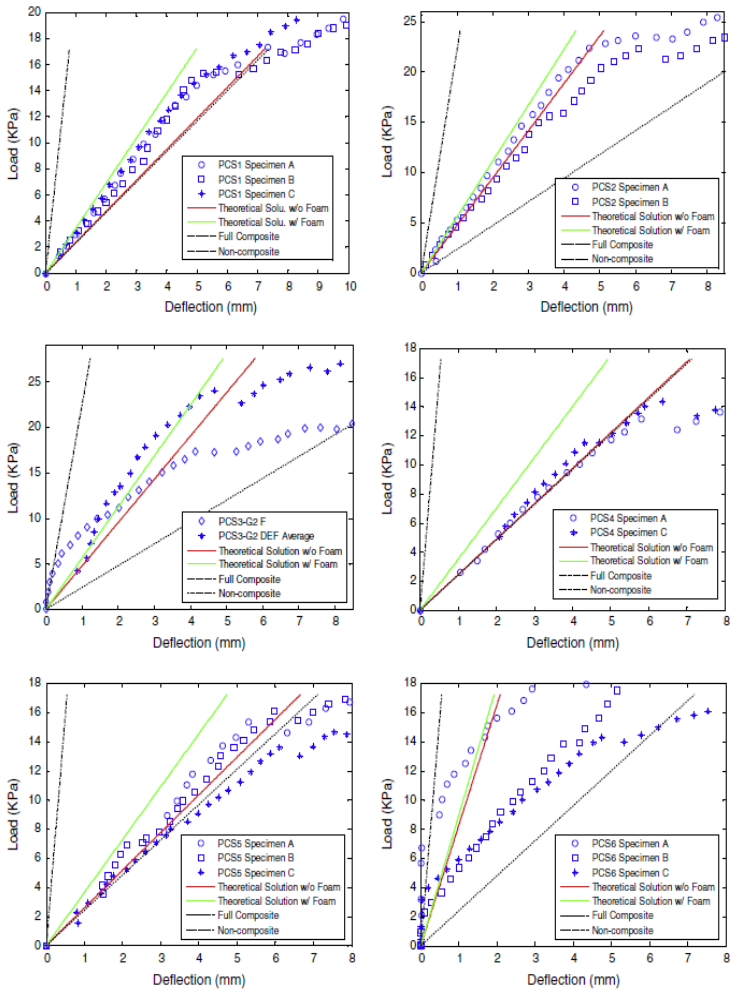

Figure 2-23 Naito et al.'s data (2011) vs Bai and Davidson's predictions (Bai and Davidson 2015)

2.2 Composite Action

Composite action is a principle that describes the degree to which two or more independent bodies cooperate to accommodate a specified loading scenario. The principle of composite action is used to design composite beams (beams which are made up of multiple materials) and reinforced concrete, but more applicable to this research, it is also used to design sandwich panel walls. Sandwich panel walls can be designed as fully-composite, partially composite, or non-composite. Composite action occurs when there is a shear transfer mechanism which transfers load from one element to another. Essentially a shear transfer mechanism creates a point of fixity or partial fixity between two interfaces.

From the history of PCSWPs, it is apparent that the creation of the concrete sandwich panel wall was intended entirely for thermal purposes. The structural capacity of these elements was not fully realized for many more years. Designing PCSWPs to be 100% composite is still a major challenge today. It is currently unknown how to design for partial composite action.

2.2.1 Thermal Efficiency

Thermal efficiency has been the main goal of PCSWPs since their inception. However, previous research has shown that there is room for improvement. The goal is to achieve as much thermal resistance as possible to prevent heat transfer from one side of the panel to the other. It is clear that the most efficient system currently achievable would be to have no steel penetrate the insulating layer, and eliminate as much steel as possible

throughout the panel. There has been much research on different materials to use as shear connectors, the most successful of which are FRP based materials.

The most attractive characteristic for constructing PCSWPs are that they are an environmentally friendly, thermally efficient, and cost effective solution as a building envelope. Primarily, they serve as a thermally resistant building envelope. By improving their thermal performance, the desire to integrate these elements into all buildings increases. Though there are already significant economic incentives for taking advantage of the structural capacity of PCSWPs, they need to be thermally exceptional to optimize their benefits and make PCSWPs more marketable.

2.3 FRP Shear Transfer Mechanism

Shear transfer mechanisms, also known as shear connectors, are elements that tie the concrete wythes together. This fixity prevents independent association of structural elements. If the elements are fully-composite, this forced interaction requires equivalent load distribution and strain compatibility. As discussed in the history portion of this report, these connectors have varied greatly from simple steel pins to FRP trusses. Compared to steel, GFRP has a higher tensile strength while being 75% lighter. It is both electrically and thermally non-conductive. There are many different ways to form, or mold, GFRP. It can be extruded, injected, or woven. The different manufacturing processes create different structural properties.

2.3.1 Mold Injected GFRP

Mold injected GFRP becomes very brittle due to the random alignment of fibers within the component. There are many advantages to mold injecting GFRP. It is

extremely cost effective when compared to other processes. Molding is a very fast process when compared to extruding or weaving. The constraints on shape are almost nonexistent.

2.3.2 Extruded GFRP

When GFRP is extruded, all the fibers are aligned in the same direction and essentially “cast” in the polymer. This polymer can be many different things but is usually epoxy based. When the fibers are all aligned, the component becomes ductile because all of the fibers are being loaded in the same direction. Fiber alignment can be optimized to accommodate many different loading scenarios as long as the loading scenario is known previous to design. When GFRP is extruded, the component develops a strong and weak axis. If the component is loaded parallel to the alignment of the strands, it is extremely strong. If the component is loaded perpendicular to the alignment of the strands, it is less-strong. The extrusion process is difficult and time consuming causing individual component costs to rise dramatically. The shape of the component with extruded GFRP simply requires a homogenous cross-section perpendicular to the fiber alignment. After the component is cast in polymer, additional machining may take place to create the desired final product. For the purpose of creating a shear connector, machining is performed to create the necessary deformations to embed the connector into the concrete.

2.3.3 Weaved GFRP

The last common manufacturing process is weaving. To weave GFRP, you must align the fibers in the desired pattern. This is done with either a machine, or often by

hand. The fibers are frequently situated loosely, if the fibers were stretched tightly, the desired shape may become unattainable. After the fibers are placed in the desired configuration, the polymer is poured around the fibers and allowed to cure. This process is advantageous, especially when the desired outcome is dependent on fiber alignment, and that alignment is not continually parallel throughout the component. For the application of this project to PCSWPs, the most common application of weaving GFRP results in a truss like configuration. This is because elements within the component are designed to experience different forces (compression and tension) at different times. This requires the fibers to be aligned, but in various directions. Weaving is time consuming, and therefore expensive. Another downside to this procedure is that components are not going to be identical every time. The standard deviation of the product is very large.

2.4 Design Methods

As noted in Section 2.1, the design methods for PCSWPs have varied greatly over time. As with any building element, the longer it has been in use, the greater our understanding of the product becomes, consequently leading to an increase in building regulations. A history of the design of PCSWPs was covered in Section 2.1. In most studies presented in that section, the number of shear connectors was never addressed. There are three methods that address this issue. These are the principles of mechanics, the ACI simplified method, and the PCI method.

2.4.1 Principles of Mechanics

Using the principles of mechanics, the analogous shear force, τ, can be obtained for any given load. By applying the appropriate load factor, the design shear force can be

determined. This force is calculated at the concrete-foam interface, where the force is at an associated maximum (Figure 2-24).

$$\tau = \frac{V_{max} Q_t}{I_{total} b} \quad (2\text{-}39)$$

$$q_{req} = \frac{V_{max} Q_t}{I_{total}} \quad (2\text{-}40)$$

Where:

τ = maximum shear force to be transferred

V_{max} = maximum shear force due to the applied loading

Q_t = first moment of area above the concrete-foam interface

I_{total} = cross-sectional moment of inertia of the entire panel

b = width of the panel cross-section

q_{req} = maximum applied shear flow

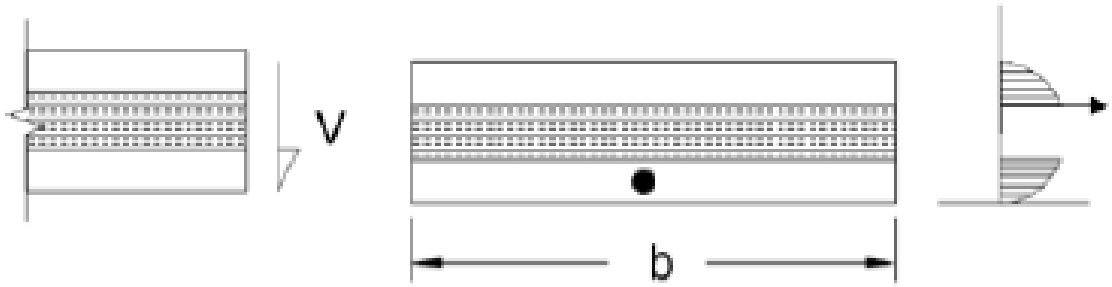

Figure 2-24 Evaluation of shear by principles of mechanics (Bunn 2011)

After the required shear flow, q_{req}, is obtained, calculating the number of required shear connectors equals:

$$N_{req} \geq \frac{q_{req}}{q_{connector}} \quad (2\text{-}41)$$

Where:

N_{req} = number of connectors required at a certain cross-section

q_{req} = from Eq. (2-40)

$q_{connector}$ = shear flow capacity of the connector

2.4.2 ACI Simplified Method

By ACI 318 (2014), shear stress, τ, is the maximum shear force acting on the panel. The shear stress acting at the concrete-foam interface is based on b*d, or the full effective cross-section. Because of this, shear flow is calculated as:

$$q_{req} = \frac{V_{max}}{d} \quad (2\text{-}42)$$

Where:

d = distance between resultant tension and compression forces (Figure 2-25)

By substituting the required shear flow associated with Eq. (2-42) into Eq. (2-41), one can determine the required number of shear connectors at any given panel cross-section.

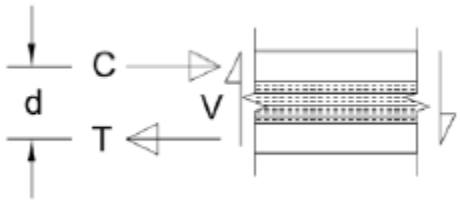

Figure 2-25 Definition of distance, d, from Eq. (2-42) (Bunn 2011)

2.4.3 PCI Method

The third method, requires that the full capacity of the panel be used when calculating the associated composite action. The shear stress, τ, is calculated at the maximum moment region (Seeber et al. 2004). It is allowed to use the lesser of the tension, T_{max}, or compression, C_{max}, forces when calculating the shear stress at the maximum moment region. Another assumption made, is that due to composite action, the entire depth of the exterior wythe is acting in compression. The required shear flow capacity, q_{req}, can be computed as follows:

$$V_{req} = \min \begin{cases} T_{max} \\ C_{max} \end{cases} \tag{2-43}$$

$$T_{max} = A_{ps} f_{ps} + A_s f_y \tag{2-44}$$

$$C_{max} = 0.85 f_c^{'} b t_c \tag{2-45}$$

$$q_{req} = \frac{V_{req}}{d_L} \tag{2-46}$$

Where:

A_{ps} = area of prestressing steel in tension wythe

f_{ps} = stress in prestressing strand

A_s = area of steel in tension wythe (excluding prestressing)

f = yield stress of steel in tension wythe (excluding prestressing)

f_c' = concrete compressive strength

b = width of cross-section

t_c = thickness of compression wythe

d_L = length of panel from M_{max} to the nearest support

Just as in the ACI method, one can determine the required number of connectors by substituting Eq. (2-46) into Eq. (2-41).

CHAPTER 3

EXPERIMENTAL PROGRAM

The experimental portion of this research was to test several different proprietary and non-proprietary FRP shear connector systems by fabricating and testing 49 small scale “push-off” specimens to apply direct shear to the connectors. By determining the shear load versus shear deformation behavior of each system at the specimen and associated component level, engineers can make more informed decisions about the full scale behavior of PCSPW’s.

3.1 Push-off Specimen Configurations

The push-off test specimens were all either 3-3-6-3-3 panels or 4-4-8-4-4 panels, with only connector spacing number changing per manufacturer recommendations. The

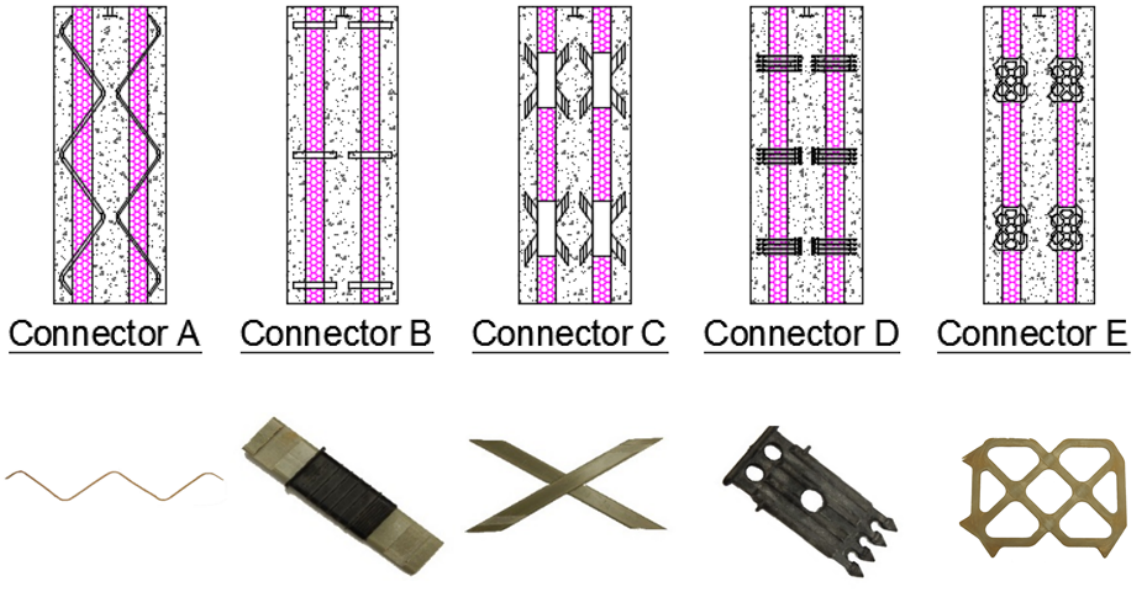

Figure 3-1 Push-off Specimen diagram and photographs of each connector

panels simulate two back to back 3-3-3 or 4-4-4 panels such that the connectors can be loaded directly in shear, rather than bending. Each specimen was 3 feet wide by 4 feet tall and contained a variety of connectors and configurations from five companies (A, B, C, D, and E) (see Figure 3-1). Each specimen was made up of three concrete wythes and two foam wythes. Foam types that were used include: Extruded Polystyrene (XPS), Polyisocyanurate (ISO), and Expanded Polystyrene (EPS). The concrete was reinforced concentrically with No. 3 grade 60 rebar spaced every 6 inches (exact spacing of rebar was contingent upon the accommodation of connectors).

3.2 Test Matrix

Table 1 presents the test matrix for the push off specimens. The matrix reflects three main variables: 1) connector type, 2) foam type, and 3) concrete/foam interface bond. The dashed lines in the table below exist because companies B and C do not supply expanded polystyrene foam with their connectors.

Each connector group tested was manufactured using Glass Fiber Reinforced Polymer (GFRP); however, not all companies used the same manufacturing process. Each Connector is discussed in detail in sections 3.2.1-3.2.5.

3.2.1 Connector A

Connector A is a pultruded GFRP truss (Section 2.4.3). For the push-off specimens in this thesis, connectors were designed to occupy a 48” section and varied in width depending on the thickness of the insulating wythe. Four connectors were evenly spaced throughout each specimen, two in each wythe. Spacing of six inches off of center was recommended by the manufacturer and was used as the spacing in this report. Figure

Table 3-2 Test Matrix for Five-Wythe Push-Off Specimens

TEST MATRIX FOR FIVE-WYTHE PUSH-OFF SPECIMENS							
			A	B	C	D	E
Foam Type	Wythe	Bond					
Expanded Polystyrene (EPS)	3"	B	AEPS3B	-*	-*	DEPS3B	EEPS3B
		UB	AEPS3UB	-*	-*	DEPS3UB	EEPS3UB
	4"	B	AEPS4B	-*	-*	DEPS4B	EEPS4B
		UB	AEPS4UB	-*	-*	DEPS4UB	EEPS4UB
Extruded Polystyrene (XPS)	3"	B	AXPS3B	BXPS3B	CXPS3B	DXPS3B	EEPS3B
		UB	AXPS3UB	BXPS3UB	CXPS3UB	DXPS3UB	EEPS3UB
	4"	B	AXPS4B	BXPS4B	CXPS4B	DXPS4B	EEPS4B
		UB	AXPS4UB	BXPS4UB	CXPS4UB	DXPS4UB	EEPS4UB
Polyisocyanurate (ISO)	3"	B	AISO3B	BISO3B	CISO3B	DISO3B	EEPS3B
		UB	AISO3UB	BISO3UB	CISO3UB	DISO3UB	EEPS3UB
	4"	B	AISO4B	BISO4B	CISO4B	DISO4B	EEPS4B
		UB	AISO4UB	BISO4UB	CISO4UB	DISO4UB	EEPS4UB
*Fabricator does not use EPS with their system							

3-2 shows a blown up photograph of the connector. A detailed diagram of the push-off specimen is shown in Figure 3-3.

Figure 3-2 Connector A Close-up

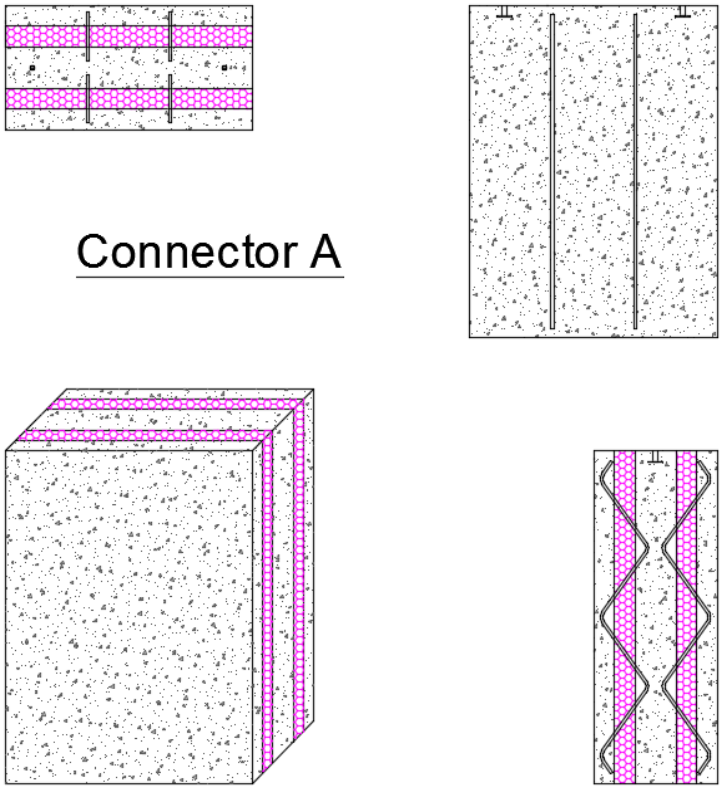

Figure 3-3 Detailed diagram of the push-off specimen design for connector A.

3.2.2 Connector B

Connector B is an extruded GFRP connector and is considered a structurally-composite connector (Section 2.4.2). The main structural component is an extruded GFRP bar, which requires notching a small section of material on each end such that the concrete is able to enable mechanical interlock with the connector. The connector is designed for a 2 inch embedment length in the concrete wythes. See Figure 3-4 for a photograph of the connector.

Figure 3-4 Connector B Close-up

Twelve connectors were used in each specimen, six in each wythe. Two rows of three were spaced nine inches from center leaving nine inches of cover to the outside edge of the panel (see Figure 3-5).

3.2.3 Connector C

Also an extruded GFRP product, connector C uses extruded GFRP bars, oriented in an X shape. Connector C is actually the combination of two independent connectors, similar to Connector B, embedded into the concrete. The combination of the two independent connectors that form an "X," will be considered one connector. See Figure 3-6 for a close up photograph of connector C. As with Connector B, this GFRP connector required post extrusion machining to enhance mechanical interlock with the concrete. Eight connectors were placed in each specimen, with four specimens inserted in each

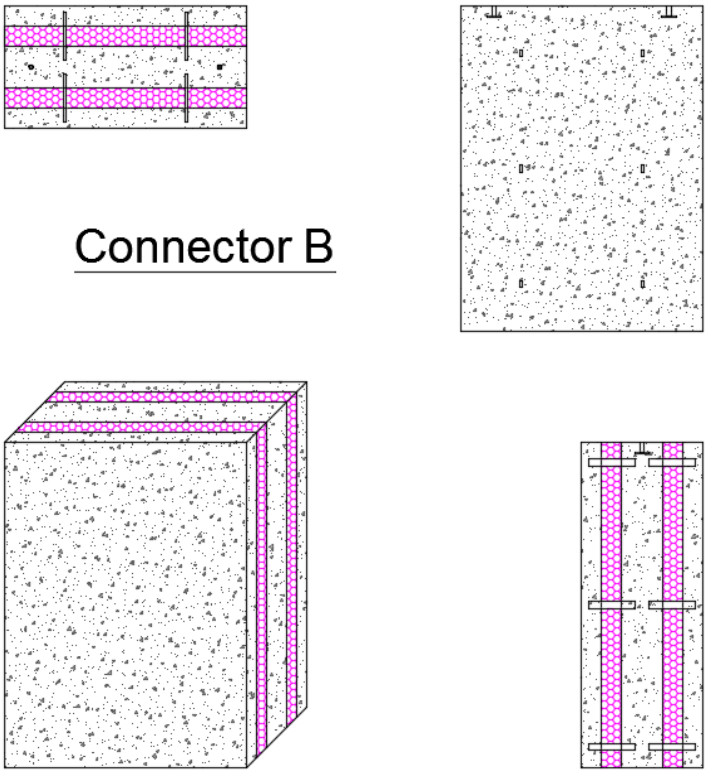

Figure 3-5 Detailed diagram for push-off specimen for connector B.

Figure 3-6 Connector C Close-up

wythe. There were two rows of two connectors, each spaced nine inches from center (See Figure 3-7).

3.2.4 Connector D

Connector D is a mold injected GFRP product (Section 2.4.1) that has randomly aligned and distributed glass fibers in a thermoplastic matrix. Connector D is designed for 1.5 inch embedment into a concrete wythe and is 3 inch wide and $\frac{1}{2}$ inch thick. Connector D has an asymmetrical design developed for construction efficiency (see Figure 3-8)

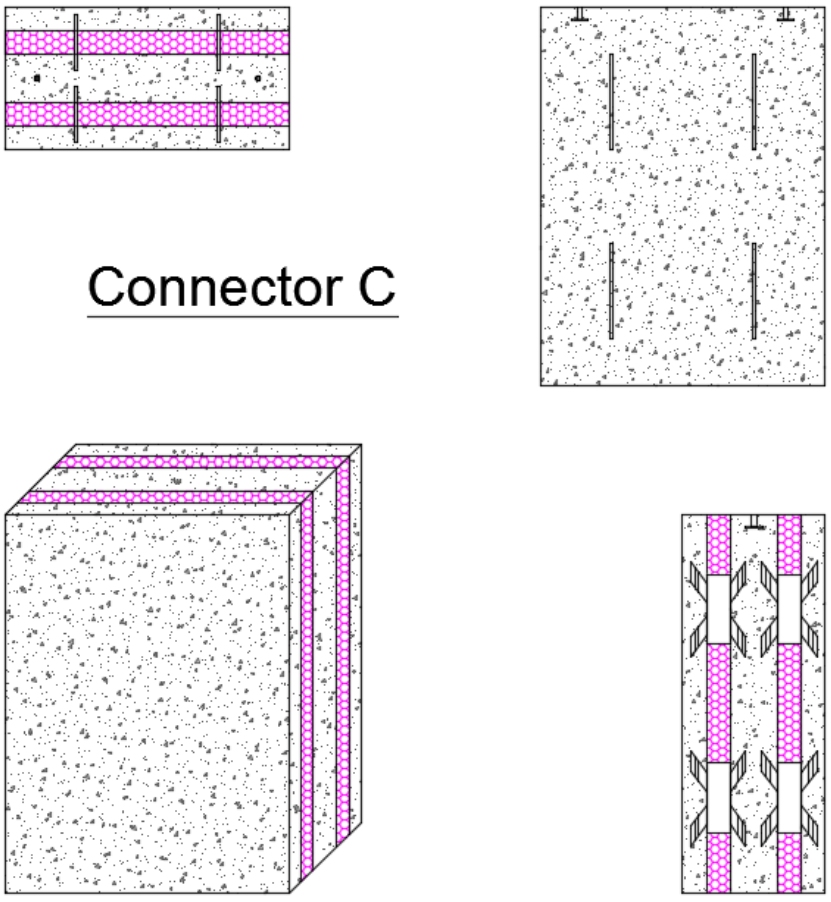

Figure 3-7 Detailed diagram for push-off specimen for connector C.

Figure 3-8 Connector D Close-up

Mold injection greatly reduces the cost of each connector and can be produced on demand for each individual job. For this thesis, twelve connectors were used in each specimen. Connectors were spaced at two rows of three, each spaced nine inches from center, per the manufacturers' recommendation (see Figure 3-9).

3.2.5 Connector E

Connector E is a hand woven GFRP shear connector. Pultrusion is the fabrication method of choice because of the change in fiber alignment throughout the connector. This connector is designed like a small truss (see Figure 3-10). It is five inches wide, seven inches long, and one-eighth inch thick. Four connectors were used in each wythe, eight connectors per specimen. Each row of two connectors was spaced nine inches off of center (refer to Figure 3-11).

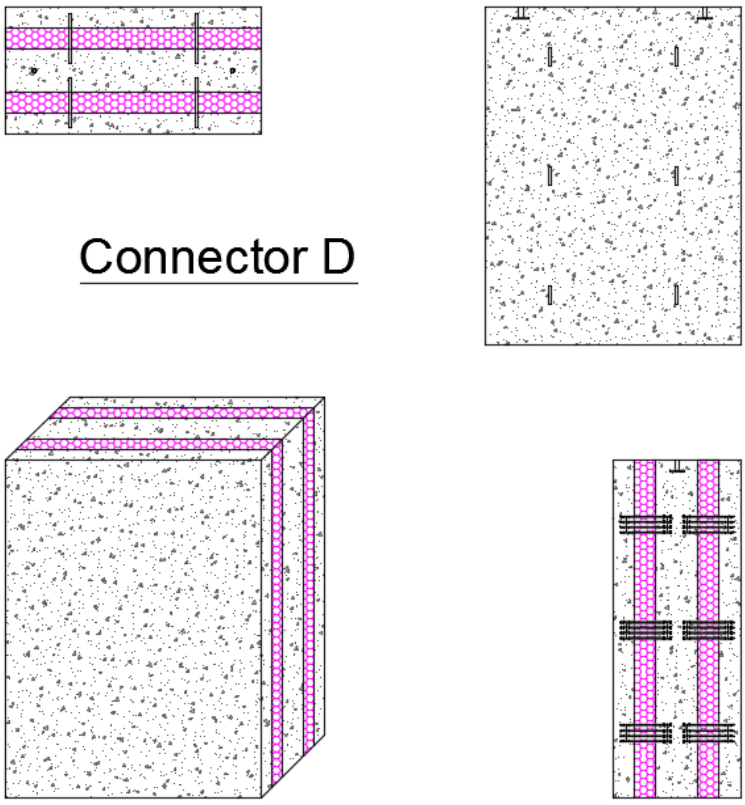

Figure 3-9 Detailed diagram for push-off specimen for connector D.

Figure 3-10 Connector E Close-up

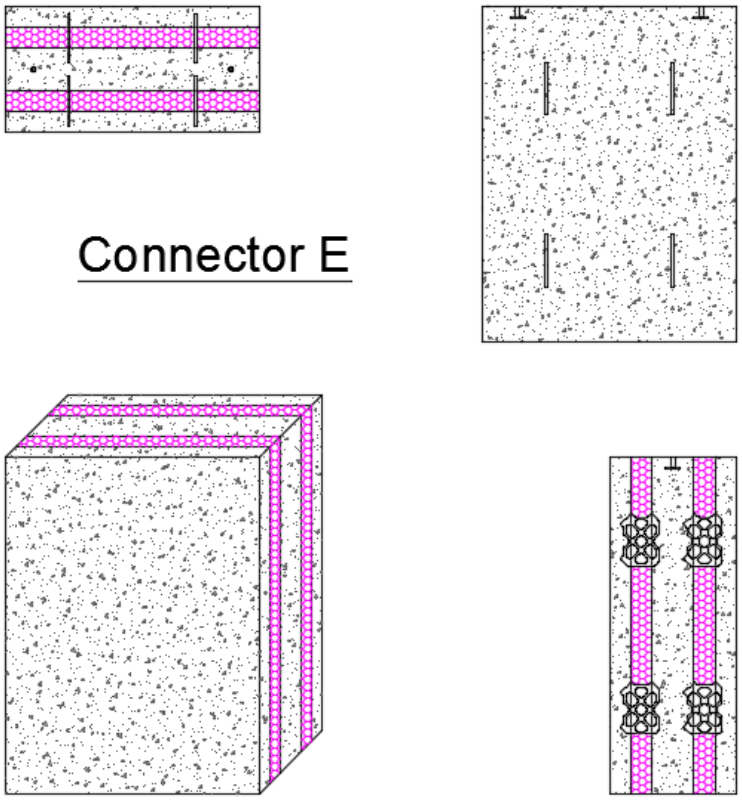

Figure 3-11 Detailed diagram for push-off specimen for connector E.

3.3 Construction of Wall Panels

Specimens were cast horizontally, one layer at a time. Forms were built out of HDO (high-density overlay) plywood and manufactured by Plum Creek Company. The first wythe was cast immediately followed by the insertion and vibration of the connectors and foam. The forms were stripped and taller forms constructed in their place. Once taller forms were in place, the center wythe was poured and immediately followed by the insertion and vibration of the connectors and foam. Forms would be stripped and the tallest forms would be constructed, after which the final concrete wythe would be cast. The unbonded specimens used a plastic sheet between the foam and concrete

surfaces to eliminate the bond. Once concrete strength was achieved (>4000 psi), the specimens were prepared for testing. In hind sight, the tallest forms should have been set up from the beginning and a custom screed constructed for each layer of concrete poured. This would have saved considerable construction time.

3.3.1 Form Setup

Initial form set up involved a floated formwork to keep the specimens supported off of the ground surface. This procedure was performed as a precaution to ensure that the specimens could be easily moved should the lifting anchors not perform as expected. The formwork was supported off of the ground 1.5 inches, every two feet. Form board was then placed on top of the boards to create the bottom of the form.

After the base of the form was constructed, the walls of the formwork were cut to the precise depth. For the 3-3-6-3-3 specimens, form boards were created with a 3 inch, 12 inch, and 18 inch depths. For the 4-4-8-4-4 specimens, boards were cut with a 4 inch, 16 inch, and 24 inch depth. For the initial pour, the three inch walls were fixed in place with a doug-fir-larch stud grade 2x4. Once walls were fixed around the perimeter, separators needed to be put in place to isolate each specimen. Separators were constructed with HDO plywood. They were fixed in place using one screw in each wall of the formwork. This only required minimal fixation because lateral pressures due to the wet concrete equalized on both sides of the wall. Special care was taken during placement of the concrete to ensure separator immobility, pressure equalization, and perpendicularity. After the separators were placed, forms were sprayed with form oil to

reduce chemical bond to the formwork, and allow for efficient form stripping of formwork.

3.3.2 Rebar Ties and Configuration

Tying rebar was done with a professional tie wire twister with looped tie wires (see Figure 3-12 & Figure 3-13). Rebar was spaced 6 inches from the edges and then every 12 inches where permissible.

Spacing was contingent upon accommodation of shear connector embedment. Rebar was supported on horizontal formwork using slab bolsters (exterior wythes) and rebar chairs (center wythe). Rebar was placed concentrically within each wythe.

3.3.3 Preparing to Pour

Prior to pouring the concrete, lifting anchors needed to be placed (center wythe only), foam needed to be prepared, and shear connectors needed to be staged for rapid placement into the wet mud. Preparations were also taken to allow for rapid, easy clean up. The pick points were recessed to ensure no conflict would arise during testing. In order to ensure pick-points would remain attached to the formwork during pouring, high strength glue was used to glue the rubber recess (the blue hemisphere in Figure 3-14) to

Figure 3-12 Professional Tie Wire Twister & Looped Tie Wires.

Figure 3-13 Tying rebar prior to inserting it in the formwork

Figure 3-14 Pick points attached to divider and centered within the middle wythe.

the separator. Special care was taken during casting to ensure the pick points were intact. This included a physical check after the concrete was poured prior to finishing.

Each pick point was made of steel and was capable of lifting 1.2 tons. Each specimen was equipped with two pick points symmetrically placed at the top of the specimen in the center wythe. A clutch was then used to lift the specimens and move them into place.

Foam needed to be prepared for placement. In the case of Connector A, this simply involved covering the unbonded specimens with plastic, making sure that the truss penetrated the barrier completely, as well as seaming the barrier discontinuities with duct tape (see Figure 3-15). Foam was shipped to the testing facility from the fabricator. The fabricator preinstalled the connectors and cut the foam to the specified dimensions.

For Connectors B, C, and D, the preparation phase involved placement of the bond inhibitor for unbonded specimens and insertion of connectors for all specimens. The foam used for Connectors B, C, and D was provided by the manufacturer. The foam

Figure 3-15 Seaming of the bond inhibitor using duct tape.

came pre-cut to dimension and include apertures for connector insertion. Connectors are shown inserted into foam in Figure 3-16.

For Connector E, foam was ordered independently of the connectors. Therefore, preparation of the foam required sizing the foam to correct dimension, creating apertures for connectors, and providing the bond inhibitor where applicable. The cutting was done with a hot knife, which had adequate precision, but was much less precise than the factory machined specimens sent from other fabricators. Connector E is shown placed in the foam after the casting of the first wythe in Figure 3-17.

Preparation of shear connectors prior to pouring involved nothing for connector A, insertion for connectors B, C, and D, and staging for connector E. In preparing for easy clean-up, a quartz-based sand was generously spread across the work area, under the form work. The sand acted as a barrier between the wet concrete and concrete floor upon which the forms were placed. Water containers were placed in various areas around the formwork to ensure all instrumentation and tools would be properly cleaned off after use. Tools were accounted for and placed in the work area where they would be easily accessible for fluidity of pour.

Figure 3-16 Left: Connector B, Middle: Connector C, Right: Connector D

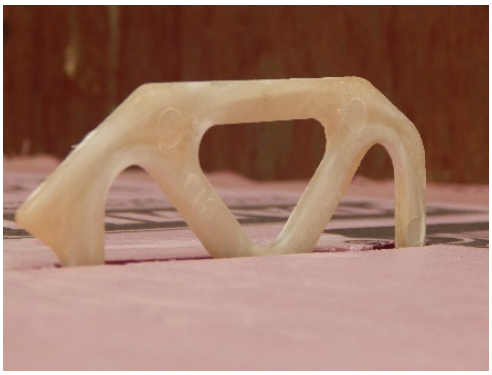

Figure 3-17 Connector E placed in foam.

3.3.4 Casting Concrete

Concrete was cast one wythe at a time. After forms were set, foam was prepared, and connectors staged, concrete was delivered and poured into the formwork. Special care was taken to ensure that the separators remained perpendicular to the base and stayed in place. Uneven lateral pressures were eliminated by manually equalizing the amount of concrete on either side of the separator. Concrete was vibrated into the forms using a pencil vibrator. A screed was drawn across the top of the formwork walls to ensure maximum volume occupancy. After the proper amount of concrete was in the formwork, a trowel was used to smooth the surface of the wet mud in preparation of placing the foam and connectors into the concrete.

Part way through the concrete pour, a sample was taken from the truck to create nine-4 inch diameter cylinders, and determine the unit-weight of the concrete. All of this was done according to the appropriate document published by the American Society for Testing and Materials; ASTM C143, ASTM C31, and ASTM C138 respectively.

Upon troweling the surface of the concrete foam was placed on top of the wet concrete and connectors were inserted into the wythe. After the connectors and foam were in place, a pencil vibrator was put in contact with every connector to ensure the concrete would adhere to the connector.

Once the concrete, foam, and connectors were all in place, special care was taken to clean off all equipment and surfaces. An example of the completed first layer can be seen in Figure 3-18.

After the concrete had set up, the walls of the formwork were removed (see Figure 3-19). It became very important that the formwork be very clean before the next

Figure 3-18 An example of a completed first layer. Concrete has been poured and foam and connectors have been put in place.

Figure 3-19 Freshly removed first layer of formwork. Scraping the hardened paste off of the concrete form base.

forms were put into place. Often this required scraping away at the hardened paste that would leak under the wall of the formwork during pouring (See Figure 3-19). After all of the concrete was loose from the form, an air hose was used to blow away any remaining debris.

After the formwork was clean, the second set of forms were fixed into place. This included the insertion of the rebar, propping the rebar on the chairs, and gluing the rubber recess for the pick point into place (see Figure 3-20). Attention was given to location of each specimen prior to burying it in cement. This was done to ensure that an unbonded EPS foam wythe containing Connector A, received an unbonded EPS foam wythe containing Connector A on top of the second wythe as an example.

Once the necessary preparations were made to pour the second wythe, concrete was ordered, and the same process used to construct the first wythe was repeated for the

Figure 3-20 Prepared second wythe. Rebar, pick points, and form work are all in place. Note: the caution tape is simply used to remove concrete quickly after pour.

second wythe, with one exception. Because the second wythe contained the lifting anchors, a physical check was performed to ensure that none of the pick points were removed during the pouring process. After the concrete cured, the formwork was removed (see Figure 3-21) and the last set of forms were put into place (See Figure 3-22).

After the formwork was in place and the necessary preparations were made, the process outlined for the first wythe was repeated, with the exception that there was no foam nor connectors to be placed within the top wythe. Because the exposed surface of the concrete is a final product, special care was taken to finish the concrete surface (see Figure 3-23). The finished product was allowed to harden before the forms were removed (see Figure 3-24).

Figure 3-21 Formwork removed after concrete for the second wythe is allowed to cure.

Figure 3-22 The highest set of forms is in place, ready to pour the last concrete wythe.

Figure 3-23 Taking special care to put a finished surface on the final wythe of the concrete.

Figure 3-24 Finished product waiting to cure.

3.3.5 Lifting and Storing Specimens

After the specimens cured for 7 days (from the third pour), removal from the form bed was permissible. This was done by removing the blue rubber recess, see Figure 3-14, exposing the head of the pick point. Once the head was exposed, the proprietary clutch was activated as shown in Figure 3-25. Up to this point, the specimen was horizontal (see Figure 3-26). Prior to lifting, the specimen was labeled with the appropriate code associated with the specimen from Table 1. The area was vacated to ensure the safety of the crane operator. Proper safety equipment was acquired. Once the specimen was lifted into the air (see Figure 3-27), it was transported to the storage area where it was allowed to cure for an additional 21 days, or until concrete strength was achieved.

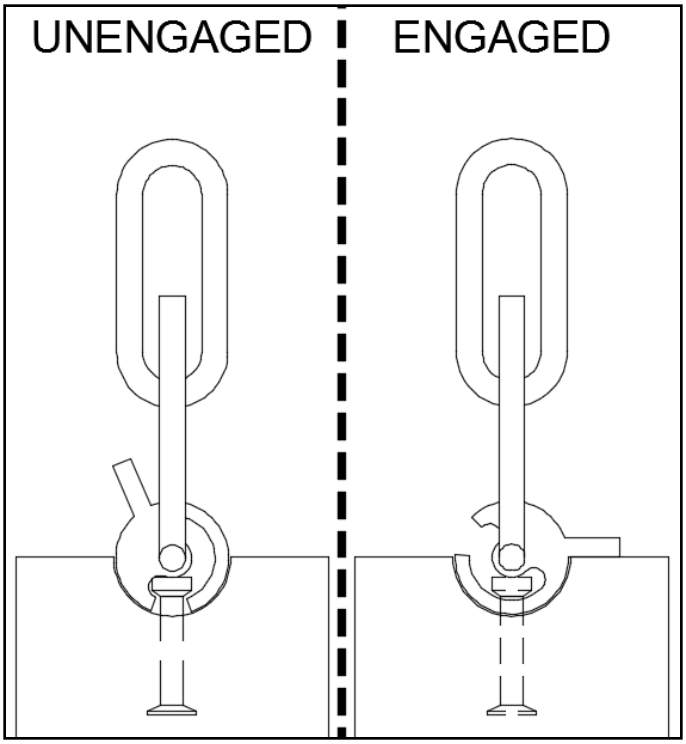

Figure 3-25 Activation of the clutch around the pick point.

Figure 3-26 Horizontal specimen ready to be lifted.

Figure 3-27 Specimen is vertical and ready for storage.

3.4 Material Properties

Due to limited material and budget, all of the specimens could not be poured at once. There were three different sets of specimens created using the same process. There were a total of nine pours (three pours per set, one pour for each wythe poured).

Concrete cylinder compressive tests were performed according to ASTM C39. Tabulated values of the material properties are shown in Table 3-3 below. Other pertinent information regarding the concrete used is tabulated in Table 3-4. These values are calculated from ACI 318-14 (American Concrete Institute, 2014). A visual comparison of the concrete compressive strength is shown in graphical form in Figure 3-28.

Table 3-3 Material Properties of Concrete

				Compressive strength (psi)			
Set	Pour	Slump	Unit Weight of Concrete	(Days of Curing)			
	(#)	(in)	$lb/(ft^3)$	28	14	7	3
1	1	9	138.79	5124.39	3736.49	1823.03	911.52
	2	7.5	139.80	5550.13	4152.13	2690.58	1345.29
	3	5	133.95	6264.74	4925.24	4134.74	2067.37
	Average	-	**137.51**	**5646.42**	**4271.29**	**2882.78**	**1441.39**
2	1	6.5	141.54	5861.28	4445.88	3402.88	1701.44
	2	7.5	134.70	5531.03	4184.03	2497.87	1248.93
	3	9.25	136.60	4979.96	3613.96	1593.76	796.88
	Average	-	**137.61**	**5457.42**	**4081.29**	**2498.17**	**1249.08**
3	1	8.5	139.65	5211.53	3815.03	2084.91	1042.46
	2	5	139.20	6195.50	4803.50	2766.32	1383.16
	3	6	138.65	5916.19	4529.69	3562.60	1781.30
	Average	-	**139.17**	**5774.41**	**4382.74**	**2804.61**	**1402.31**

Table 3-4 Material Properties of Concrete

Material Properties of Concrete				
	w_c	f'_c	f_t	E_c
Set	pcf	psi	psi	psi
1	137.51	5646.42	563.56996	3998690
2	137.61	5457.42	554.0578	3935487
3	139.17	5774.41	569.92137	4116901

3.5 Push Test Setup

The Push-off specimen test setup is illustrated in Figure 3-29. Push-off specimens were loaded by placing a ram and load cell on the wide center wythe and supported at the bottom of the outer wythes with concrete filled hollow structural section (HSS) tubes. The load was transferred to the specimen through a wide flange spreader

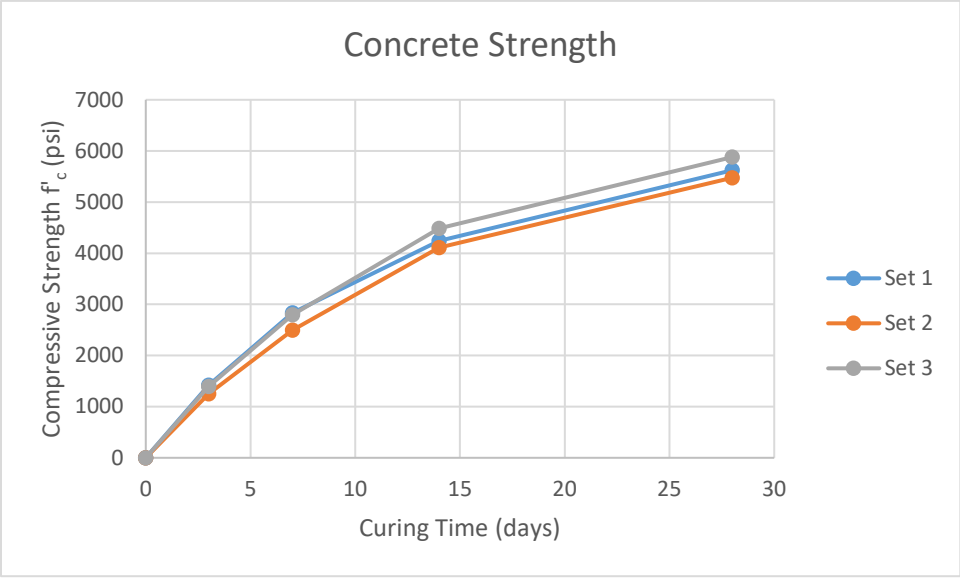

Figure 3-28 Graphical representation of the average concrete compressive strengths tabulated in Table 2.

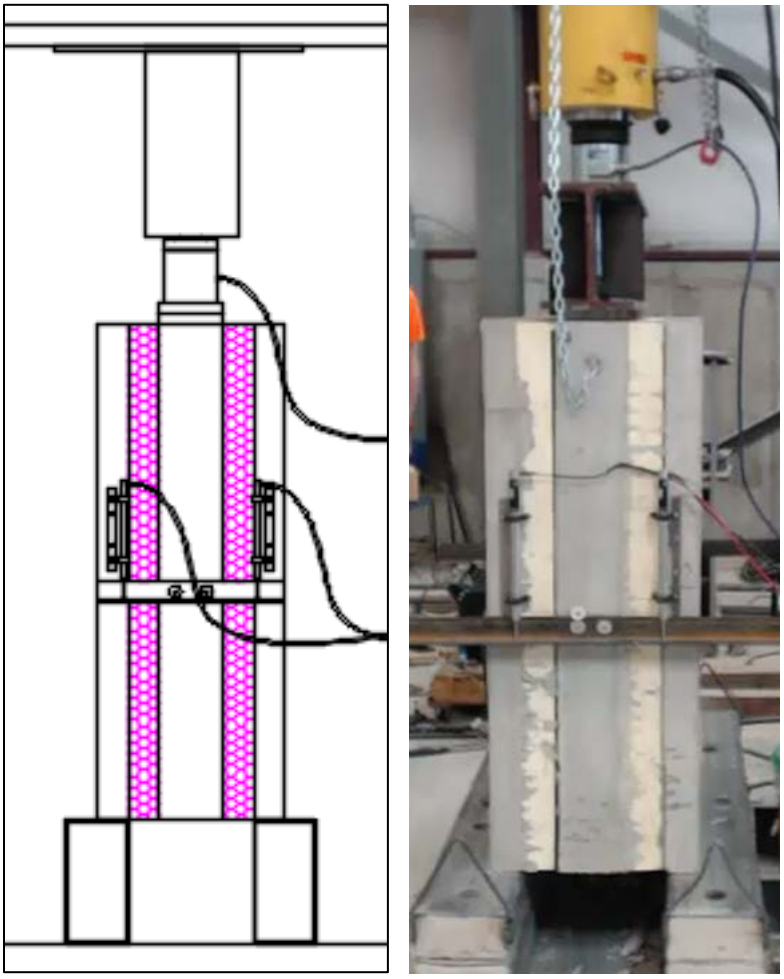

Figure 3-29 Diagram (left) and photograph (right) of test set up.

beam, which in turn passed the load into the specimen directly in line with the connectors. The specimen was supported only on the outer wythes at the bottom. Extra care was taken to ensure the specimen was flush on the supports. Relative displacement of the inner wythe to the outer wythes was measured in four places and averaged to determine the reported displacements. The Linear Variable Differential Transformers (LVDTs) were attached to the outer wythes using a custom built bracket (Figure 3-30 & Figure 3-31). Displacements were measured by fixing a small piece of mild steel to the

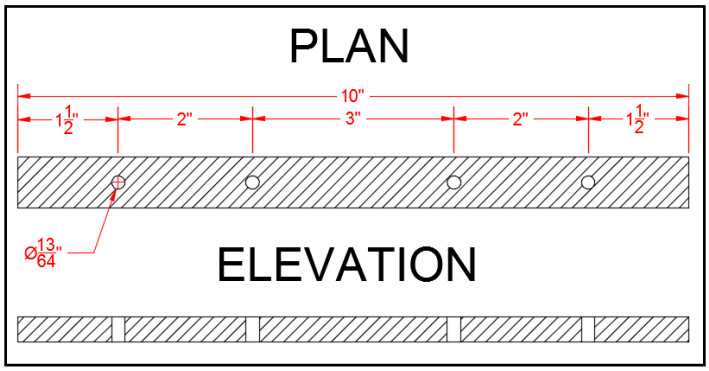

Figure 3-30 Specially designed mounting bracket used to attach LVDT's to specimen.

center wythe, providing a reference point for LVDT's to measure from (see Section 3.6). A load cell was placed at the ram-to-spreader beam interface to measure the overall applied load (see Figure 3-29). As a safety precaution, a loose chain was firmly attached

Figure 3-31 Special bracket fixed to the specimen. LVDT attached to the bracket using #10-32 machine screws.

to the center wythe to prevent catastrophic failure or related injury. Careful observation was given to the tautness of the chain. Never was the chain taut during loading.

3.6 Instrumentation

The LVDTs used for this testing were newly purchased with NIST traceable calibration in February 2015. The transducers were attached to the specimen using the specially fabricated bracket shown in Figure 3-30. The two holes closest to the left and right edges in the diagram, where threaded to accommodate a #10-32 machine screw. The inner holes were used to nail the bracket to the specimen. Nails were pounded using a .22 caliber powder actuated fastening tool. The bracket can be seen in use in Figure 3-31.

The Geokon load cell calibration was verified in February 2015 using a Tinius Olsen testing machine with NIST traceable calibration, last calibrated March 2014. The equipment used to collect data was the Bridge Diagnostics Inc.-Structural Testing System (BDI-STS).

3.6.1 Linear Variable Differential Transformer Locations

The Linear Variable Differential Transformers (LVDT) were mounted such that the contact point between the mild steel angle and the plunger of the LVDT was at the vertical midpoint of the associated wythe. There was an LVDT attached to the edge of each exterior wythe, to make a total of four shear displacement measurements. These measurements were averaged to determine the actual shear displacement of the center wythe relative to the exterior wythes.

CHAPTER 4

TEST RESULTS FOR PUSH-OFF TESTS

4.1 Introduction

In this study, 41 pure shear push-off specimens were created to evaluate the shear stiffness of the various commercially available sandwich panel wall shear connectors. This chapter presents the results of this testing. The variables studied were connector type, foam thickness, foam type and foam bond. This study included 5 different connectors. For convenience of data presentation, each connector was assigned a letter descriptor and are as follows: Nu-Tie connector (Connector A), Thermomass CC Connector (Connector B), Thermomass X Connector (Connector C), HK Composite Connector (Connector D), and Delta Tie (Connector E). Due to project constraints, only a single specimen of each type could be constructed so there is no statistical information available regarding the connector strength and stiffness values, making some comparisons difficult. Design, fabrication, and test setup for the push-off specimens is presented in the preceding chapter.

4.2 Material Testing

Concrete cylinder compressive tests were performed for all specimens tested. Due to limited material, space, and budget, all the push-off specimens could not be poured at once. Each specimen required three separate concrete pours (one per wythe), and specimens were created in three different sets due to space restrictions for a total of nine pours (three sets with three pours each). Cylinders were created from the concrete

midway through each pour. All concrete cylinders were 4-inch diameter, with compressive tests performed according to ASTM C39.

Tabulated values of the push-off specimen material properties are shown in Table 4-1 below with other pertinent information regarding the concrete shown in Table 4-2. These values are calculated from ACI 318-14 (American Concrete Institute 2014). A visual comparison of the concrete compressive strength is shown in graphical form in Figure 4-1.

Table 4-1 Material properties of concrete for push-off specimens

				Compressive strength (psi)			
Set	**Pour**	**Slump**	**Unit Weight of Concrete**	**(Days of Curing)**			
	(#)	(in)	(lb/ft^3)	28	14	7	3
1	1	9	138.79	5124.39	3736.49	1823.03	911.52
	2	7.5	139.80	5550.13	4152.13	2690.58	1345.29
	3	5	133.95	6264.74	4925.24	4134.74	2067.37
	Average	**-**	**137.51**	**5646.42**	**4271.29**	**2882.78**	**1441.39**
2	1	6.5	141.54	5861.28	4445.88	3402.88	1701.44
	2	7.5	134.70	5531.03	4184.03	2497.87	1248.93
	3	9.25	136.60	4979.96	3613.96	1593.76	796.88
	Average	**-**	**137.61**	**5457.42**	**4081.29**	**2498.17**	**1249.08**
3	1	8.5	139.65	5211.53	3815.03	2084.91	1042.46
	2	5	139.20	6195.50	4803.50	2766.32	1383.16
	3	6	138.65	5916.19	4529.69	3562.60	1781.30
	Average	**-**	**139.17**	**5774.41**	**4382.74**	**2804.61**	**1402.31**

Table 4-2 Material Properties of Concrete for push-off specimens

	w_c	f'_c	f_t	E_c
Set	pcf	psi	psi	psi
1	137.51	5646.42	563.56996	3998690
2	137.61	5457.42	554.0578	3935487
3	139.17	5774.41	569.92137	4116901

4.3 Push-off Test Results

Each push-off specimen was loaded through failure. Figure 4-2 presents an example Shear Load versus Shear Deformation plot. All load displacement curves had an initial elastic peak response. After this initial peak, the connectors began to exhibit

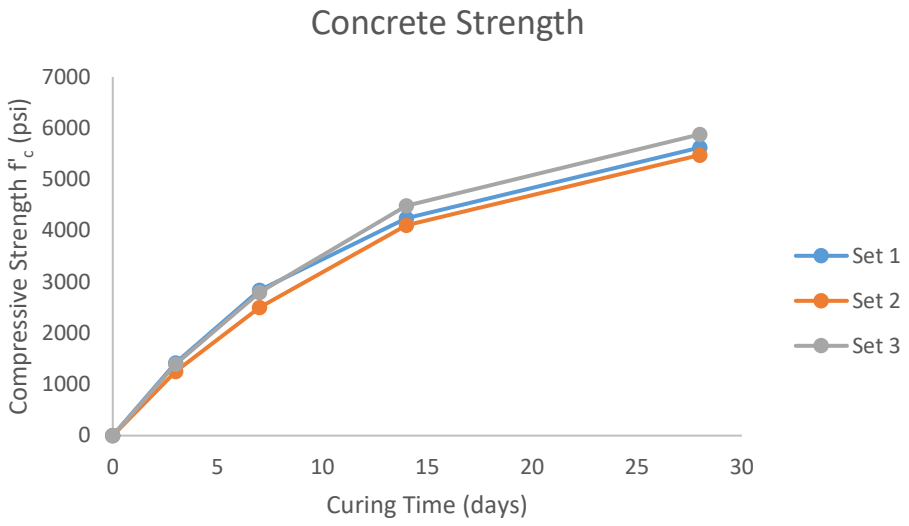

Figure 4-1 Graphical representation of average concrete compressive strengths in Table 4-2

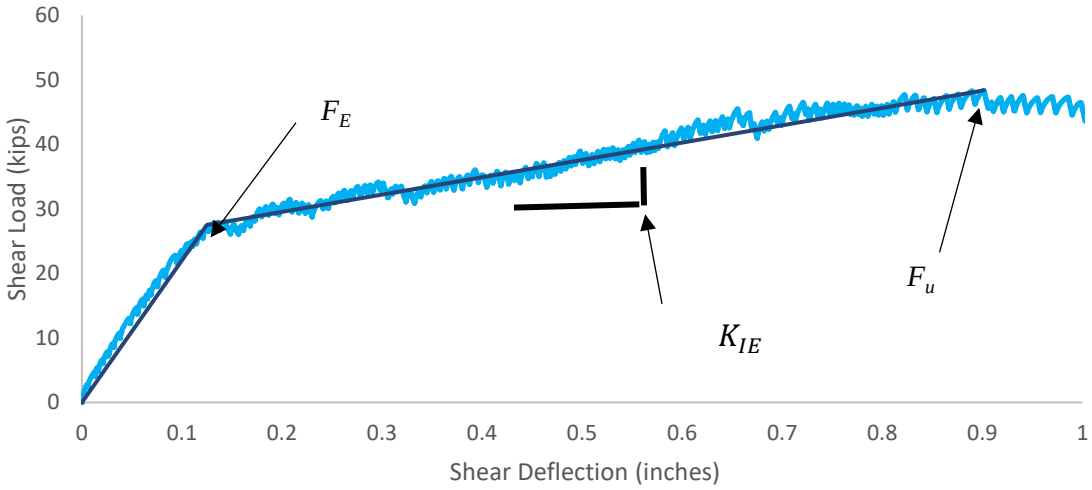

Figure 4-2 Load-Deformation Curve & Visually Identifying the Yield Point

reduced stiffness until peak load. Many of the connectors maintained significant load past this peak load while continuing to deform, whereas, others failed soon after they reached peak load. This section will provide a brief overview and summary of all connector types and each connector will be reviewed specifically in the following subsections.

On a load-deflection diagram, the elastic stiffness of the specimen the initial slope of the load deformation curve. For design purposes, this curve is idealized into two categories: the elastic portion, K_e, and the plastic portion, K_{ie} (Figure 4-2). The stiffness can be calculated as the derivative of the curve, which for our idealized case of two sections is equal to:

$$K_E = \frac{F_E}{\Delta_E} \tag{4-1}$$

$$K_{IE} = \frac{F_u - F_E}{\Delta_U - \Delta_E} \tag{4-2}$$

Where:

K_E = elastic stiffness

K_{IE} = inelastic stiffness of plastic stiffness

F_E = elastic load limit

F_u = ultimate capacity or peak load

Δ_E = deflection corresponding to the elastic load limit

Δ_U = deflection corresponding to the ultimate capacity

Utilizing Equations (4-1) and (4-2), elastic and plastic stiffnesses were calculated for each connector and calculated per connector.

Figure 4-3 presents an ultimate strength (F_u) comparison for all specimens. Connector A with 3-in. bonded XPS insulation produced the strongest individual shear connection (16.8 kips each), while connector D with 4-in. unbonded EPS insulation produced the smallest shear connection (1.39 kips each), though in this instance there may have been a fabrication issue. There was a consistent reduction in strength between 3-in. and 4-in. wythe specimens, but connector C with ISO and connector D with XPS experienced little to no reduction in strength.

Each unbonded specimen produced a reduction in ultimate strength for its respective connector. The amount of reduction in ultimate strength varied greatly, however. For example, connector A with EPS produced a reduction of approximately

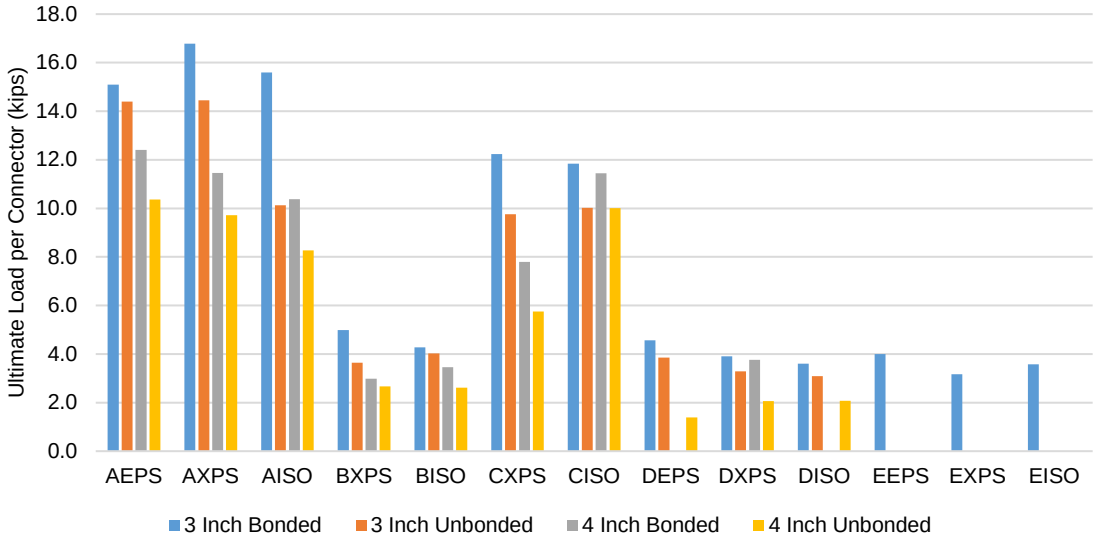

Figure 4-3 Ultimate Load Comparison for All Connectors Individually

10% when unbonded, while connector D with EPS produced an approximately 70% difference when unbonded.

Foam type did contribute to the ultimate strength as well, but the results were also inconsistent (especially with the ISO). This variation is expected to be because the ISO surfaces were not consistent between manufacturers. The ISO foam selected for each was part of the manufacturer's system/recommendation, and therefore what a precast producer would receive upon purchase. Some ISO surfaces were smooth plastic or metallic foil while others had a paper surface (Figure 4-4). The vastly differing properties of each of these materials causes them to bond differently with the concrete, possibly leading to inconsistencies in bonded and unbonded behavior for the ISO. Ultimate strengths were typically higher with XPS, but connector D experienced higher loads with EPS.

Figure 4-4 Different types of polyisocyanurate foam and their associated face finishing

An “elastic limit” load (F_E) and “elastic” stiffness (K_E) were identified from the load deformation curve of each push-off specimen. This was done by visually identifying the yield point as shown in Figure 4-2. Figure 4-5 shows the maximum elastic force (F_E) observed during testing for each connector configuration. Although fatigue testing was not performed, it was assumed that F_E should be the maximum force allowed in the connector during service loading scenarios as damage may accumulate at higher loads.

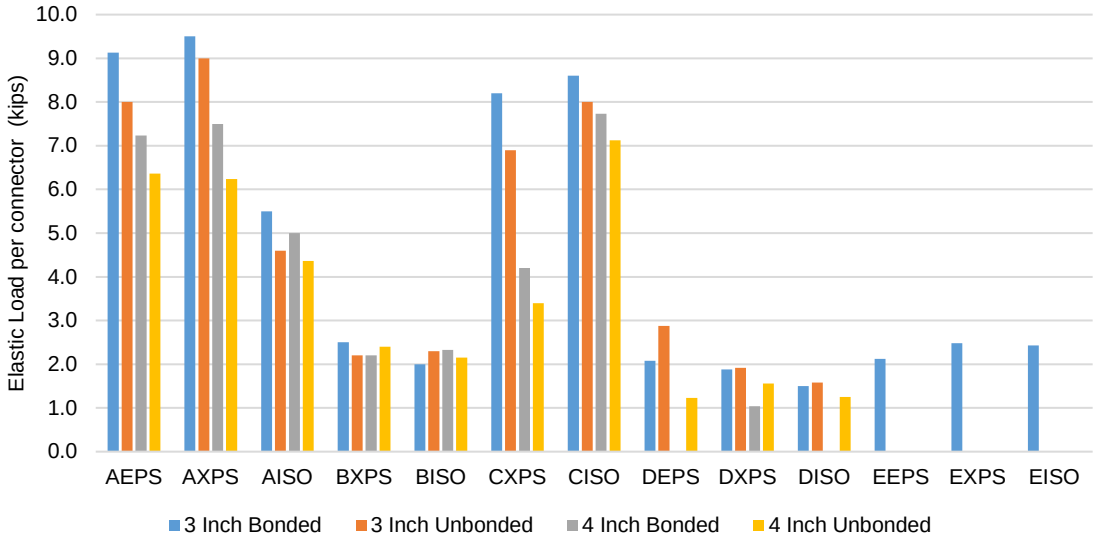

Figure 4-5 Elastic Load Limit (F_E) Comparison for All Specimen Configurations

Figure 4-5 allows a visual comparison of elastic load limits for all push-off specimens in this paper. The connectors that exhibited a high ultimate strength, F_u, in Figure 4-3 also presented with a similar F_E, relative to the other connectors. Connector A with XPS had the highest F_E value (9.5 kips), but Connector A with ISO was significantly lower than the EPS and XPS combinations. This is likely due to the difference in ISO surface treatment used with the fabricators system as previously discussed, which might cause inconsistent bond. There was relatively little difference between the Connector A ISO bonded and unbonded. Similar relationships between insulation, wythe thickness and bond performance are observed with respect to F_E.

Figure 4-6 presents the elastic stiffness values for the push-off specimens tested in this program. Connector B resulted in the lowest K_E values with as low as 6 kips/in in combination with the 4-in. unbonded specimens, whereas several Connector A specimens

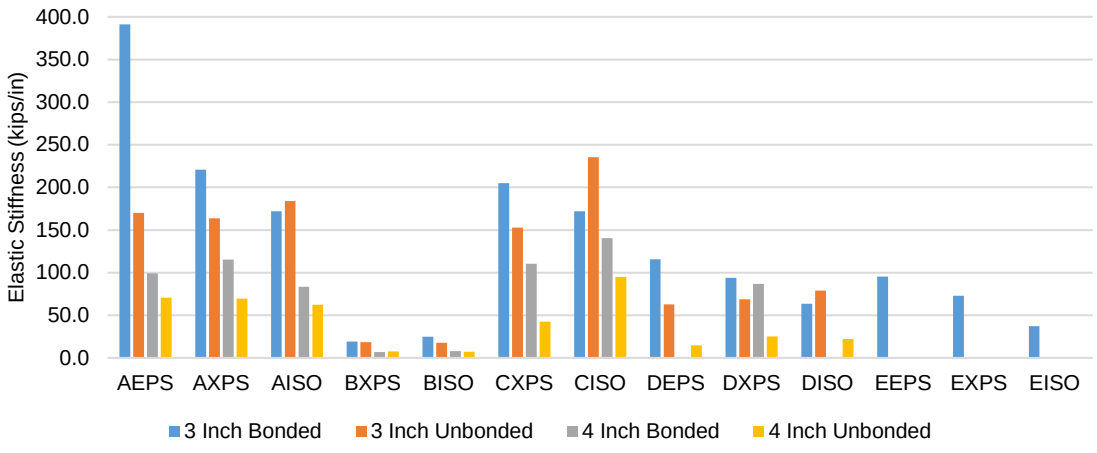

Figure 4-6 Elastic Stiffness Comparison for All Connector

exceeded 150 kips/in. Surprisingly, although Connector D specimens had displayed lower relative strengths with respect to the other connectors, they had a similar stiffness to the other connector specimens in many instances. Connectors A and C showed significantly higher stiffness and strength. This is likely due to their truss-like fiber orientation which allows more efficient horizontal load transfer as opposed to the load transfer mechanism of Connectors B and D, which is similar to dowel action or pure shear.

Both unbonded ISO scenarios for connectors A and C displayed higher elastic stiffness values than their bonded counterparts. This was unexpected and may be evidence of highly variable bond behavior and/or insulation behavior. Generally, 4-in. wythes, bonded and unbonded, exhibit significantly lower stiffness than the observed reductions in strengths in Figure 4-2 and Figure 4-5. Similar observations can be made from the inelastic stiffnesses presented in Figure 4-7.

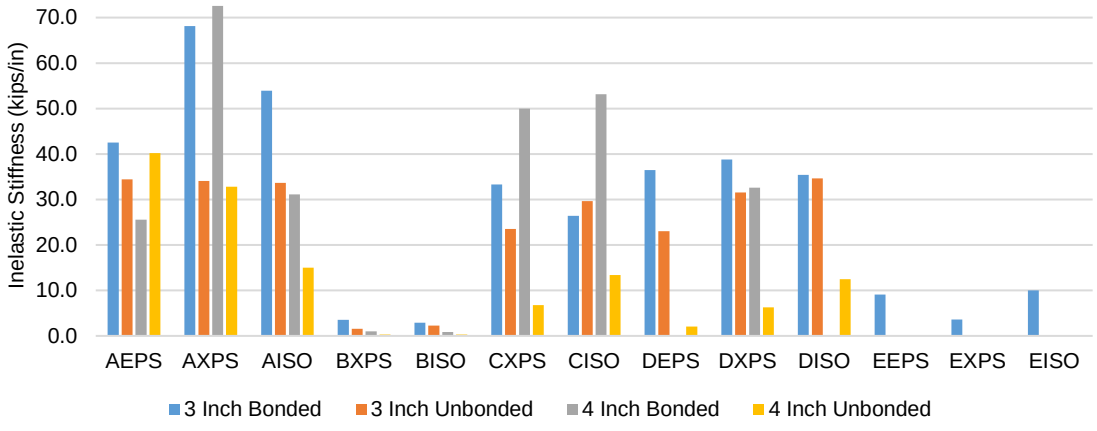

Figure 4-7 Inelastic Stiffness Comparison for All Connector

It should be expressly noted that the differences in strength and stiffness should not be the sole factor in selecting a shear component. Cost, durability, ease of fabrication and customer support should also be considered when selecting a system. Also, connector configuration is important to performance (Olsen and Maguire 2016).

4.3.1 Experimental Results for Connector A

Figure 4-8 and Figure 4-9 display plots of shear load versus shear deflection for all Connector A 3-in. and 4-in. specimens, respectively. There is a reduction in all mechanical values when comparing the 4 in. specimens to the 3 in. specimens, as expected. Connector A seems to be affected by the bond of the foam to the concrete since, in all cases, the bonded specimens have larger strengths and stiffnesses than the

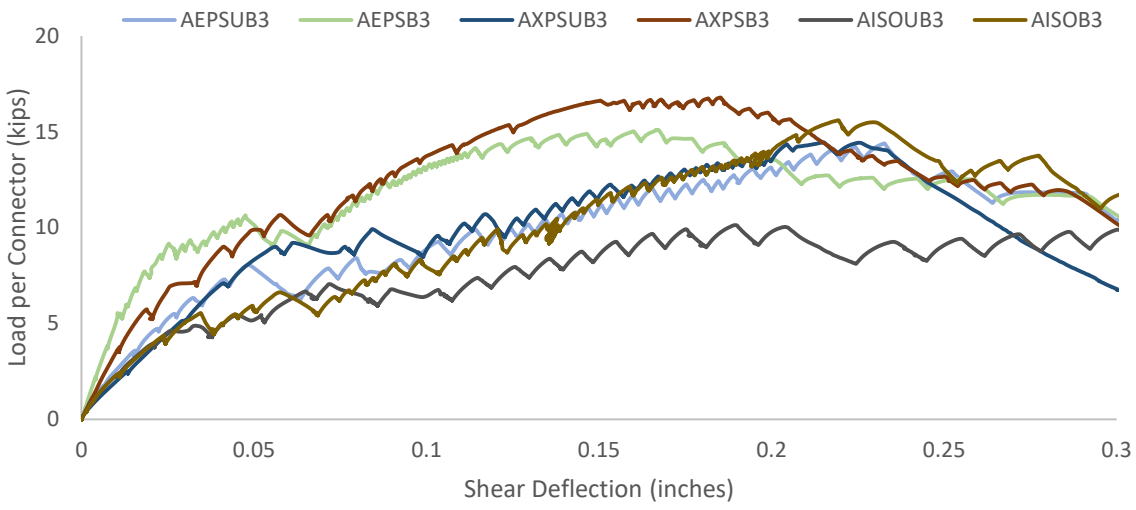

Figure 4-8 Chart of all 3-in. specimens for Connector A

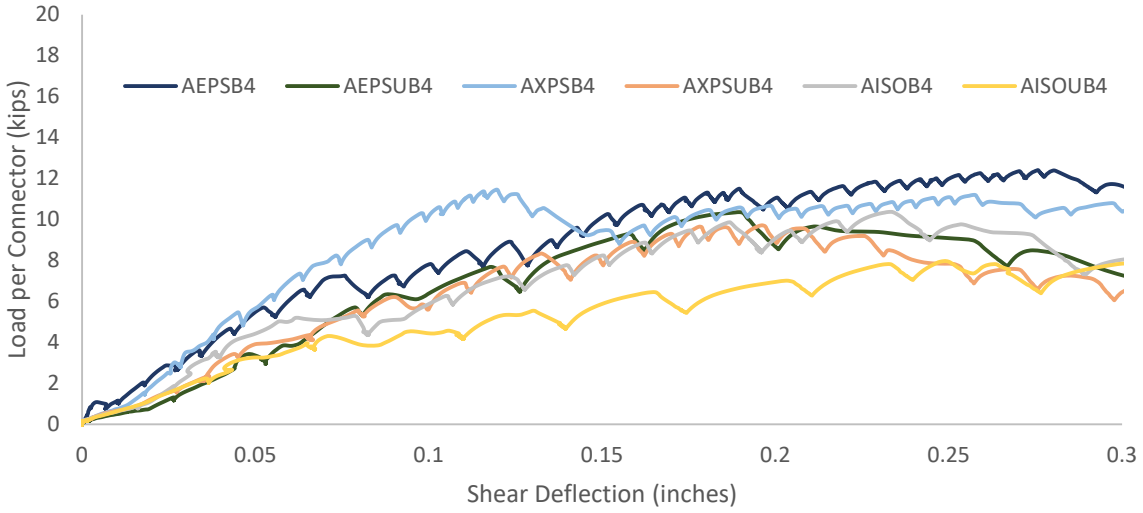

Figure 4-9 Chart of all 4-in. specimens for Connector A

unbonded specimens. This did not hold true for all the other connectors as presented in the following sections. Table 4-3 and Table 4-4 present the tabulated capacities of the specimen and the stiffnesses, respectively.

4.3.2 Experimental Results for Connector B

Figure 4-10 and Figure 4-11 display plots of shear load versus shear deflection for all Connector B 3-in. and 4-in. specimens, respectively. There is a reduction in all mechanical values when comparing the 4 in. specimens to the 3 in. specimens, as expected. Connector B seems to behave similarly whether the foam is bonded or not. Table 4-5 and Table 4-6 present the tabulated capacities of the specimen and the stiffnesses, respectively.

Table 4-3 Observed Experimental Capacity of Connector A

	Ultimate Capacity of Specimen				Ultimate Capacity of Connector			
	3 Inch		4 Inch		3 Inch		4 Inch	
	(kips)	*(kips)*	*(kips)*	*(kips)*	*(kips)*	*(kips)*	*(kips)*	*(kips)*
	B	UB	B	UB	B	UB	B	UB
AEPS	60.4	57.6	49.7	41.5	15.1	14.4	12.4	10.4
AXPS	67.2	57.8	45.9	38.9	16.8	14.4	11.5	9.7
AISO	626	40.5	41.5	33.1	15.6	10.1	10.4	8.3

Table 4-4 Elastic and plastic stiffness for all Connector A push-off specimens

Specimen			AEPS3B	AEPS3UB	AEPS4B	AEPS4UB	AXPS3B	AXPS3UB	AXPS4B	AXPS4UB	AISO3B	AISO3UB	AISO4B	AISO4UB
Elastic Stiffness	K_E	(kips/in)	391	170	100.0	69.4	221	163.6	115.4	69.3	172	184	83.3	62.5
Inelastic Stiffness	K_{EL}	(kips/in)	42.2	34.3	24.5	41.3	68	34.0	72.5	31.3	54.7	32.7	31.1	15.0

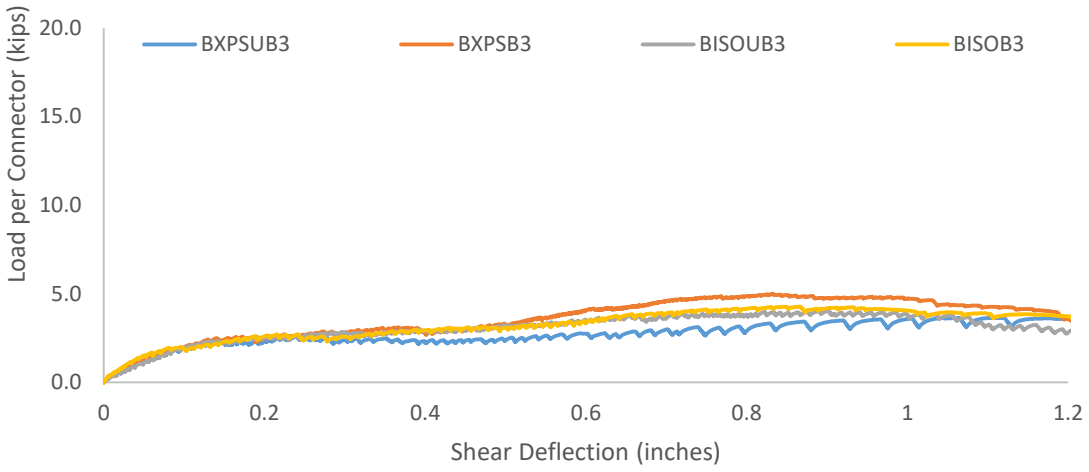

Figure 4-10 Chart of all three-inch specimens for connector B

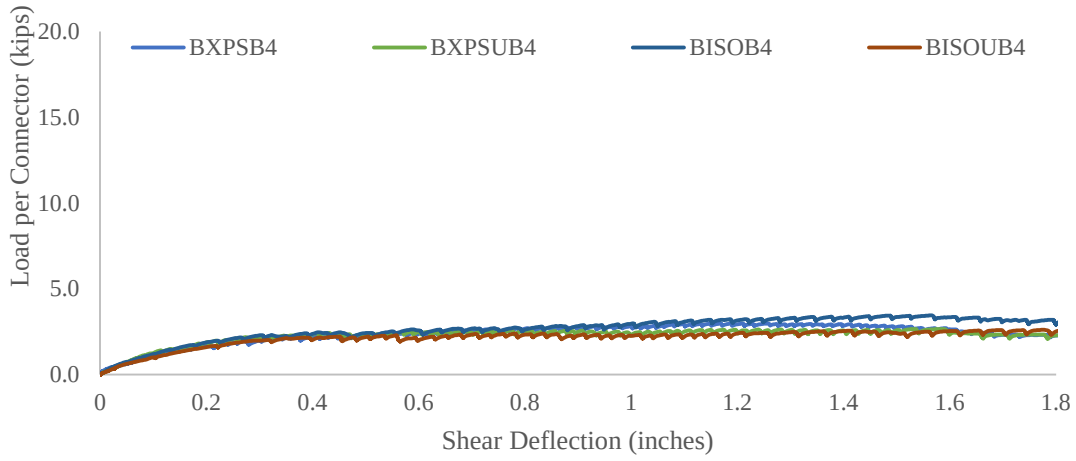

Figure 4-11 Chart of all 4-in. specimens for Connector B push-off specimens

Table 4-5 Observed experimental capacity of Connector B

	Ultimate Capacity of Specimen				Ultimate Capacity of Connector			
	3 Inch		4 Inch		3 Inch		4 Inch	
	B	UB	B	UB	B	UB	B	UB
BXPS	59.91	43.71	35.77	31.95	4.99	3.64	2.98	2.66
BISO	51.32	48.38	41.49	31.42	4.28	4.03	3.46	2.62

Table 4-6 Elastic and plastic stiffness for all Connector B push-off specimens

Specimen			BXPS3B	BXPS3UB	BXPS4B	BXPS4UB	BISO3B	BISO3UB	BISO4B	BISO4UB
Elastic Stiffness	K_{EL}	(kips/in)	19.2	18.3	7.0	7.7	25	17.7	7.8	7.2
Inelastic Stiffness	K_{EL}	(kips/in)	3.5	1.5	1.0	0.3	2.9	2.2	0.9	0.3

4.3.3 Experimental Results for Connector C

Figure 4-12 and Figure 4-13 display plots of shear load versus shear deflection for all Connector C 3-in. and 4-in. specimens, respectively. There is a reduction in all mechanical values when comparing the 4 in. specimens to the 3 in. specimens, except for the Connector C ISO bonded 4 in. specimen, which had very similar values compared to the 3 in. specimens in the same series. Connector C was affected by the foam to concrete bond, although is it less pronounced in the 3 in. specimens and in nearly every case the strength and stiffness is significantly reduced when unbonded. Note that the manufacturer does not recommend Connector C for 3 in. specimens and some connectors in the 3 in. wythes experienced compression blow out as discussed later in this chapter. Table 4-7 and Table 4-8 present the tabulated capacities of the specimen and the stiffnesses, respectively.

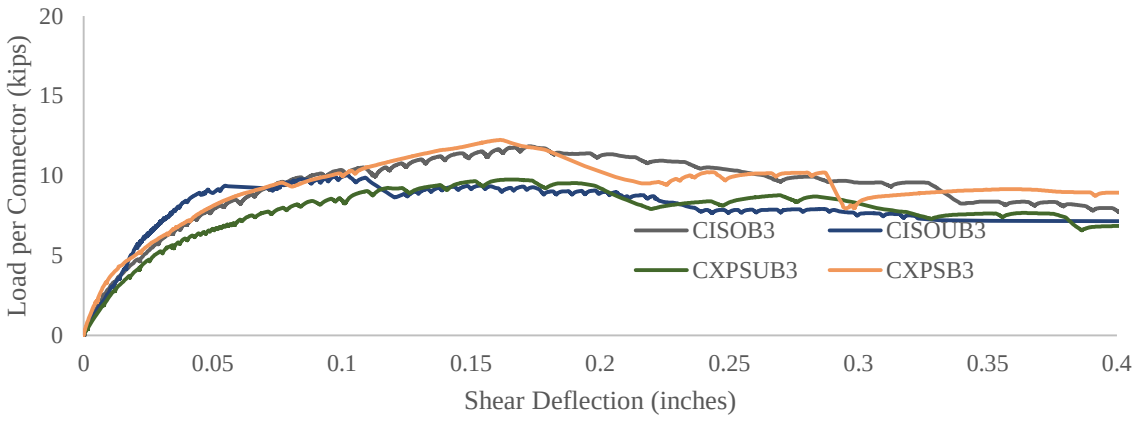

Figure 4-12 Chart of all 3-in. specimens for Connector C

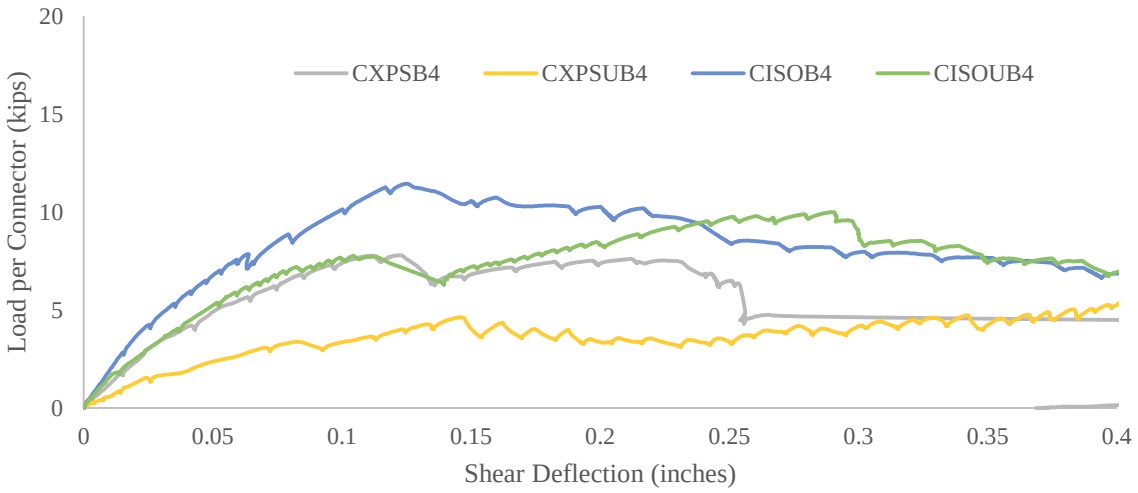

Figure 4-13 Chart of all 4-in. specimens for Connector C

Table 4-7 Observed Experimental Capacity of Connector C

	Ultimate Capacity of Specimen				Ultimate Capacity of Connector			
	3 Inch		4 Inch		3 Inch		4 Inch	
	B	UB	B	UB	B	UB	B	UB
CXPS	97.85	78	62.37	46	12.23	9.76	7.8	5.75
CISO	94.74	80.21	91.61	80.04	11.84	10.03	11.45	10.01

Table 4-8 Elastic and plastic stiffness for all Connector C push-off specimens

Specimen			CXPS3B	CXPS3UB	CXPS4B	CXPS4UB	CISO3B	CISO3UB	CISO4B	CISO4UB
Elastic Stiffness	K_{EL}	(kips/in)	205	153	110	42.5	172	235	140	94
Inelastic Stiffness	K_{EL}	(kips/in)	34.7	23.5	50	6.8	26.5	29.4	53.1	13.6

4.3.4 Experimental Results for Connector D

Figure 4-14 and Figure 4-15 display plots of shear load versus shear deflection for all Connector B 3-in. and 4-in. specimens, respectively. There is a reduction in all mechanical values when comparing the 4 in. specimens to the 3 in. specimens. Connector D had significantly reduced ductility when compared to the other connectors, especially for the 3 in. specimens. This is due to its randomly aligned fibers and dowel action failure mode. Based on these results, it appears that foam type and has little effect on the strength and stiffness of Connector D. Bond does influence strength and stiffness, however it is negligible. Table 4-9 and Table 4-10 present the tabulated capacities of the specimen and the stiffnesses, respectively. Interestingly, considering its overall strength, Connector D has a very high elastic stiffness, which would be a very favorable property for controlling elastic deflections and cracking.

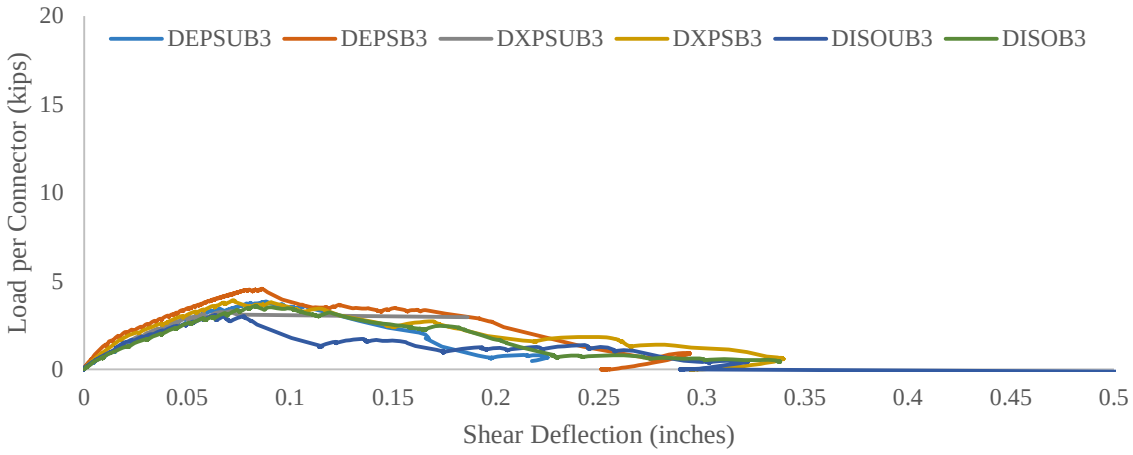

Figure 4-14 Chart of all 3-in. specimens for Connector D

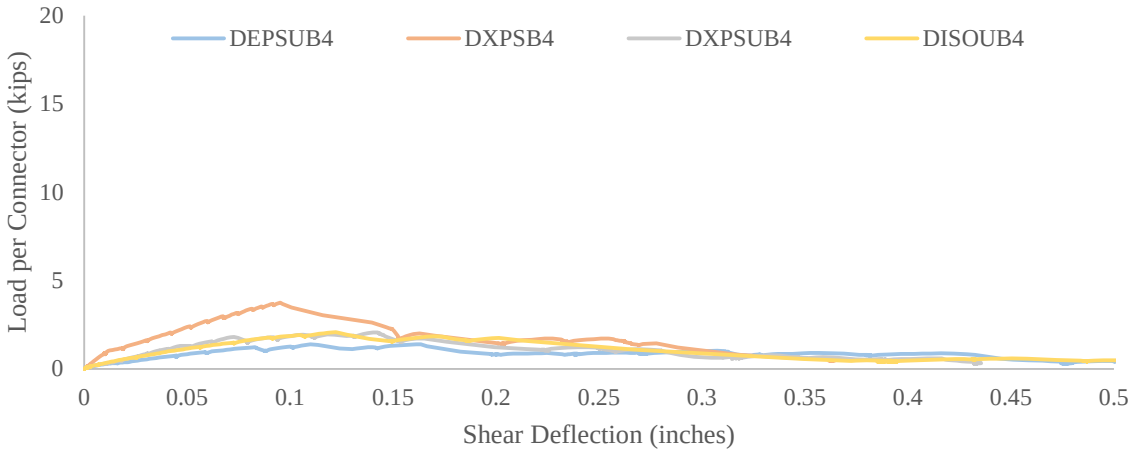

Figure 4-15 Chart of all 4-in. specimens for Connector D

Table 4-9 Observed experimental capacity of Connector D

	Ultimate Capacity of Specimen				Ultimate Capacity of Connector			
	3 Inch		4 Inch		3 Inch		4 Inch	
	B	UB	B	UB	B	UB	B	UB
HKEPS	54.00	46.18	-	16.73	4.50	3.85	-	1.39
HKXPS	46.92	39.52	45.08	24.74	3.91	3.29	3.76	2.06
HKISO	43.26	37.03	-	24.98	3.60	3.09	-	2.08

Table 4-10 Elastic and plastic stiffness for all Connector D push-off specimens

Specimen			DEPS3B	DEPS3UB	DEPS4B	DEPS4UB	DXPS3B	DXPS3UB	DXPS4B	DXPS4UB	DISO3B	DISO3UB	DISO4B	DISO4UB
Elastic Stiffness	K_{EL}	(kips/in)	115	62.9	-	14.8	94.8	68.6	86.7	25.2	63.6	79.0	-	22.2
Inelastic Stiffness	K_{EL}	(kips/in)	37.6	23	-	2.0	38.8	31.6	32.6	6.3	35.4	34.6	-	12.4

4.3.5 Experimental Results for Connector E

Figure 4-16 displays a plot of shear load versus shear deflection for all Connector E specimens. For Connector E, only 3-in. specimens were tested because the 4-in. specimens were unacceptable for testing. Based on the little information gathered, there does not seem to be a significant influence of foam type on the strength, but the ISO specimen had reduced elastic stiffness. Connector E had lower ductility than the rest, except for connector D. Table 4-11 presents the tabulated stiffness of each specimen.

4.3.6 Failure Modes of Shear Connectors

In general, glass fiber-reinforced polymer (GFRP) and nearly all other polymers and FRP products are considered brittle when compared to material like steel. However, the GFRP shear connectors tested, have exhibited many different modes of failure including: delamination, rupture, pull-out, push through and dowel action (pure shear).

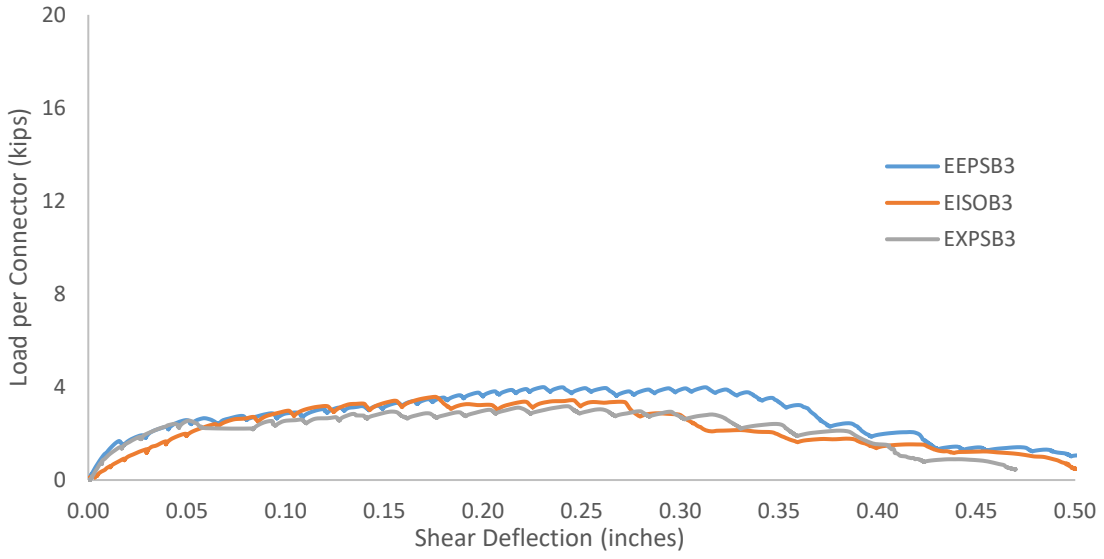

Figure 4-16 Chart of all 3-in. specimens for Connector E

Table 4-11 Elastic and plastic stiffness for all Connector E push-off specimens

Specimen			EEPS3B	EEPS3UB	EEPS4B	EEPS4UB	EXPS3B	EXPS3UB	EXPS4B	EXPS4UB	EISO3B	EISO3UB	EISO4B	EISO4UB
Elastic Stiffness	K_{EL}	(kips/in)	95.5	-	-	-	72.7	-	-	-	37.4	-	-	-
Inelastic Stiffness	K_{EL}	(kips/in)	9.1	-	-	-	3.6	-	-	-	10.0	-	-	-

4.3.6.1 Connector A (Nu-Tie Connector)

Connector A was a pultruded GFRP bar. It was 48 inches long and there were four of them in each specimen. Load was applied parallel to the connector and engaged the connector by putting the legs of the truss into either tension or compression. All specimens were loaded to failure. Figure 4-17 shows specimen AISOUB3. This failure was very typical for all connector A specimens. It shows a tensile rupture caused by rupture of the tension leg of the truss. Figure 4-18 shows specimen AISOUB4, which failed in pullout. Pullout was not common for this connector type and is likely to have been fabrication related. Figure 4-19 is failure due to shear fracture an unbonded EPS specimen.

Figure 4-17 Tensile rupture in unbonded specimen with ISO foam

Figure 4-18 Pullout failure in unbonded specimen with ISO foam

Figure 4-19 Shear fracture failure in unbonded specimen with EPS foam

4.3.6.2 Connector B (Thermomass CC Connector)

Connector B was an extruded connector symmetric in cross-section except for the machined deformations constructed to aid in the creation of bond development. Twelve connectors were equally and symmetrically spaced in each specimen. Load was applied perpendicular to the long axis of the connector and loaded to failure. Because these connectors were loaded perpendicular to the grain of the connector, relatively large deformations were observed, leading to greater variety of failures as well. Dowel action and the delamination of fibers, was the most common failure.

Figure 4-20, Figure 4-21 and Figure 4-22 depict different connector delamination patterns. Another commonly observed failure was that of shear rupture, also caused by pure shear. (See Figure 4-23). Pull-out was also observed with Connector B. When a

Figure 4-20 Dowel action causing delamination along the width of Connector B

connector failed due to pull-out, other failure mechanisms were also present. Figure 4-24 shows connector B failing in pullout, but bending fracture is also observable. Figure 4-25 shows a clean and clear shear fracture of connector B.

Figure 4-21 Dowel action failure of Connector B

Figure 4-22 Dowel action occurring along the length of Connector B

Figure 4-23 Shear fracture observed in Connector B

Figure 4-24 Pullout occurring with Connector B in combination with bending fracture

Figure 4-25 Shear fracture of Connector B

4.3.6.3 Connector C (Thermomass X Connector)

Much like Connector B, Connector C is a pultruded connector with machined ends to enable mechanical bond. Unlike Connector B, Connector C is loaded axially due to the compression and tension struts which develop because of its shape. Eight Connectors were equally and symmetrically spaced in each specimen. Load was applied in line with the connectors. Delamination and rupture were the most common cases of failure. In the case of the 3-in. specimens, the connector punched through the concrete on the outside of the specimen. This was somewhat expected as these connectors are not recommended for 3 in. concrete wythes, but were tested that way for the comparison study. Figure 4-26, Figure 4-27, and Figure 4-28 show various types of rupture and delamination. Figure 4-29 is a great example of a shear fracture. This fracture takes place in the compression leg of the “X.”. Figure 4-30 and Figure 4-31 show the failure of 3-in. specimens caused by punch through of the connector.

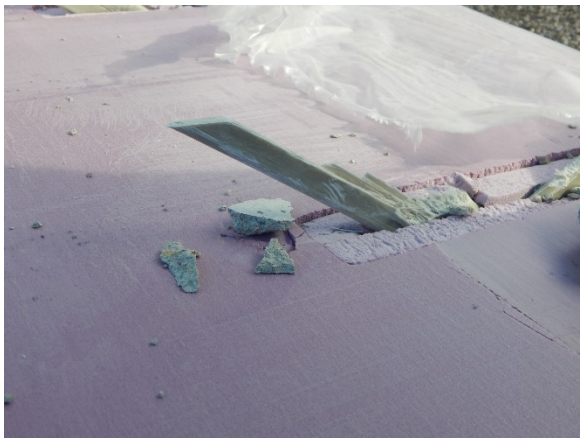

Figure 4-26 Delamination observed in a 4-in. unbonded XPS specimen

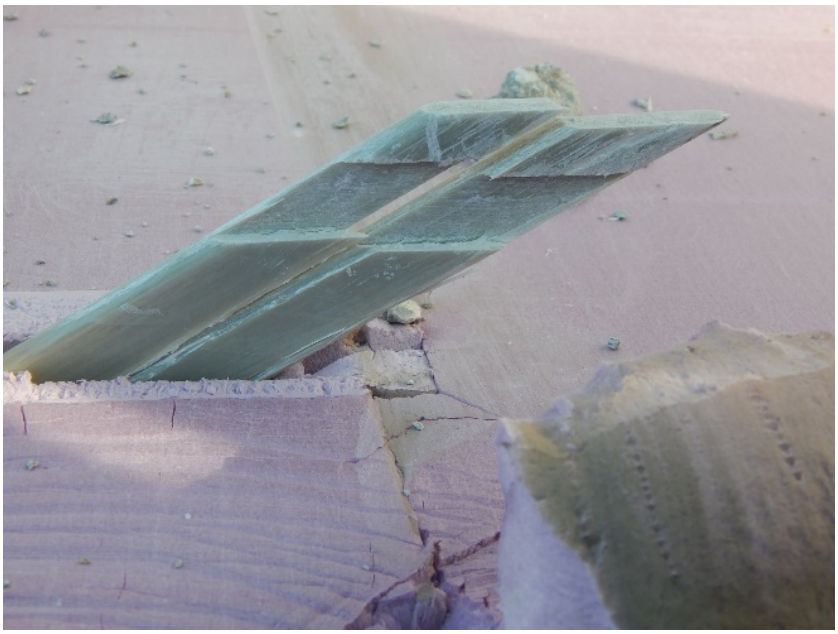

Figure 4-27 Dowel action in a 4-in. bonded XPS specimen

Figure 4-28 Delamination / shear rupture in a 4-in. bonded XPS specimen

Figure 4-29 Shear fracture and dowel action of Connector C

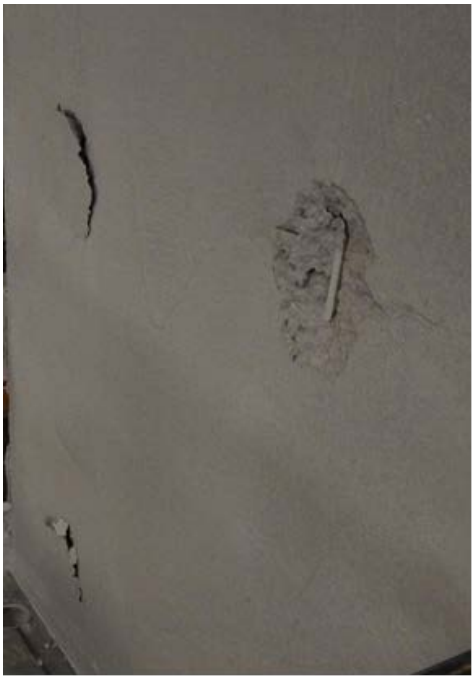

Figure 4-30 Punch through observed in all 3-in. specimens with Connector C

Figure 4-31 Punch through close-up

4.3.6.4 Connector D (HK Composite Connector)

Connector D was a mold injected connector with randomly aligned fibers. Twelve connectors were equally and symmetrically spaced in each specimen. Load was applied in line with the connectors. Shear rupture / dowel action was the only observable failure mode in Connector D. Fracture always occurred on both ends of the connector. There were no instances where fracture occurred on one end and not the other. Pull out was not observed. Connector D does, however, have the most uniquely shaped embedment regions of all the connectors. Figure 4-32 through Figure 4-34 show the shear fractures of connector D from multiple angles.

Figure 4-32 Shear fracture of Connector D (full specimen)

Figure 4-33 Shear fracture of Connector D, both ends fractured

Figure 4-34 Close-up of shear fracture of connector D

4.3.6.5 Connector E (Delta Tie Connector)

For Connector E, eight connectors were equally and symmetrically spaced in each specimen. Load was applied in line with the connectors. Connector E exhibited only one type of failure: tensile rupture. This woven connector displayed a consistent failure mode. The truss formation of Connector E always failed in its tension members. Figure 4-35 shows the completely ruptured specimen. Figure 4-36 and Figure 4-37 depict the tension legs of the truss failed while the compression leg is mostly intact. Due to internal truss shape of Connector E, it fails with rupture of the tension leg of the connector, but the overall shape of the connector is similar to that of Connector B and D and also its behavior. For Connector E, the foam was not engaged as much as it was for A and C, which had more angled connectors.

Figure 4-35 Three inch bonded EPS connector E tensile rupture of all connectors

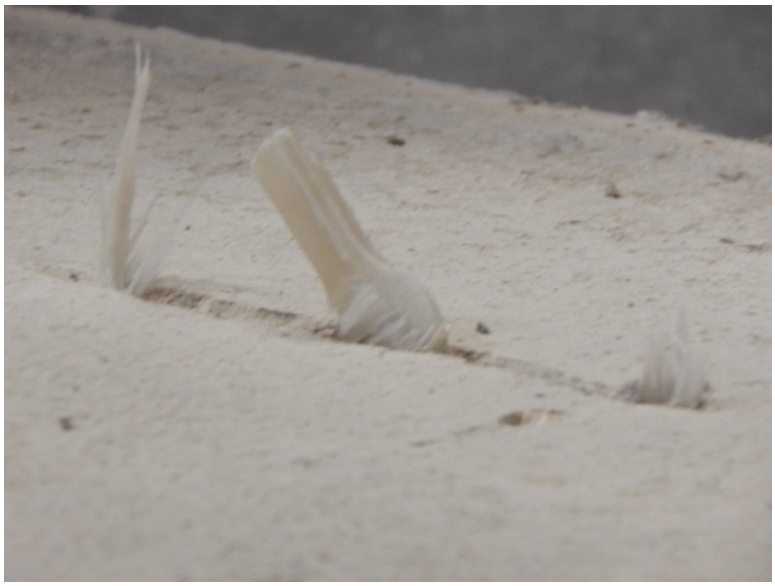

Figure 4-36 Tensile rupture of connector E, note compression leg still intact

Figure 4-37 Tensile rupture of tension strut in truss.

4.3.7 Recommended Design Curves

The shear load versus deformation information from the above connectors is a valuable design value for partially composite sandwich panel walls. Using the concept illustrated in Figure 4-2 one can use the values summarized in Table 4-12. Future effort should investigate statistical information regarding the shear strength and stiffness in order to properly and safely set limits on elastic stresses and failure stresses in the connectors during different loading scenarios. As of now it seems prudent to limit connector forced to the elastic range (F_E, Δ_E) for elastic behavior like cracking and deflections. Furthermore, for the ultimate limit state it may be prudent to limit connector forces and deformations to F_U and Δ_U to force failure of the wythes rather than a probably more brittle failure of the connectors.

Table 4-12 Summary of recommended design curves for all connectors

Connector	Foam	Bond Interface	F_E (Kips)	K_E (Kips/in.)	F_U (Kips)	K_{IE} (Kips/in.)	Δ_E (in.)	Δ_U (in.)
A	3EPS	Bonded	9.13	391.30	15.10	42.54	0.023	0.166
	3EPS	Unbonded	8.00	170.21	14.39	34.45	0.047	0.233
	4EPS	Bonded	7.23	99.04	12.41	25.58	0.073	0.276
	4EPS	Unbonded	6.36	70.67	10.36	40.20	0.090	0.190
	3XPS	Bonded	9.50	220.93	16.79	68.11	0.043	0.150
	3XPS	Unbonded	9.00	163.64	14.44	34.04	0.055	0.215
	4XPS	Bonded	7.50	115.38	11.46	72.53	0.065	0.120
	4XPS	Unbonded	6.24	69.33	9.72	32.82	0.090	0.196
	3ISO	Bonded	5.50	171.88	15.60	53.91	0.032	0.219
	3ISO	Unbonded	4.60	184.00	10.12	33.66	0.025	0.189
	4ISO	Bonded	5.00	83.33	10.37	31.12	0.060	0.233
	4ISO	Unbonded	4.36	62.29	8.27	15.01	0.070	0.331
B	3XPS	Bonded	2.50	19.23	4.99	3.55	0.130	0.833
	3XPS	Unbonded	2.20	18.33	3.64	1.53	0.120	1.064
	4XPS	Bonded	2.20	7.00	2.98	1.02	0.314	1.168
	4XPS	Unbonded	2.40	7.67	2.66	0.29	0.313	1.535
	3ISO	Bonded	2.00	25.00	4.28	2.89	0.080	0.867
	3ISO	Unbonded	2.30	17.69	4.03	2.24	0.130	0.901
	4ISO	Bonded	2.33	7.77	3.46	0.89	0.300	1.565
	4ISO	Unbonded	2.15	7.17	2.62	0.32	0.300	1.778
C	3XPS	Bonded	8.20	205.00	12.23	33.29	0.040	0.161
	3XPS	Unbonded	6.90	152.78	9.76	23.51	0.045	0.168
	4XPS	Bonded	4.20	110.53	7.80	49.95	0.038	0.110
	4XPS	Unbonded	3.40	42.50	5.75	6.79	0.080	0.426
	3ISO	Bonded	8.60	172.00	11.84	26.40	0.050	0.173
	3ISO	Unbonded	8.00	235.29	10.03	29.65	0.034	0.102
	4ISO	Bonded	7.73	140.55	11.45	53.13	0.055	0.125
	4ISO	Unbonded	7.12	94.93	10.01	13.41	0.075	0.290
D	3EPS	Bonded	2.08	115.56	4.56	36.47	0.018	0.086
	3EPS	Unbonded	2.88	62.61	3.85	23.05	0.046	0.088
	4EPS	Unbonded	1.23	14.84	1.39	2.05	0.083	0.163
	3XPS	Bonded	1.88	94.80	3.91	38.78	0.020	0.073
	3XPS	Unbonded	1.92	68.57	3.29	31.57	0.028	0.072
	4XPS	Bonded	1.04	86.67	3.76	32.61	0.012	0.095
	4XPS	Unbonded	1.56	25.16	2.06	6.27	0.062	0.142
	3ISO	Bonded	1.50	63.56	3.60	35.43	0.024	0.083
	3ISO	Unbonded	1.58	79.00	3.09	34.62	0.020	0.064
	4ISO	Unbonded	1.25	22.24	2.08	12.45	0.056	0.123
E	3EPS	Bonded	2.12	95.45	3.99	9.09	0.022	0.230
	3XPS	Bonded	2.48	72.73	3.17	3.63	0.034	0.245
	3ISO	Bonded	2.43	37.38	3.58	10.04	0.065	0.177

4.4 Summary and Conclusions

The preceding chapter describes the testing of 41 pure shear push-off specimens, created to evaluate the shear stiffness of the various commercially available sandwich panel wall shear connectors. The variables studied were connector type, foam thickness, foam type and foam bond. Due to project constraints, only a single specimen of each type could be constructed so there is no statistical information available regarding the connector strength and stiffness values. The following conclusions can be made from the push-off testing:

1. For pin type connectors that fail mainly in dowel action (Connectors B and D) or behave like a pin connector (Connector E) foam type and bond play a negligible role in strength and stiffness.
2. For truss type connectors (Connectors A and C) that are loaded mainly in tension or compression when shear is applied to the specimen, foam type and bond plays a more significant role in strength and stiffness.
3. Connector types vary widely in stiffness, strength, and ductility
4. Future effort should investigate statistical information regarding the shear strength and stiffness in order to properly and safely set limits on elastic stresses and failure stresses in the connectors during different loading scenarios.

CHAPTER 5

SIMPLE MODEL TO PREDICT ELASTIC FULL SCALE BEHAVIOR

Predicting sandwich panel elastic stresses and deformations is paramount for design. Several researchers have developed techniques to predict sandwich panel deformations. Prediction methods vary significantly in complexity and accuracy as observed in section 2.1.

Full scale test data from Naito et al. (Naito, et al., 2011) for a precast concrete sandwich panel was compared to a complex mechanics based model created by Bai and Davidson (Bai & Davidson, 2015) and the simplified beam and spring element model below. The precast panels tested by Naito et al. (Naito, et al., 2011) were 3 inch x 3 inch x 3 inch wythe panels, which were 32 inches wide and 12 feet long. Connector B shear transfer mechanisms were placed at 16 inches on center starting 8 inches from the end of the panel, using extruded expanded polystyrene (EPS). Concrete was 8,800 psi concrete with an estimated elastic modulus of 5,350 ksi.

The analytical model created used commercial matrix analysis software package and any commercial or personal matrix analysis software could produce an identical model and could also be easily built into commercial wall panel analysis and design software. The very simple model, shown in Figure 5-1, uses only beam and spring elements combined with the appropriate material values, boundary conditions, and the results for the shear connector testing presented in this thesis. Beam elements are assigned the individual gross properties of each wythe, separated by the distance between the wythe centroids. Link elements, assigned connector B shear stiffness, bridge the gap

between the wythes in this case at 8 inches on-center along the panel length. The test specimen had shear connectors placed at 16 inch centers, starting at 8 inches from the end of the beam. Spring elements corresponding to the location of the shear connectors were assigned a shear stiffness equal to the K_e value associated with specimen BXPS3B in Table 9 of this publication. The remaining links, which represent a lumped insulation stiffness, between the links representing the composite connectors, were assigned a shear stiffness equivalent of 17 kip/inch based on the shear modulus (estimated at 200 psi) and the tributary geometry of the insulation wythe (32 inches wide x 8 inches tributary length x 3 inches thick) and a rigid longitudinal stiffness. Point loads were assigned at each node on one face corresponding to the pressure, multiplied by the tributary width between nodes. All links were assigned a longitudinal stiffness of 45 kip/in based on the tributary geometry and an assumed Young's modulus of XPS insulation (estimated at 500 ksi).

Figure 5-2 presents the comparison between the three identical test specimens (denoted PCS5 A, B and C) from Naito et al. (Naito, et al., 2011). The beam and spring model shows congruence with the observed test data and the complex mechanical model

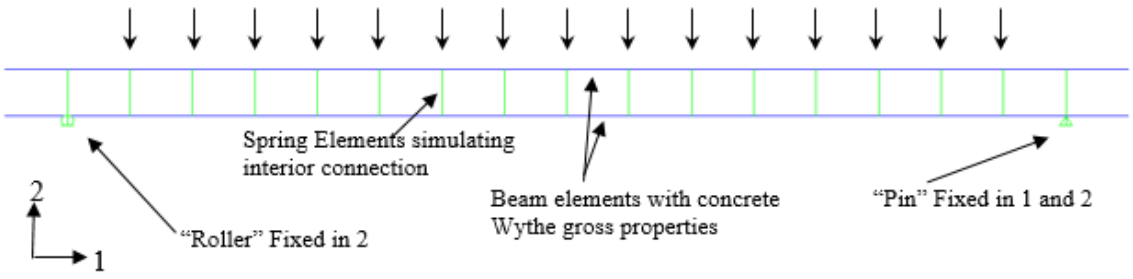

Figure 5-1 Simple FEM model used to predict full-scale behavior

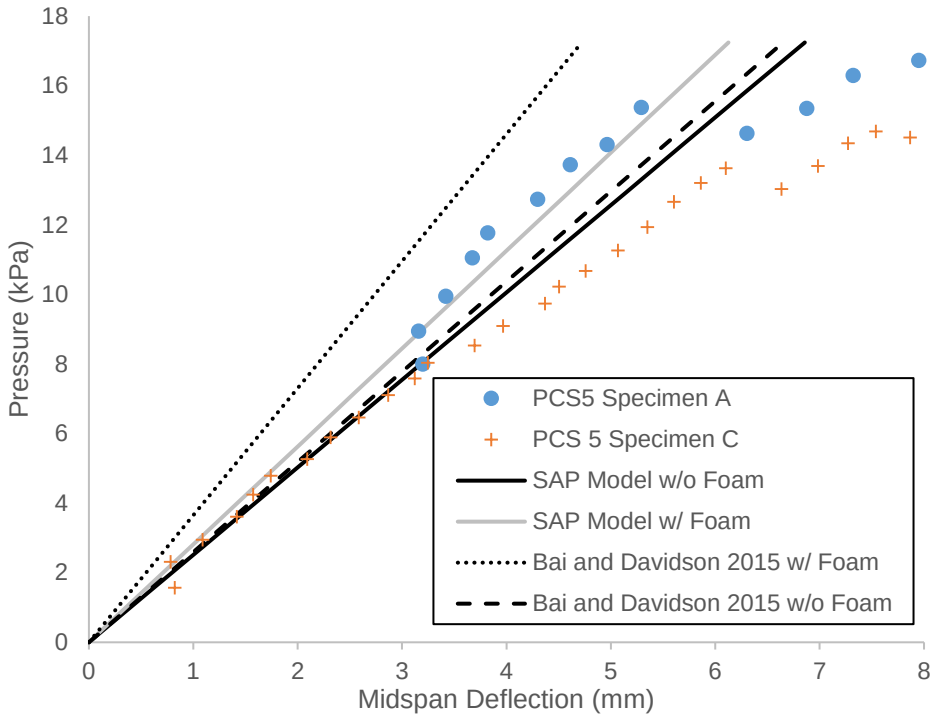

Figure 5-2 Comparison of the Beam Spring Model in elastic range, to Naito et al.'s test data, and Bai & Davidson's mathematical model.

presented by Bai and Davidson (Bai & Davidson, 2015). The beam and spring model is limited to elastic deflections, although if inelasticity were introduced (non-linear springs and beam elements) ultimate deflections and strength can likely be determined, however this may not be necessary for most designs.

The beam and spring model has only been validated using connector B shear connectors, for a single wall panel configuration. The authors are in the process of testing full scale specimens for all connectors in this study, and will be able to determine how valid the beam and spring model is in all situations. Regardless, the beam spring model presented here is a promising option for elastic analysis of precast sandwich wall panels

with composite shear connector systems, including those with unsymmetrical wythes and irregular connector patterns, inclusion of P-δ and P-Δ effects. Based on preliminary evaluation, using this model, it should be possible to tailor percent composite action at cracking checks, deflection checks by distributing connectors over the wall panel, while maintaining elastic behavior within the connectors.

For instance, in an example panel 8 feet wide, 30 feet long, with a 30 feet span, under 50 psf lateral load, with concrete compression strength of 8000 psi and elastic modulus 5100 ksi, ignoring P-δ and P-Δ, can be simulated with various connector patterns. For a generic connector with individual unbonded stiffness of K_e = 50 kip/in, Figure 5-3 presents the difference between adding connectors in a uniformly distributed fashion or triangularly distributed with connectors concentrated near the panel ends. With

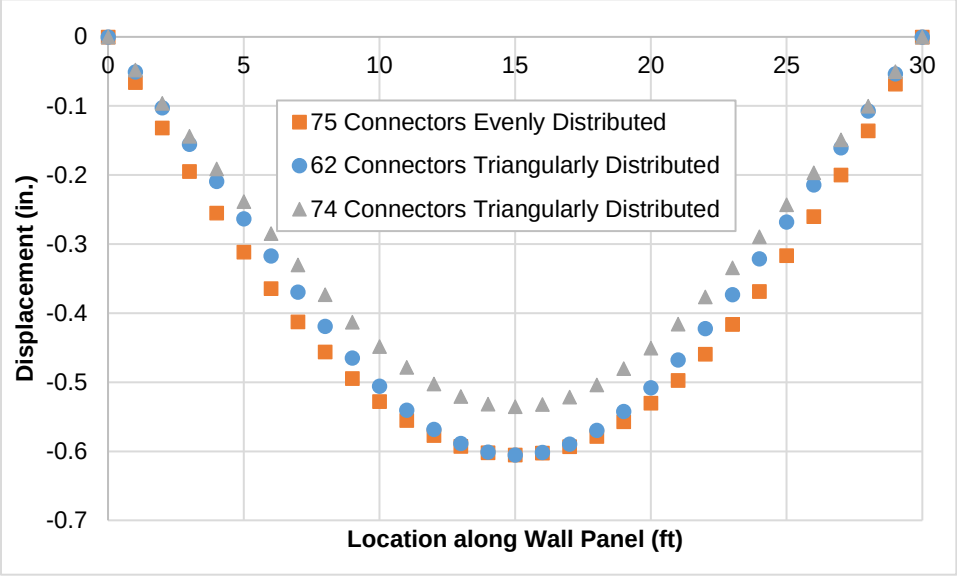

Figure 5-3 Deflection comparison with different connector distributions.

the same number of connectors (~75), deflection could be reduced 10% by changing connector distribution. Deflection for the uniformly distributed connectors was matched with 16% fewer connectors (74 connectors versus 62 connectors, see Figure 5-3) when using a triangular connector distribution and locating more near the ends.

Distribution of connector force did change for these different connector patterns. Figure 5-4 presents a plot of connector force along the length. For the uniformly distributed connectors, the maximum connector force is located 4 feet from the end, while for both triangularly distributed models, maximum connector force occurred 8 feet from the end. Furthermore, the uniformly distributed connectors exhibited a higher maximum connector force. These results indicate designers should be aware of where

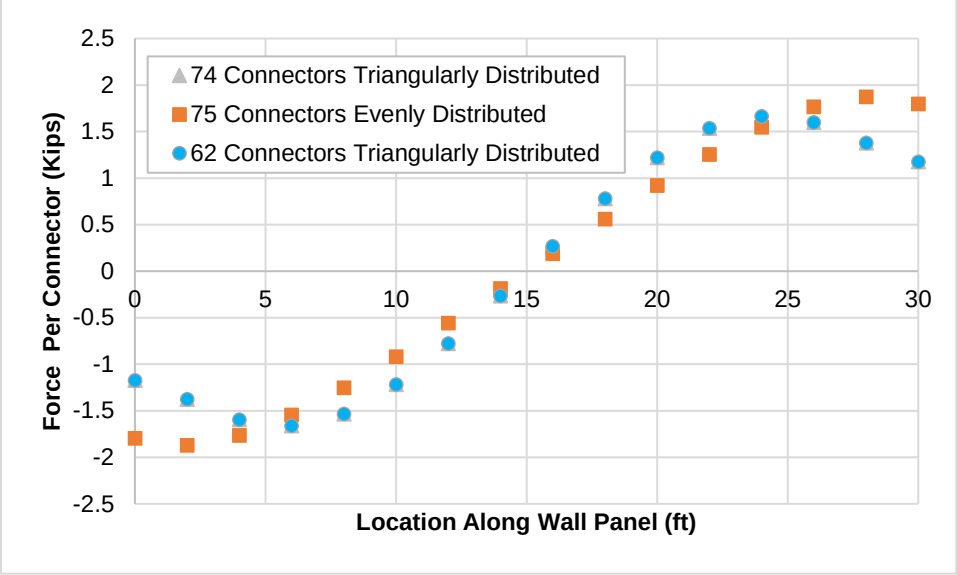

Figure 5-4 Force per connector for different connector distributions.

connectors are highly loaded, especially at service limit states where connector forces should remain elastic.

Currently, when a designer uses commercial wall panel software, they are asked to input a degree of composite action (in percent) for evaluation of cracking, elastic deflections, and ultimate load. Most connector systems are considered to have a standard degree of composite action for each design limit state, but this is not necessarily the case. Figure 5-5 presents the same panel as described above, with varying levels of uniformly distributed shear connectors. As the number of shear connectors increases, the panel becomes stiffer and approaches the fully composite line. This implies that using additional connectors of the same stiffness will provide different levels of composite action. These results indicate that the degree of composite action for a given system,

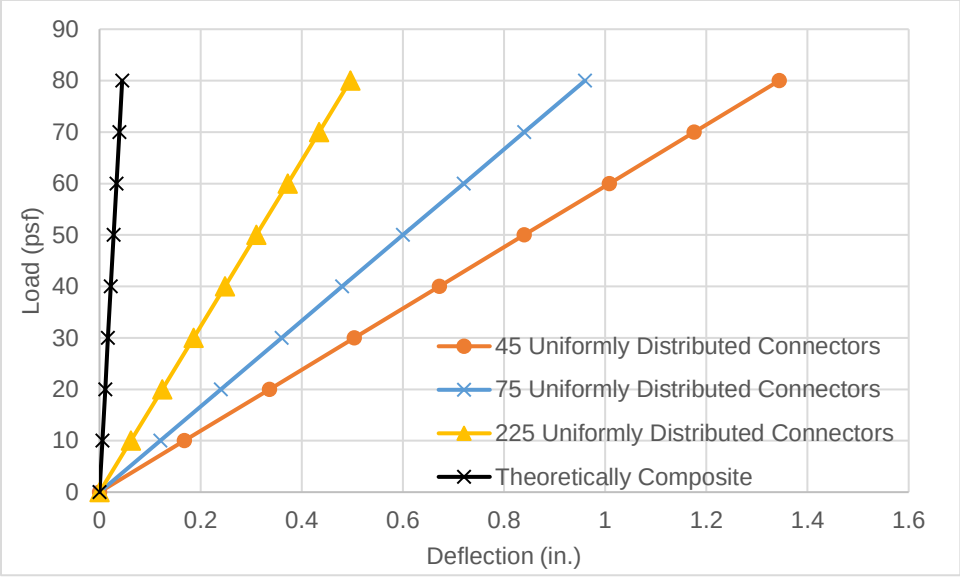

Figure 5-5 Example elastic load versus deformation relationship.

deflections, cracking and even ultimate capacity is not a single number and is directly related to the stiffness provided by the shear connectors. Adding more connectors, or redistributing connectors towards the panel ends, as described above, will present an apparent increase in composite behavior, regardless of the manufacturer's connector system. There is likely a practical limit to the amount of composite action available to a given system due to differences in strength, stiffness, and the total number of connectors that can practically be fabricated in a wall panel for a given system.

CHAPTER 6

SUMMARY AND CONCLUSIONS

6.1 Summary

In this report, a thorough literature review and history of composite action in PCSWP was presented and current design philosophies were described. To develop general methods to predict PCSWP behavior, an experimental program was undertaken in which push-off PCSWP specimens were designed, fabricated and tested at the Utah State University SMASH lab. Using this valuable experimental data, a matrix based elastic model was presented to predict important elastic deflections and cracking moments.

6.2 Push-off Testing

A total of 41 pure shear push-off specimens were created to evaluate the shear stiffness of the various commercially available sandwich panel wall shear connectors. The variables studied were connector type, foam thickness, foam type and foam bond. Due to project constraints, only a single specimen of each type could be constructed so there is no statistical information available regarding the connector strength and stiffness values. The following conclusions can be made from the push-off testing:

1. For pin type connectors that fail mainly in dowel action (Connector B and D) or behave like a pin connector (Connector E), foam type and bond play a negligible role in strength and stiffness.

2. For truss type connectors (Connectors A and C) that are loaded mainly in tension when shear is applied to the specimen, foam type and bond plays a more significant role in strength and stiffness.
3. Connector types vary widely in stiffness, strength and ductility
4. Bi-linear design curves were developed to be used in the prediction methodologies and limits on connector forces/deformation.
5. Future effort should investigate statistical information regarding the shear strength and stiffness in order to properly and safely set limits on elastic stresses and failure stresses in the connectors during different loading scenarios.

6.3 Elastic Prediction Methods

In this section, a method to predict elastic deformations and cracking was developed. The Beam-Spring model is a simple, general, matrix analysis framework that allows for accurate prediction of sandwich panel behavior. It is limited to elastic behavior, although if inelasticity were introduced to the Beam-Spring model (non-linear springs and beam elements), ultimate deflections and ultimate strength could likely be determined, though this may not be necessary.

The Beam-Spring Model presented herein is a promising option for elastic analysis of precast concrete sandwich panel walls using composite shear connector systems, including those with unsymmetrical wythes, axial forces and irregular connector patterns, including P-δ and P-Δ effects.

REFERENCES

Adams, R. C., Leabu, V., Barber, J. S., Cordon, W. A., Florian, J. O., Galezewski, S., . . . Burchett, K. R. (1971). Design of Precast Concrete Wall Panels. *Journal of the American Concrete Institute, 98*(7), 504-513.

Al-Rubaye, S., Sorensen, T., & Maguire, M. (2017). Investigating Composite Action at Ultimate for Commercial Sandwich Panel Composite Connectors. *Precast/Prestressed Concrete Institute*.

American Concrete Institute. (2014). *Building Code Requirements for Structural Concrete (ACI 318-14).* Farmington Hills, Missouri, USA: American Concrete Institute.

Bai, F., & Davidson, J. S. (2015). Analysis of Partially composite Foam Insulated Concrete Sandwich Structures. *Journal of Engineering Structures, 91*, 197-209.

Bunn, W. G. (2011). *CFRP Grid/Rigid Foam Shear Transfer Mechanism for Precast, Prestressed Concrete Sandwich Wall Panels.* North Carolina State University, Department of Civil Engineering. Raleigh: North Carolina State University.

Chang, M., Maguire, M., & Sun, Y. (2017, September). Framework for Mitigating Human Bias in Selection of Explanatory Variables for Bridge Deterioration Modeling. *Journal of Infrastructure Systems, 23*(3). doi:http://dx.doi.org/10.1061/(ASCE)IS.1943-555X.0000352#sthash.crl6UQWl.dpuf

Collins, F. T. (1954, February 24). Precast Concrete Sandwich Panels for Tilt-up Construction. *Journal of the American Concrete Institute, 26*, 149-164.

Dorafshan, S., Maguire, M., & Qi, X. (2016, August). Automatic Surface Crack Detection in Concrete Structures Using OTSU Thresholding and Morphological Operations.

Einea, A., Salmon, D. C., Fogarasi, G. J., Culp, T. D., & Tadros, M. K. (1991). State-of-of-the-Art of Precast Concrete Sandwich Panels. *PCI Journal, 36*(6), 78-98.

Einea, A., Salmon, D. C., Tadros, M. K., & Culp, T. D. (1994). A New Structurally and Thermally Efficient Precast Sandwich Panel System. *PCI Journal, 39*(4), 90-101.

Frankl, B. A., Lucier, G. W., Hassan, T. K., & Rizkalla, S. H. (2011). Behavior of Precast, Prestressed Concrete Sandwich Wall panels Reinforced with CFRP Shear Grid. *PCI Journal, 56*(2), 42-54.

Jones, G. F., & Jones, R. W. (1999). Steady-State Heat Transfer in an Insulated, Reinforced Concrete Wall: Theory, Numerical Simulations, and Experiments. *Journal of Energy and Buildings, 29*, 293-305.

Lee, B. J., & Pessiki, S. (2004). Analytical Investigation of Thermal Performance of Precast Concrete Three-Wythe Sandwich Wall Panels. *PCI Journal, 49*(4), 88-101.

Lee, B. J., & Pessiki, S. (2007). Design and Analysis of Precast, Prestressed Concrete, Three-Wythe Sandwich Wall Panels. *PCI Journal, 52*(4), 70-83.

Lee, B. J., & Pessiki, S. (2008). Experimental Evaluation of Precast, Prestressed Concrete, Three-Wythe Sandwich Wall Panels. *PCI Journal, 53*(2), 95-115.

Maguire, M., Collins, W. N., Halbe, K. R., & Roberts-Wollmann, D. L. (2016, Mar/Apr). Multi-Span Members with Unbonded Tendons: Ultimate Sstrength Behavior. *ACI Structural Journal; Farmington Hills*, 195-204.

Naito, C. J., Hoemann, J. M., Shull, J. S., Saucier, A., Salim, H. A., Bewick, B. T., & Hammons, M. I. (2011). *Precast/Prestressed Concrete Experiments Performance on Non-Load Bearing Sandwich Wall Panels.* Lehigh University, Department of Ciivl and Environmental Engineering. Tyndall Air Force Base: Air Force Research Laboratory; Materials and Manufacturing Directorate.

Olsen, J., Al-Rubaye, S., Sorenson, T., & Maguire, M. (2017). Developing a General Methodology for Evaluating Composite Action in Insulated Wall Panels. *Precast/Prestressed Concrete Institute*. Retrieved from http://digitalcommons.usu.edu/cee_facpub/3531

Pantelides, C. P., Rajeev, S., & Reaveley, L. D. (2008). Structural Performance of Hybrid GFRP/Steel. *Journal of Composites for Construction, 12*(5), 570-576.

Pettigrew, C. S., Barr, P. J., Maguire, M., & Halling, M. W. (2016, September). Behavior of 48-Year-Old Double-Tee Bridge Girders Made with Lightweight Concrete. *Journal of Bridge Engienering, 21*(9). doi:http://dx.doi.org/10.1061/(ASCE)BE.1943-5592.0000921#sthash.2NHOdtPP.dpuf

Rizkalla, S. H., Hassan, T. K., & Lucier, G. (2009). FRP Shear Transfer Mechanism for Precast, Prestressed Concrete Sandwich Load-Bearing Panels. *American Concrete Institute Fall 2009 Convention: Thomas T.C. Hsu Symposium. 265*, pp. 603-625. New Orleans: American Concrete Institute.

Salmon, D. C., & Einea, A. (1995). Partially Composite Sandwich Panel Deflections. *Journal of Structural Engineering, 121*, 778-783.

Salmon, D. C., Einea, A., Tadros, M. K., & Culp, T. D. (1997). Full Scale Testing of Precast Concrete Sandwich Panels. *American Concrete Institute Structural Journal, 94*(4), 354-362.

Seeber, K. E., Andrews, R. J., Baty, J. R., Campbell, P. S., Dobbs, J. E., Force, G., . . . Wescott, H. E. (1997, March). State-of-the-Art of Precast/Prestressed Sandwich Wall Panels. *PCI Journal, 42*(2), 92-134.

Seeber, K., Anderson, N. S., Barrett, C. T., Brecher, E. F., Cleland, N. M., D'Arcy, T. J., . . . Wynings, C. E. (2004). *PCI Design Handbook; Precast and Prestressed Concrete* (6th ed.). (L. D. Martin, & C. J. Perry, Eds.) Chicago, Illinois, USA: Precast/Prestressed Concrete Institute. Retrieved 2015

Woltman, G., Tomlinson, D., & Fam, A. (2013). Investigation of Various GFRP Shear Connectors for Insulated Precast Concrete Sandwich Wall Panels. *Journal of Composites of Construction, 3*(17), 711-721. doi:10.1061/(ASCE)CC.1943-5614.0000373